

**AN INVESTIGATION INTO THE APOPTOTIC INDUCING EFFECT
OF FUSARIC ACID ON HUMAN LYMPHOCYTES AND ITS ROLE
IN CELL GROWTH INHIBITION**

BY

ATISHKAR RAMAUTAR

B Sc (HONS) UDW

**Submitted in partial fulfillment of the requirements for the degree of
Masters in Medical Science in the Department of Physiology, Faculty of
Medicine, University of Natal, Durban.**

2003

Abstract

Fusaric acid (FA) (5-butylpicolinic acid) is a divalent ion chelating agent that has low affinity for Ca^{2+} and Mg^{2+} and a high affinity for other essential metal ions such as Fe^{2+} , Mn^{2+} , Zn^{2+} and Cu^{2+} . Its mode of action therefore may involve its interference with various transition metal ions and thus may be analogous to picolinic acid. Fusaric acid inhibits the proliferation of numerous cell lines *in vitro*. In the current *in vitro* study the effects of FA on peripheral blood lymphocytes was studied. Lymphocytes from a healthy volunteer were treated with varying concentrations of FA (3 μM , 6 μM , 25 μM , 50 μM , 100 μM , 200 μM , 400 μM and 1000 μM) to assess the toxins apoptotic inducing potential. The 'Comet Assay' (Single cell gel electrophoresis), DNA fragmentation and Annexin V flous assays were employed to assess apoptosis. These assays proved that FA induces apoptosis in human lymphocytes. Lymphocytes were also incubated with phytohaemagglutinin (PHA) (10 $\mu\text{g/ml}$) and increasing doses of FA (10, 50, 100 and 200 μM). After 24, 48 and 72 hours of incubation an aliquot of the cells was stained with propidium iodide and subjected to flow cytometric analysis to assess the DNA configuration. Phytohaemagglutinin stimulation led to a significant increase of the S-phase of the cell cycle after 48 and 72 hours of incubation. All the PHA induced effects were reduced by co-incubation with increasing doses of FA. Lymphocytes were inhibited in the S-phase at 100 and 200 μM concentration of FA. The current study shows that the *in vitro* inhibitory effects of FA can be demonstrated using flow cytometric technology on a cellular level. Fusaric acid leads to an inhibition of cell cycle progression in peripheral blood lymphocytes.

DECLARATION

This study represents the original work of the author and has not been submitted in any form to another University. The use of work by other authors has been duly acknowledged in the text.

The research described in this study was carried out in the Department of Physiology, Faculty of Medicine, University of Natal, Durban, under the supervision of Professor A. A. Chuturgoon.

A. RAMAUTAR

PUBLICATIONS

Papers submitted for publication 2003

1. M. F. Dutton, A. A. Chuturgoon and A. Ramautar. Fusaric acid induced DNA damage in human lymphocytes detected by the comet assay. *Mutation Research*.
2. M. F. Dutton, A. A. Chuturgoon and A. Ramautar. Induction of apoptosis in human lymphocytes by fusaric acid. *Environmental Health Perspectives*.
3. M. F. Dutton, A. A. Chuturgoon and A. Ramautar. Inhibition of growth of human lymphocytes by fusaric acid. *Environmental Health Perspectives*.
4. M. F. Dutton, A. A. Chuturgoon and A. Ramautar. Changes in mitochondrial transmembrane potential of human lymphocytes induced by fusaric acid. *Environmental Health Perspectives*.

Acknowledgements

I would like to thank my mum and dad for their constant support encouragement and patience in this work and my brothers for their technical assistance.

I would like to thank Professor A. A. Chuturgoon for his constructive criticism and invaluable advice throughout the lab work and writing of this dissertation.

I would also like to thank the following people:

Professor M. F. Dutton for his advice on fusaric acid and financial support (NRF busary).

Professor M. Mars for assistance in statistical analysis.

All my friends for their constant encouragement.

And Miss D Ramduth for her invaluable assistance throughout my lab work especially in flow cytometry.

Table of contents

	Page
Abstract	I
Declaration	II
Publications	III
Acknowledgements	IV
List of Figures	XII
List of tables	XVII
Chapter 1	
1 Introduction	1
1.2 Literature review	2
1.2.1 Mycotoxins	2
1.2.2 White blood cells	3
1.2.2.1 Lymphocyte function and ultrastructural features	3
1.2.3 The other white cells	5
1.2.3.1 The monocytes	5
1.2.3.2 Neutrophils	6
1.2.3.3 Eosinophils	7
1.2.3.4 Basophils	8
1.3 Cell cycle regulation	9
1.3.1 Regulation of the cell cycle	9
1.4 Mode of action of mycotoxins	11
1.4.1 Nucleic acids as receptors	11

1.4.2 Proteins as molecular receptors	12
1.4.3 Mycotoxin effects on energy production	12
1.4.4 Effects of mycotoxins on cellular respiration	13
1.4.5 Uncoupling of oxidative phosphorylation	13
1.4.6 Alteration of membrane permeability	14
1.5 Picolinic acid	15
1.5.1 Cytotoxic effect of picolinic acid	15
1.5.2 Antitumour activity	17
1.6 Fusaric acid (5-butylpicolinic acid)	18
1.6.1 The effect of fusaric acid on animals	20
1.6.2 Antihypertensive activity of fusaric acid	21
1.6.3 The relation of fusaric acid to niacin	23
✓ 1.7 Apoptosis	24
1.7.1 Apoptosis and cytotoxins	25
1.7.2 Sensing toxin induced damage	27
1.7.3 Modes of protection against toxin induced death	27
1.7.4 Bcl-2	29
1.7.5 Ionic regulation	30
1.7.6 Caspases	30
1.7.7 Caspase activation	32
1.8 Apoptosis and the mitochondria	35
1.8.1 The formation of channels by the Bcl-2 family to facilitate protein transport	35

1.8.2 The interaction of Bcl-2 with other proteins to form channels	35
1.8.3 Bcl-2 family members may cause rupture of the mitochondrial membrane	35
1.9 CD95 and apoptosis	37
1.9.1 CD95 Signal transduction	39
Chapter 2	
2. Cytotoxicity testing : MTT assay	41
2.1 Materials and Method	42
2.1.1 Materials	42
2.1.1.2 Cell culture media	43
2.1.2 Methods	43
2.1.2.1 Lymphocyte isolation	43
2.1.2.2 Cell counting and viability	44
2.1.2.3 Preparation of the MTT salt	44
2.1.2.4 Lymphocyte treatments	44
2.2 Results and Discussion	45
Chapter 3	
3. Single cell gel electrophoresis	50
3.1 Analysis of DNA breakage in the SCGE assay	53
3.2 Principles that determine the behaviour of DNA in the SCGE	

assay	53
3.3 Applications of the SCGE assay	54
3.4 DNA damage and repair studies	54
3.5 Biomonitoring	55
3.6 Determination of genotoxicity	57
3.7 Materials and Method	58
3.7.1 Materials	58
3.7.2 Methods	58
3.7.2.1 Blood preparation and treatments	58
3.7.2.2 Slide preparation	58
3.7.2.3 Electrophoresis	60
3.7.2.4 Staining	60
3.7.2.5 Image analysis	60
3.7.2.6 Statistical analysis	61
3.8 Results and Discussion	61
Chapter 4	
4. DNA Fragmentation analysis	70
4.1 The role of endonuclease in DNA fragmentation	71
4.2 DNA Digestion is influenced by pre- existing chromatin organization	72
4.3 Materials and Method	74
4.3.1 Materials	74
4.3.2 Methods	74

6.2.3 Lipid scramblase	111
6.3 Annexins	112
6.3.1 Annexin structure	112
6.3.2 Implications of the annexin structure	114
6.4 Materials and Method	115
6.4.1 Materials	115
6.4.2 Methods	116
6.4.2.1 Preparation of lymphocytes for flow cytometry	116
6.4.2.2 Flow cytometric analysis	116
6.4.2.3 Data analysis	117
6.5 Results and Discussion	117
Chapter 7	
7. Cell cycle analysis	127
7.1 Cell cycle and flow cytometry	127
7.2 Detection of cyclins in individual cells using flow cytometry	131
7.3 Materials and Method	135
7.3.1 Materials	135
7.3.2 Methods	135
7.3.2.1 Chemicals required	135
7.3.2.2 Preparation of lymphocyte samples	135
7.3.2.2.1 Fixation	136
7.3.2.2.2 Debris removal	136

7.3.2.2.3 DNA Staining	136
7.3.2.2.4 Statistical analysis	137
7.4 Results and Discussion	137
8 Conclusion	145
9 References	148
10 Appendices	163
Appendix 1	163
Appendix 2	164
Appendix 3	165
Appendix 4	166
Appendix 5	167
Appendix 6	168

List of Figures

	Page
Figure 1a Light micrograph of lymphocyte.	5
Figure 1b Electron micrograph of lymphocyte illustrating ultrastructural features.	5
Figure 2 Light micrograph of monocyte.	6
Figure 3 Light micrograph of neutrophil.	7
Figure 4 Light micrograph of eosinophil.	7
Figure 5 Light micrograph of basophil.	8
Figure 6 Schematic diagram of cell cycle.	10
Figure 7 Structure of fusaric acid.	18
Figure 8 The nature of the substrate and the exact position of the cleavage site in the primary sequence can lead to diverse results by caspase action.	32
Figure 9 The three modes of caspase activation.	34
Figure 10 Various proposed mechanisms of Bcl-2 action.	36
Figure 11 Cytotoxic T lymphocytes can kill target cells by CD95.	39
Figure 12 Cleavage of the tetrazolium ring in the MTT salt.	42
Figure 13 Mean percentage lymphocyte viability at various concentrations of FA.	47
Figure 14 Fluorescence micrographs showing individual Chinese hamster V79 comets processed in the SCGE assay.	51
Figure 15a <i>T. thermophila</i> cells before cell lysis.	56
Figure 15b Cells centrifuged at $1000 \times g$ and then electrophoresed.	56
Figure 15c-d cells collected by natural sedimentation then electrophoresed.	56

Figure 16a Untreated control cells.	57
Figure 16b Lymphocytes treated with AZT.	57
Figure 17 Diagrammatic representation of SCGE assay.	59
Figure 18 Control cell exhibiting no DNA damage (untreated).	62
Figure 19a Mild degree of DNA damage exhibited by short migration of DNA (6 μ M FA).	62
Figure 19b Cell exhibiting moderate degree of DNA damage (50 μ M FA).	63
Figure 19c Cell exhibiting extreme DNA damage (100 μ M FA).	63
Figure 20a Untreated control cells with no DNA damage.	64
Figure 20b Cells treated with 3 μ M FA with little DNA damage.	64
Figure 20c Cells treated with 6 μ M FA with minor DNA damage.	64
Figure 20d Cells treated with 50 μ M FA with increased DNA damage.	64
Figure 20e Cells treated with 100 μ M FA with major DNA damage.	64
Figure 21 Fragmentation profiles of FA treated lymphocytes at various concentrations after 4 and 24 hours.	77
Figure 22 Fragmentation profiles of FA treated lymphocytes at various concentrations after 4 and 48 hours.	78
Figure 23 Semithin section (a) and low power transmission electronmicrograph (TEM); b of prednisolone-treated rat thymus. (<i>Asterisk</i> T-Iymphoblast, <i>stars</i> early apoptotic cells, <i>arrows</i> late apoptotic cells).	83
Figure 24a The nucleus of an early apoptotic cell. The coiled chromatin threads of the supranucleosomal level of organization, textured as	

30-nm globules, are seen (<i>arrows</i>). <i>Bar</i> 100 nm.	84
Figure 24b The nucleus of a late apoptotic cell.	84
Figure 25 Typical control lymphocyte (24Hours).	90
Figure 26 FA treated lymphocytes (24 hours).	91
Figure 27 400 μ M FA treated lymphocyte (24hours) exhibiting nuclear migration to the periphery of the nucleus which is characteristic of apoptosing cells. \times 15000 mag	92
Figure 28 Mitochondria of control lymphocyte (24 hours) associated with normal paralell arrays of cristae (black arrow). \times 60000 mag	93
Figure 29 1000 μ M FA treated lymphocytes (24 hours).	94
Figure 30 200 μ l FA treated lymphocyte exhibiting budding of numerous membrane bound vesicles from the apoptotic cell.	95
Figure 31 The stages of apoptosis in fusaric acid treated lymphocytes.	96
Figure 32 Lymphocyte treated with 200 μ M fusaric acid for 24 hours exhibiting large vacuole. \times 2500 mag	97
Figure 33 Lymphocyte treated with 200 μ M fusaric acid for 24 hours exhibiting numerous vacuoles of different sizes. \times 2500 mag	98
Figure 34 Nucleus of control lymphocyte exhibiting distinct nuclear pores (<i>arrows</i>). \times 20000 mag	99
Figure 35 Nucleus of control cell displaying laminar across nuclear pore. \times 60000 mag	99
Figure 36 Endoplasmic reticulum of control cell (arrow). \times 40000 mag	100
Figure 37 Diagrammatic representation of functional components	

and light scatter in a flow cytometer.	105
Figure 38 Annexin V-FITC can be used as a sensitive probe for the presence of PS on the outside of the plasma membrane of apoptosing cells.	106
Figure 39 Dual parameter three dimensional contour plot exhibiting healthy apoptotic and necrotic cells.	107
Figure 40 Dot plot exhibiting live, apoptotic and necrotic cells.	107
Figure 41 The regulation and physiology of membrane phospholipid asymmetry.	109
Figure 42 a) The alpha helices of annexin V, b) The three dimensional structure of annexin V, c) The three binding sites of annexin V.	113
Figure 43 Flow cytometric analysis of apoptosis in FA treated lymphocytes.	120
Figure 44a Control 3D contour and dot plots at 1 hour incubation.	121
Figure 44b 50 μ M FA 3D contour and dot plots at 1 hour incubation.	121
Figure 44c 200 μ M FA 3D contour and dot plots at 1 hour incubation.	121
Figure 44d Control 3D contour and dot plots at 4 hour incubation.	122
Figure 44e 50 μ M FA 3D contour and dot plots at 4 hour incubation.	122
Figure 44f 200 μ M FA 3D contour and dot plots at 4 hour incubation.	122
Figure 44g Control 3D contour and dot plots at 24 hour incubation.	123
Figure 44h 50 μ M FA 3D contour and dot plots at 24 hour incubation.	123
Figure 44i 200 μ M FA 3D contour and dot plots at 24 hour incubation.	123
Figure 45 Typical flow cytometric histogram representing various phases of the cell cycle.	130

Figure 46 Three dimensional contour plot of cells in various phases of the cell cycle.	131
Figure 47 Schematic diagram of the occurrence of various cyclins at different time points in the cell cycle.	132
Figure 48a Positive control exhibiting normal distribution of phases after 24 hours.	139
Figure 48b Slight decrease in G ₀ /G ₁ and G ₂ /M peaks after 10μM FA treatments.	139
Figure 48c More pronounced decrease in G ₀ /G ₁ and G ₂ /M peaks after 200μM FA treatments.	139
Figure 49a Positive control exhibiting pronounced S phase.	140
Figure 49b All phase peaks smaller than positive control due to 10μM FA although S phase still prominent.	140
Figure 49c All phase peaks smaller than positive control due to 200μM FA treatment.	140
Figure 50a Full expression of PHA indicated in all phase peaks after 72 hours.	141
Figure 50b Significant decrease in all phase peaks due to 10μM FA treatment after 72 hours.	141
Figure 50c Fusaric acid has almost totally stopped replication of cells as exhibited by an absence of an S phase and a very small G ₂ /M phase.	141

List of tables

		Page
TABLE 1	Metabolic activity of lymphocytes treated with fusaric acid.	46
TABLE 2	Demonstration of DNA damage induced in human lymphocytes by FA using the SCGE assay.	65
TABLE 3	<i>In vitro</i> processing of lymphocytes for transmission electron microscopy.	87
TABLE 4	Percentages of apoptosis and necrosis in lymphocytes at various time intervals.	119
TABLE 5	Cyclins and their partner CDKs during the cell cycle.	133
TABLE 6	Percentages of cells in different phases of the cell cycle after treatment with FA at various time intervals.	138

Chapter 1

1. Introduction

Fusaric acid (FA) is a toxic metabolite produced by numerous *Fusarium* species in maize and other cereal grains including barley, wheat millets and sorghum. Studies have demonstrated FA contamination as high as 35.76mg/kg of swine feed and 135mg/kg in high moisture maize occurring simultaneously with other mycotoxins such as deoxynivalenol and zearalenone. Although the maize destined for human consumption is not screened for FA contamination, the likelihood of exposure of FA in humans is a high probability, since 79-100% of grain and animal feed samples on farms were found to be contaminated with FA (Smith and Sousadias, 1993).

The biological half life of FA in blood approximates 12 hours (Matta and Wooten, 1973). With such a long duration of action and given that FA has been used in clinical trials to treat Parkinson's disease, the effect of the toxin on human lymphocytes has to date not been documented. This study was designed to evaluate the effect of FA on human lymphocytes and its effect on cell growth inhibition. The aims of this study were:

- a) To assess the cytotoxicity of FA on normal human lymphocytes.
- b) To determine the apoptotic inducing potential of FA on normal healthy lymphocytes.
- c) To determine the effects of FA on the cell cycle of normal human lymphocytes.

1.2 Literature review

1.2.1 Mycotoxins

Mycotoxins along with other fungal products, such as antibiotics, alkaloids and gibberellins are often referred to as secondary metabolites. These mould produced toxins are contaminants of a wide variety of foods and feeds. Ingestion of these secondary metabolites may cause a range of toxic responses from acute toxicity to long term or chronic health disorders. Primary metabolites are the summation of an interrelated series of enzyme-catalysed chemical reactions which provide the organism with energy, synthetic intermediates and key macromolecules such as protein and DNA. Secondary metabolism involves mainly synthetic processes, the end products of which are secondary metabolites and are of no particular importance to the organisms economy. These secondary metabolites are produced at only one stage of the life cycle, have obscure physiological functions and are not essential to the growth of the producing organism. The selection of the ability of the fungus to produce mycotoxins probably lies in the roots of protective or competitive advantages (Coulombe, 1993).

The effects of mycotoxins has been tested *in vitro* and *in vivo* in various cellular systems. Blood is a tissue which consists of a variety of cells suspended in a fluid medium called plasma. It is clinically the key intermediate in the functioning of all organs. Functioning principally as a vehicle for the transport of gases, nutrients, metabolic waste products, cells and hormones throughout the body. It can therefore be implicated in the transport of mycotoxins, thus creating a link between systemic diseases and their respective aetiological factors.

1.2.2 White blood cells

The white cell series consist of two main classes subdivided into five cell types. The two classes are granulocytes and agranulocytes, named according to the granularity of their cytoplasm and general nuclear characteristics. The three different types of granulocytes are neutrophils, eosinophils and basophils named according to the staining characteristics of their specific granules.

The agranulocytes consist of the lymphocytes and monocytes which are so named because they do not contain cytoplasmic granules readily visible under the light microscope. White blood cells are particularly important because they play a fundamental role in the bodies immune response (Wheater *et al.*, 1987).

1.2.2.1 Lymphocyte function and ultrastructural features

Lymphocytes (Fig 1a and 1b) are key players in all the immune responses and in contrast to all the other leucocytes, their activity is always directed against specific foreign agents. Lymphocytes identify foreign substances in the body and produce antibodies and cells that specifically target them. It takes between several days to weeks for lymphocytes to recognise and attack new foreign substances.

The main lymphocyte sub-types are :

1. B-cells - Special B cells produce specific antibodies, proteins that help destroy foreign substances.
2. T-cells - T-cells attack virus-infected cells, foreign tissue, and cancer cells. They also produce a number of substances that regulate the immune response.

3. Natural killer cells - Among other functions, natural killer cells destroy cancer cells and virus-infected cells through phagocytosis and by producing substances that can kill such cells.
4. Null cells - An early population of lymphocytes bearing neither T-cell nor B-cell differentiation antigens.

B- lymphocytes have a lifespan of 10-20 days and T-lymphocytes can survive for several months. Lymphocytes are the smallest cells in the white cell series, larger only than erythrocytes. They have virtually no cytoplasm and are found in the blood, in all tissue and in lymphoid organs, such as lymph nodes, the tonsils, thymus gland, spleen and Peyer's patch. They are the second most common leukocyte in circulating blood and make up 20-45% of the differential white cell count. The amount of cytoplasm varies with the state of activity of the lymphocyte. The nucleus of lymphocytes is usually small, rounded and often indented and the chromatin is moderately condensed. The nucleoli are usually not visible. The thin layer of cytoplasm contains a few mitochondria, a rudimentary golgi apparatus, little or no endoplasmic reticulum and a comparatively large number of free ribosomes. The plasma membrane has a few irregular pseudopodia (Wheater *et al.*, 1987).

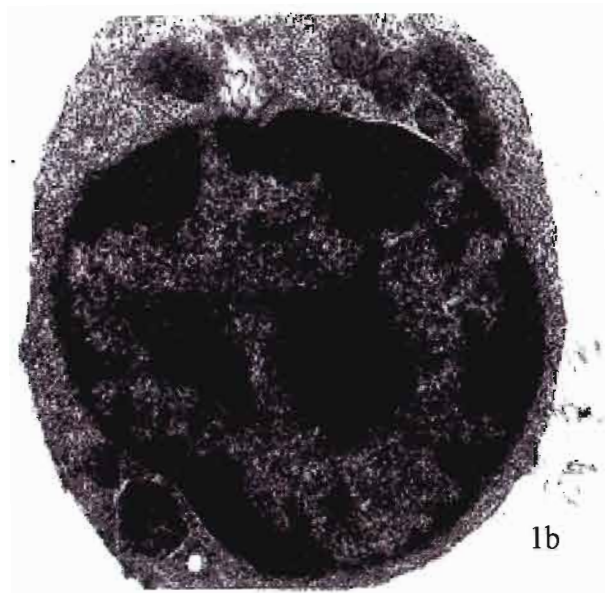
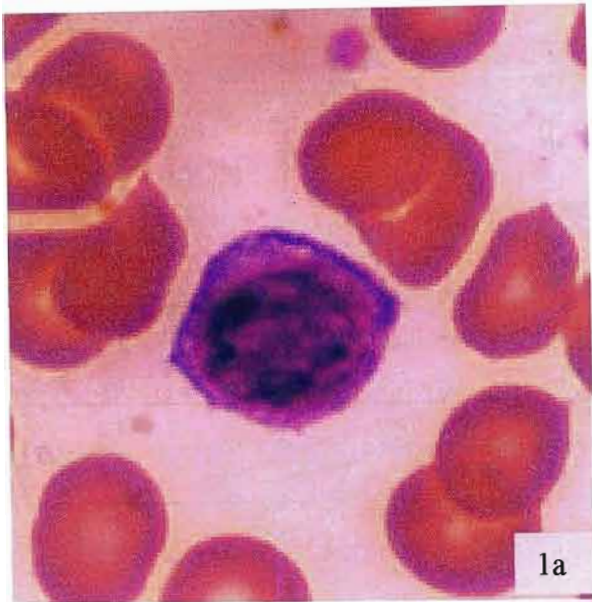


Figure 1a Light micrograph of lymphocyte. 1b Electron micrograph of lymphocyte illustrating ultrastructural features (www.hsc.virginia.edu/./pathology/educ/innes/text/nh/wcb.html).

1.2.3 Other white cells

1.2.3.1 The monocytes

The monocytes (Fig 2) are the largest white blood cells and constitute approximately 2-10% of leucocytes in the peripheral blood. They are characterized by a large eccentrically placed nucleus which stains less intensely than that of other leucocytes. The nucleus is usually indented. It may at times even appear bilobed or even horseshoe like. Lysosomes are abundantly found in the cytoplasm. Ultrastructural evaluations reveal relatively diffuse rough endoplasmic reticulum, well developed golgi apparatus and abundant mitochondria.

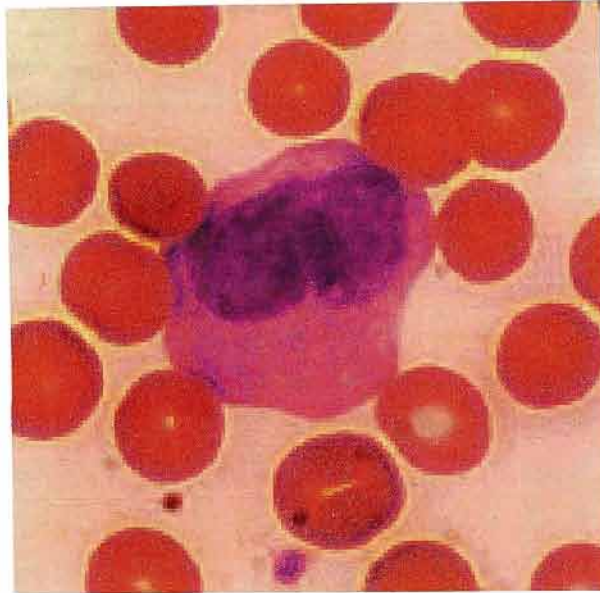


Figure 2 Light micrograph of monocyte
(www.hsc.virginia.edu/./pathology/educ/innes/text/nh/wcb.html).

1.2.3.2 Neutrophils

Neutrophils (Fig 3) are the most abundant leukocyte accounting for 40-75% of circulating leucocytes. The most characteristic feature of the neutrophil is its lobulated nucleus. As many as five lobes may be discernible at a time. The main function of neutrophils is to phagocytose invading microorganisms. They are the main leucocytes involved in acute inflammatory response.

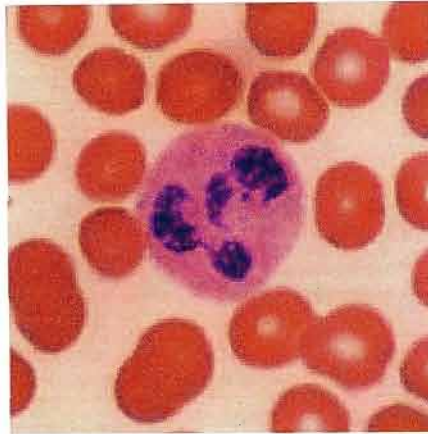


Figure 3 Light micrograph of neutrophil (www.hsc.virginia.edu/.../pathology/educ/innes/text/nh/wcb.html).

1.2.3.3 Eosinophils

These leucocytes are less common than neutrophils. They are characterized by a bilobed nucleus which is packed with large eosinophilic specific granules of uniform size. Evidence suggests that eosinophils are directly involved in the destruction of some parasites. They are usually attracted to sites of inflammation and are highly phagocytic for antigen-antibody complexes.

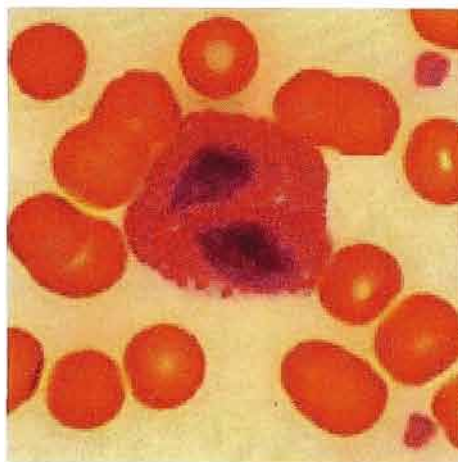


Figure 4 Light micrograph of eosinophil (www.hsc.virginia.edu/.../pathology/educ/innes/text/nh/wcb.html).

1.2.3.4 Basophils

Basophils (Fig 5) are the least common of the leucocytes making up approximately 1% of leucocytes in the circulating blood. These leucocytes are also bilobed and contain numerous large, densely basophilic specific granules. Basophils liberate heparin into the blood. Heparin can prevent blood coagulation and can speed up the removal of fat particles from the blood after fatty meals. Basophils play an important role in certain allergic reactions because of the type of antibody that causes allergic reaction, IgE type, which has a special propensity to become attached to basophils. The reaction of the specific antigen with the antibody causes the basophil to rupture liberating large quantities of histamine, bradykinin, serotonin, heparin, slow reacting substances of anaphylaxis, and a number of lysosomal enzymes. This process results in allergic manifestations.

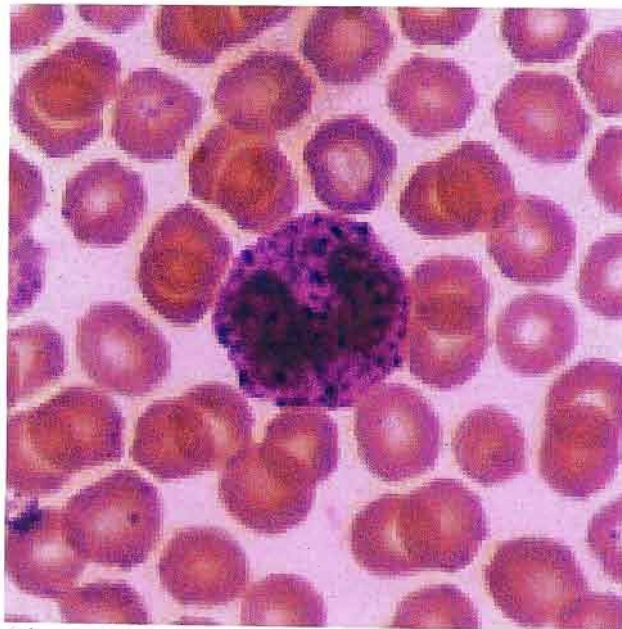


Figure 5 Light micrograph of basophil
(www.hsc.virginia.edu/./pathology/educ/innes/text/nh/wcb.html).

1.3 Cell cycle regulation

In a proliferating cell population 4 distinct phases can be recognized: the G_1 (Gap1)-, S (Synthesis)- (DNA synthesis phase), G_2 (Gap2)- and M-phase (mitosis). The G_1 stage stands for "GAP 1". The S phase is the stage when DNA replication occurs. During the M phase, nuclear (chromosomes separate) and cytoplasmic (cytokinesis) division occurs.

Based on their differences in DNA content these phases can be discriminated, except for the G_2 - and M-phase, which both have an identical DNA content. A schematic drawing of the cell cycle can be seen in figure 6.

1.3.1 Regulation of the cell cycle

Cell division (and thus tissue growth) control is very complex. The following terms are some of the features that are important in regulation, and places where errors can lead to cancer. Cancer is a disease where regulation of the cell cycle goes wrong and normal cell growth and behaviour is lost.

Cyclin dependent kinase, (CdK) along with cyclins, are major control switches for the cell cycle, causing the cell to move from G_1 to S or G_2 to M.

Maturation promoting factor (MPF) includes the CdK and cyclins that triggers progression through the cell cycle.

p53 is a protein that functions to block the cell cycle if the DNA is damaged. If the damage is severe this protein can cause apoptosis (cell death).

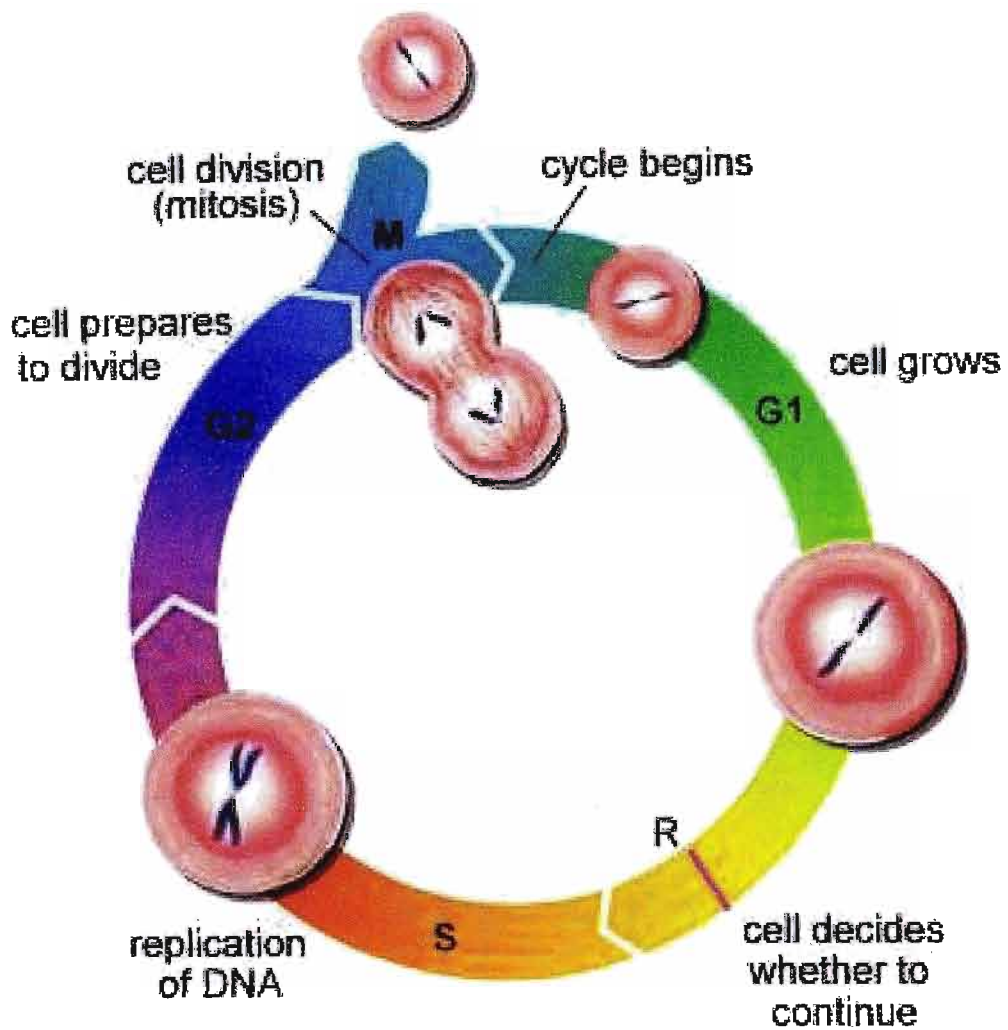


Figure 6 Schematic diagram of cell cycle

(www.learninglab.co.uk/headstart/cycle3.htm).

G1- GAP 1

G2- GAP 2

S- DNA replication occurs

M- Nuclear and cytoplasmic division occurs

1.4 Mode of action of mycotoxins

Mycotoxins may impair vital biochemical processes by reacting with critical molecular receptors which may be DNA, RNA, functional proteins, enzyme cofactors or membrane constituents. The relative significance of a molecular receptor of a mycotoxin is determined by :

- a) its affinity for the active form of the toxin,
- b) its role in vital biochemical processes,
- c) the persistence of the lesion it bears,
- d) the severity of the consequences of the lesion.

Damage occurring in DNA and RNA are of particular importance. Not only do they destroy the structural integrity of these informational molecules, but their biosynthesis is interrupted. Important reactions that occur are non-specific electrophilic attacks on the nucleophilic centres of the receptor molecules, usually, nitrogen, oxygen, and sulphur heteroatoms in proteins and nucleic acids. The occurrence of adduction at the active site of a critical receptor, causes a sufficient conformational change of the receptor causing chemical injury and impairment of the receptor. Receptor mycotoxin adduction can be removed from the cell by a number of processes, including spontaneous decomposition of the covalent bonds, receptor turnover and specific repair processes (Hsieh, 1987).

1.4.1 Nucleic acids as receptors

Nucleic acids are often critical targets of genotoxic mycotoxins. The nucleophilic heteroatoms in the organic bases of nucleic acids are often the targets of electrophilic

metabolites of mycotoxins, forming covalent adducts. Alterations in the precise structures of DNA and RNA leads to impaired template activity of these molecules. Synthesis of nucleic acids may be inhibited and in point mutations this may lead to the synthesis of erroneous macromolecules. The result of such adduction *in vivo* may be cellular death or in some instances transformation to the cancerous condition (Hsieh, 1987).

1.4.2 Proteins as molecular receptors

Proteins are the most common receptors in cells due to the presence of nucleophilic N, O, and S heteroatoms in their functional groups. Both non-specific irreversible covalent and specific reversible non-covalent binding by mycotoxins are instrumental in altering the structure and activities of proteins. Once bound to mycotoxins, proteins may serve as carriers to transport reactive metabolites, or as reservoirs of the toxins to stabilize and prolong cellular exposure to the toxins (Hsieh, 1987).

1.4.3 Mycotoxin effects on energy production

One of the main effects of acute exposure to mycotoxins is inhibition of cellular energy production. The molecular receptors here are the enzymes that catalyse certain key reactions in the tricarboxylic acid cycle (TCA), the electron transport to oxygen and the oxidative phosphorylation for ATP production. Both non-specific-irreversible covalent and specific-reversible-noncovalent binding have been observed to occur between these enzymes and mycotoxins. Inadequate production of ATP due to the biochemical effects of toxic insult impairs cellular function and ultimately causes cell death. Some mycotoxins modify various types of adenosine triphosphatases (ATPase) disrupting functions of the plasma membrane (Hsieh, 1987).

1.4.4 Effects of mycotoxins on cellular respiration

Many mycotoxins are capable of inhibiting important enzymes involved in the TCA cycle and the electron transport chain in mitochondria. The resulting immediate cellular response to a disturbance of such metabolic processes is a reduction in oxygen consumption. Evaluation of the changes in oxygen consumption rate in cell homogenates or mitochondrial preparation involving various intermediates of the TCA cycle such as substrates, has revealed specific target sites of mycotoxin action in the electron transport chain. The *Fusarium* toxin, moniliformin is a potent inhibitor of mitochondrial pyruvate and α -ketoglutarate oxidation. Other similar enzymes exist that are responsible for the oxidative decarboxylation of pyruvate to acetyl coenzyme A and of α -ketoglutarate to succinyl coenzyme A. Both these enzymes are susceptible to arsenicals and arsenites through inactivation of lipoic acid, an essential cofactor for these enzymes. The result is the suppression of the acetyl group transfer to coenzymes. In this manner, moniliformin acts like fluoroacetate on the TCA cycle (Hsieh, 1987).

The co-occurring mycotoxin fusaric acid inhibits certain metal-containing enzymes, eg. cytochrome oxidase and is instrumental in depolarising the plasma membrane while decreasing cellular ATP levels (Arias, 1985).

1.4.5 Uncoupling of oxidative phosphorylation

Certain mycotoxins are also capable of uncoupling oxidative phosphorylation. Uncoupling of oxidative phosphorylation results in the immediate depletion of cellular ATP. Depletion of ATP may then cause mitochondrial swelling due to the failure of the cell to maintain sodium and potassium gradients. The uncoupling ability of mycotoxins may or may not be accompanied by their ability to inhibit cellular electron transport.

Aflatoxin M₁ (AFM₁) uncouples oxidative phosphorylation as well as inhibits electron transport. Aflatoxin B₁ (AFB₁) although similar to AFM₁ is more of an electron transport inhibitor. In contrast the mycotoxins luteoskyrin, emodin, and secalonic acid all uncouple oxidative phosphorylation more strongly than they inhibit the cellular respiration at site 3. Ochratoxin A (OTA) depletes cellular ATP via another mechanism. The effect of OTA is two fold. Firstly the ATP is consumed in the uptake of OTA by the mitochondria, and, more importantly, this toxin inhibits intramitochondrial phosphate transport, resulting in impairment of oxidative phosphorylation (Hsieh, 1987). The mechanism by which FA exerts its effect on cells is believed to be via its protonophore activity which can uncouple oxidative phosphorylation and thus ATP synthesis or mitochondrial electron transport which is directly inhibited at the cytochrome oxidase level by the toxin (Arias, 1985).

1.4.6 Alteration of membrane permeability

Mycotoxins may also affect cellular energy production and utilization by alteration of ATPase activity. These membrane bound enzymes are responsible for the hydrolysis of ATP to generate the energy required for active transport of cations across the cell membrane. They may also be involved in ATP synthesis and oxidative phosphorylation. Due to their association with the cell membranes, these enzymes are particularly susceptible to toxic insult. Mycotoxins that bind to ATPases may affect a variety of transport or permeability-mediated physiological and biochemical functions of various types of cells (Hsieh, 1987).

1.5 PICOLINIC ACID

1.5.1 Cytotoxic effect of picolinic acid

Picolinic acid (PA) is a powerful bidentate chelating agent and is also structurally related to nicotinic acid, a precursor in the biosynthesis of NAD^+ (Fernandez-Pol *et al.*, 1977). Picolinic acid is a naturally occurring molecule derived from the catabolism of tryptophan (Leuthauser *et al.*, 1982). One of the characteristic features of PA is that it inhibits the growth of normal and transformed cell lines (Fernandez-Pol *et al.*, 1993). Short term treatment with PA arrests normal cells in G_1 (G_0) while transformed cells are blocked in different phases of the cell cycle (Fernandez-Pol and Johnson, 1977). Picolinic acid exhibits differential cytotoxicity in growth control and survival mechanisms between normal and transformed cells. Normal rat kidney (NRK) cells for example were reversibly arrested at the G_1 stage of the cell cycle when PA was added to the culture media. Growth of transformed NRK cells was also arrested by PA but this G_1 block was not reversible. Upon removal of the block the transformed cells progressed through S and G_2 phases and then died. Long exposure to PA is cytotoxic and cell death may result in transformed cells whether they were blocked in G_1 , G_2 or at random. This was in contrast to corresponding normal cells which exhibited no toxic effects from the longer treatment with PA (Fernandez-Pol *et al.*, 1993).

The effects of kinetic and radioisotopic studies have shown that PA inhibits incorporation of iron into cells and effectively removes radioiron from cells. It is thus conceivable that the inhibition of cell proliferation *in vitro* as well as tumour growth *in vivo* by PA results, at least in part, from selective depletion of iron in the cells. The chelating effect of PA is not restricted to iron. It can chelate Zn^{2+} , Cu^{2+} and Mn^{2+} ions which are important

structural and functional components in numerous proteins associated with cell proliferation, differentiation, and protection against free radicals such as the transcriptionally active zinc finger proteins and the Cu^{2+} and Mn^{2+} containing superoxide dismutases.

Picolinic acid has a number of other biological properties such as inhibitory effects on ADP ribosylation and ribosomal RNA maturation of hormonal responses to various hormones such as prostaglandin E1 or isoproterenol, enhancement of guanine nucleotide dependant adenylate cyclase activity and macrophage activation. Picolinic acid in combination with inteferon gamma ($\text{IFN}\gamma$) has been shown to be a potent inhibitor of J2 recombinant retrovirus mRNA in murine macrophages. It is also known to act synergistically with $\text{IFN}\gamma$ in activating macrophages which leads to the expression of tumouricidal activity by macrophages (Varesio *et al.*, 1990). An interesting proposition is that in macrophages interleukin 2 (IL-2) and PA share a common mechanism of action that is susceptible to interleukin 4 (IL-4) suppression. The expression of J2 virus mRNA in relationship with the proliferative ability and tumouricidal activity of GG2EE cells was investigated when exposed to biologic response modifiers. Among these where PA and $\text{IFN}\gamma$. The results suggest that the process of activation of tumouricidal macrophages also triggers a mechanism of resistance to viral mRNA expression (Varesio *et al.*, 1990).

1.5.2 Antitumour Activity

Picolinic acid has exhibited positive antitumour activity. Picolinic acid treated mice had significantly slower increases in tumour size. The mode of PA administration in these tumour models is important. Intraperitoneal administration is rapidly excreted into the urine, with a half life of six hours (Mehler and May, 1956). Intravenous injection of PA is excreted more slowly when compared to intraperitoneal administration (Mehler and May, 1956).

The mechanism of action of the arrest of NRK cells by PA in G₁ remains unknown. Initial propositions involved the alteration of cyclic AMP metabolism, NAD⁺ metabolism or chelation of Fe³⁺ and Zn²⁺ as possible modes of action (Fernandez-Pol *et al.*, 1977). The cytotoxicity of PA could possibly involve the generation of hydroxyl radicals (Leuthauser *et al.*, 1982).

1.6 Fusaric acid (5-butylpicolinic acid)

Fusaric acid (FA) (5-butylpicolinic acid) (Fig 7) produced by several *Fusarium* species has diverse pharmacological activities in mammals which are mainly apparent in the nervous, cardiovascular and immune systems. Fusaric acid may augment the overall toxicity of other mycotoxins. Thus the major importance of FA to animal toxicity may be synergistic interactions with other naturally occurring mycotoxins. Numerous surveys of several types of cereal grain, mixed livestock and poultry feed indicated that FA is a natural contaminant of these food and feed grains. Further investigations revealed that these feed samples contained other mycotoxins in addition to FA (Bacon *et al.*, 1996).

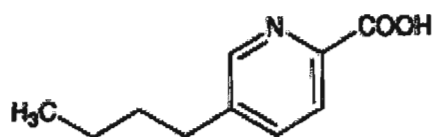


Figure 7 Structure of fusaric acid.

Fusaric acid is also a phytotoxin produced by many *formae speciales* of the fungus *F. oxysporum* Schelect. *Fusarium oxysporum* has been identified as the causal agent of tomato wilt. Studies demonstrated that tomato plants, infected with FA degrading *Pseudomonas* bacteria, were protected partially against *Fusarium* wilt caused by *F. oxysporum* (Loffler and Mouris, 1992). The mechanism of FA phytopathology is not completely understood. Studies were conducted on outer root cap cells of *Zea mays* (which contain numerous organelles) to examine ultrastructural and physiological alterations induced by FA. Alteration of membrane electrical potential occurs with 10^3 to 10^5 M FA whereas only concentrations greater than 10^4 M inhibit mitochondrial

respiration. *In vitro* FA inhibits certain metal-containing enzymes such as cytochrome oxidase and depolarises the plasma membrane while decreasing cellular ATP levels (Arias, 1985).

The phytotoxicity of FA has been ascribed to its ability to form chelate rings with heavy metals, resulting in an inhibition of enzymes such as iron porphyrin oxidase (Malini, 1966). Experiments have also found that FA which is a transition metal ion chelating agent and analogue of PA, has potent cytotoxic activity in cultured cells. The effects of FA on the growth and viability of various human cancer cell lines have demonstrated that it has potent anti-cancer activity *in vitro*. Fusaric acid has been shown to arrest cell proliferation at certain stages in the cell cycle and at higher concentrations has exhibited cytotoxicity. Investigation into the inhibition of DNA synthesis by FA showed that FA was a potent inhibitor of DNA synthesis in certain cell lines (Fernandez-Pol *et al.*, 1993). The inhibition of growth by FA may be primarily due to inhibition of the activity of the iron requiring enzyme ribonucleotide reductase. It is thought that ribonucleotide reductase, a rate controlling enzyme in the DNA synthetic pathway, is a possible target for the action of FA. It is possible that fusaric acid may act on cytosol $\text{Cu}^{2+}/\text{Zn}^{2+}$ containing- and /or mitochondrial Mn^{2+} - containing superoxide dismutase enzymes that may be important for growth and survival of cancerous cells. It may act by binding Zn^{2+} which is a structural component of certain zinc finger DNA binding proteins that are involved in cell proliferation (Fernandez-Pol *et al.*, 1993).

Preliminary experiments revealed that FA had potent cytotoxic activity in cultured cells. This led to a detailed study of the effects of FA on the growth and viability of normal WI-38 fibroblasts and various human cancer cell lines. Fusaric acid imposed a cytostatic

activity in normal human WI-38 fibroblasts which remained viable for 30-48hrs. The subsequent removal of FA allowed its effect to be reversed. The cytotoxic effect of FA on human colon adenocarcinoma cell lines (LoVo, SW48, SW480, SW742) and a human mammary adenocarcinoma cell line (MDA-MB-468) was marked. Prominent cytotoxic effects, manifested by granularity and cell destruction in all the colorectal adenocarcinoma cell lines at 24 to 72 hours after addition of FA was observed. The human mammary adenocarcinoma cell line (MDA-MB-468) were also highly sensitive to the cytotoxic effects of FA as > 80% of the cells were destroyed at 72 hours. The effect of FA on the viability of human epidermoid carcinoma KB cells was, by comparison, less pronounced as approximately 95% of KB cells resisted the pronounced cytotoxic action of FA (Fernandez-Pol *et al.*, 1993).

1.6.1 The effect of fusaric acid on animals

Fusaric acid was mixed with feed at 10, 75 and 200ppm and fed to pregnant rats. The consequence in the resulting neonates was a reduction of weight gain and pineal content of serotonin and tyrosine (Wang and Ng, 1999). Rapid eye movement (REM) sleep deprivation modified dopamine-mediated behaviour and adrenergic receptor sensitivity. Fusaric acid increased aggressiveness in REM-sleep-deprived rats. Isoproterenol diminished this degree of aggressiveness (Troncone and Tufik, 1991). The levels of homovanilic acid (HA) in rat cerebrospinal fluid were also increased by FA. This increase in HA induced by FA was accentuated by inazoxan, a selective α_2 -antagonist and prevented by methyldopa, suggesting that the rate of dopamine synthesis in norepinephrine neurons could be the chief determinant of FA stimulated elevation of homovanilic acid (Elghozi *et al.*, 1985).

Fusaric acid increased the level of tryptophan and hence serotonin in the brain, and displaced tryptophan binding to serum albumin thus increasing free tryptophan in the blood of test rats (Chaoulouff *et al.*, 1986). The diets of chickens treated with FA caused no abnormalities in behaviour, feed intake, weight gain or appearance of visceral organs. In addition, the incidence of tibial dyschondroplasia and leg shape deformities did not correlate with dietary concentration of FA. Fusaric acid enhanced vomiting and feed refusal in pigs administered with trichothecenes (Smith and Macdonald, 1991). Bacon *et al.*, (1995) found enhanced cytotoxicity when FA and FB₁ were administered simultaneously to developing chicks in ovo, thus providing direct evidence of synergism.

1.6.2 Antihypertensive activity of fusaric acid

Fusaric acid biochemically inhibits, *in vivo* and *in vitro* the enzymatic action of dopamine- β -hydroxylase (DBH) and lowers the level of endogenous adrenaline (A) and noradrenaline (NA) in brain, heart, spleen, and adrenal glands. Fusaric acid is a potent non-competitive inhibitor of DBH. Clinically it has been reported to have antihypertensive effects and to be effective in relieving tremor, rigidity and speech aberrations. More interestingly FA and L-dopa when administered together were much more effective than either given alone (Nagatsu *et al.*, 1970).

The mechanism of inhibition of FA was quite characteristic. Initially it was thought that because of the chelating ability of FA it would chelate the copper atom at the active site of the enzyme. Experiments revealed however that the inhibition was not attributable to simple chelation. The inhibition of FA was of an uncompetitive type with the substrate, indicating that this compound affects the enzyme substrate complex. Fusaric acid exhibited a mixed type of inhibition with a cofactor, ascorbate. Extensive dialysis

reversed the effect of FA but the addition of copper did not reverse the inhibition. These experiments revealed that the inhibition of FA is not due to simple chelation, but to complex interactions with the enzyme substrate complex (Nagatsu *et al.*, 1970).

The effects of the calcium salt of FA were tested in elderly hypertensive Japanese patients. In the first year it was found that the systolic and the diastolic blood pressures were lowered and no adverse effects were discernable. Patients exhibited no consistent changes in heart rate or plasma volume. The conclusions drawn were that the hypertensive response was obtained by the reduction of the total peripheral vascular resistance index (Wang and Ng, 1999). The systemic and renal hemodynamic effects of bupicamide a FA derivative was examined in 10 male patients with uncomplicated essential hypertension of moderate severity. Results revealed that diastolic, systolic and mean arterial pressures together with peripheral vascular resistance were lowered accompanied by a reflexive rise in heart rate, left ventricular ejection rate and cardiac index. The drug exhibited no other effect upon the reflexive sympathetic adjustments induced by upright tilt and the Valsalva manoeuvre. There was an increase in renal blood flow, while renal vascular resistance was reduced but glomerular filtration rate was unaffected. Dilation of the peripheral arterioles was due to vascular smooth muscle relaxation accounting for the hypotensive action of bupicamide. Side effects of the drug were headache cutaneous flushing and tachycardia (Wang and Ng, 1999).

Fusaric acid has been found to affect the levels of catecholamines in the adrenals, the heart and the kidneys. Adrenal levels of epinephrine and norepinephrine and a rise in adrenal dopamine concentration was documented after FA administration.

The fall in adrenal epinephrine was due to a decreased synthesis and an increased release. The epinephrine concentration in the kidneys, heart, plasma and urine increased. The concentrations of norepinephrine and dopamine in the heart and kidney changed in the same way as the adrenal (Wang and Ng, 1999).

1.6.3 The relation of fusaric acid to niacin

Nicotinamide adenine dinucleotide (NAD) is an important coenzyme in oxidation reduction reactions and is synthesized from niacin ie. nicotinic acid and nicotinamide. The function of NAD in the mitochondria as a coenzyme is very important. DNA strand breakage is thought to induce the critical consumption of NAD and ATP due to ADP-ribosylation and results in the decrease of reduced glutathione (GSH) content. The depletion of GSH is thought to induce oxidative stress, and to result in apoptosis. Niacin itself has many physiological and pharmacological functions in various organisms. Niacin related compounds such as PA, dipicolinic acid, and isonicotinamide have been found to induce apoptosis in HL-60 cells, while niacin itself did not. In particular PA acted as an inducer of apoptosis, although it is a natural metabolite in a side pathway of NAD biosynthesis from tryptophan in animals and exists in various organisms as a natural component (Ogata *et al.*, 2000). It may be possible that FA induces apoptosis in cells in a similar way as it is a structural analogue of PA.

1.7 APOPTOSIS

Apoptosis or programmed cell death, is derived from the greek word for "falling off" of petals from flowers or leaves from trees. This sequential death process was observed to occur in two discrete stages. In the first phase the cell undergoes nuclear and cytoplasmic condensation, eventually breaking up into a number of membrane-bound fragments containing structurally intact organelles. The second phase involves the phagocytosis and degradation of these apoptotic bodies by neighbouring cells. Apoptosis is thus a basic physiological process that plays a major role in the regulation of cell populations (Schwartzman and Cidlowski, 1993).

The earliest morphological changes during apoptosis were elucidated using light and electron microscopy. Apoptosis characteristically affects single cells or small populations of cells in an asynchronous fashion. The earliest ultrastructural changes of apoptosis include the loss of cell junctions and other specialized plasma structures such as microvilli and desmosomes. The cell undergoes a period of blebbing and contortion that is dramatically visualised in time lapse cinematography. An irreversible condensation of cytoplasmic organelles and condensation of the nuclear chromatin to form dense granular caps or toroidal structures underlying the nuclear membrane. Nuclear pores disappear from the membrane subjacent to these chromatin condensations whilst, within the nucleus the proteinaceous fibrillar centre of the nucleolus separates from its surrounding shell of osmiophillic transcription complexes. The cell then splits into a cluster of membrane bound bodies each containing a variety of organelles. The organelles found within these membrane bounded bodies are highly conserved although at times it is possible to identify side to side aggregates of cytoskeletal microfilaments and semi crystalline

associations of ribosomes (Wyllie, 1997). The apoptotic bodies produced, vary greatly in size and the numbers produced by the dying cell is proportional to the size of the dying cell. Apoptotic bodies are rapidly phagocytosed by neighbouring cells. These phagocytosing cells are usually members of the monocyte phagocyte system but can also be normal epithelial cells, vascular endothelium, or tumour cells. Once ingested apoptotic bodies are rapidly digested. In cases where the apoptotic bodies are not subjected to phagocytoses they are extruded into an adjacent lumen. These apoptotic bodies exhibit progressive dilation and degradation of cytoplasmic organelles, a process that is termed secondary necrosis (Schwartzman and Cidlowski, 1993).

The features that characterize apoptosis sharply contrast those of necrosis. Here the dying cell swells, cytosolic as well as nuclear structures alter, but the general disposition of hetero and euchromatin is maintained, as are the nuclear pores. The plasma membrane ruptures and the cytosolic contents are expelled into the extracellular space, where some of these elicit an inflammatory response (Schwartzman and Cidlowski, 1993).

1.7.1 Apoptosis and cytotoxins

Most xenobiotics attain lethal cytotoxicity according to concentration. Almost without exception toxins induce death by apoptosis even though this may occur through completely disparate mechanisms. The key in determining whether a compound/toxin induces apoptosis depends on the morphological features of the cell. The fact that a cell undergoing apoptosis is followed by a series of conserved morphological changes is perhaps not as important as the genes. The genetic approach of studying apoptosis lends insight into the mechanistic understanding of why some cells die readily and others do not (Thompson, 1995).

Analysis of the morphology of toxin induced cell death may sometimes be confounded *in vitro* and *in vivo* by kinetic considerations. Early death of cells *in vitro* and *in vivo* may render cells incapable of retaining their membrane integrity and therefore rapidly expressing the appearance of necrotic rather than apoptotic cells. In the absence of distinct morphological evidence, particularly *in vivo*, a test of whether a toxin induces apoptosis as defined as a programmed cell death is whether the amount or kinetics of cell death is genetically modulatable without varying the amount of toxin-induced damage accumulated. Intensive studies have been conducted on the intestinal tract regarding the induction of apoptosis by cytotoxins *in vivo* (Hickman and Boyle, 1996).

The degree and amount of damage delivered are the ultimate determinants of the final fate of the cell. The cytotoxic effect that a toxin has on a cell is related to the dose. This statement is a composite of three assumptions :

- i) a molecular receptor exists to which the chemical reacts to produce the response.
- ii) the response achieved and the degree of the response are related to the concentration of the agent at the receptor site.
- iii) The concentration at the site is directly related to the dose administered.

The cell receiving a toxic insult is however not a passive recipient. A cellular response to a stimulus is induced so that homeostasis can be restored to the organism. This process may involve a number of endpoints, only one of which is actually death. The manner in which numerous cell types respond to the same level of toxin- receptor interaction and engage particular endpoints is different. There are essentially two phases to the response.

- i) the first involves the events at the receptor site which may involve the level of a specific enzyme inhibition or the degree of DNA damage.

ii) the second involves the cells homeostatic adjustment to the resulting stimulus.

At a specific point in time damaged cells "commit" to a particular pathway.

1.7.2 Sensing toxin induced damage

Cells clearly possess the ability to sense damage. The most prominent of these sensors regards protein damage which initiates a heat shock response and DNA damage which initiates repair (Friedberg, 1996).

Components of the plasma membrane are instrumental in sensing and activating signalling pathways which are normally associated with ligation by cytokines and growth factors (Canman and Kastan, 1996). The Jun kinases (JNK) are one such pathway that mediate the transcriptional activation of the immediate early genes c-jun and c-fos. Toxins may induce the synthesis of ceramide via stimulation of ceramide synthase or activation of a sphingomyelinase which directly stimulates an apoptotic signalling cascade (Verheij *et al.*, 1996). This in itself is an indication that membranes are capable of sensing a vast array of toxins.

Cytotoxic damage of cells *in vitro* initiates the transcription of a variety of genes leading to growth arrest with associated stimulation of repair.

1.7.3 Modes of protection against toxin induced death

One of the major determinants of a cells survival potential is the expression of the bcl-2 family of genes. The cellular threshold for death is thought to be potentiated by the balance between pro and anti-apoptotic proteins, such as bax and bcl-2, respectively (Yang and Korsmeyer, 1996). Toxins regulate the expression of these proteins in some cell types. Some studies have demonstrated that genotoxic activation of p53 increased the

synthesis of bax in some cells. This is probably due to a p53 transcriptional activation site on the bax gene promoter (Miyashita and Reed, 1995).

Studies have demonstrated that ligation of CD40 on B-cells enhanced the cells clonogenic survival advantage after genotoxic insult. This is probably the result of CD40 induced upregulation of the expression of bcl-x_l, a suppressor of apoptosis. This illustrates the fact that a cells trophic environment is instrumental in determining its fate after encountering a toxic insult, mainly by modulating the endogenous survival threshold. Over expression of bcl-2 and bcl-x_l varies the kinetics of the onset of toxin induced apoptosis. These studies involve the toxicity of cytotoxic anti-tumour drugs with vastly disparate mechanisms of action. Over expression of these two proteins promote pleotropic drug resistance (Hickman and Boyle, 1996).

Although experiments involving the over expression of bcl-2 in a B-cell lymphoma line exhibited no effect on the damage by 5-fluorodeoxyuridine, it significantly delayed the onset of apoptosis (Fisher *et al.*, 1993). This study questions the assumption that the toxicity of an agent is defined by the amount of toxin induced damage.

Conflicting *in vitro* data exists regarding the effects of the bcl-2 protein, indicating on one hand that expression of bcl-2 provides long term survival to lymphoid cells treated with radiation or cytotoxins (Strasser *et al.*, 1993) while fibroblasts are provided with no long term survival after treatment with amphidocolin (Yin and Schimke, 1995). Bcl-2 expression may therefore actually serve to delay the onset of apoptosis rather than promote long term survival in some cells. Bcl-2 expression then may actually "buy" sufficient time for the toxin-treated cell to upregulate mechanisms of defence against

particular classes of toxins which can initiate gene amplification (Yin and Schimke, 1995).

Experiments need to be conducted to establish that the endpoints recognized by toxicologists can be related to changes in the patterns of apoptosis brought about by manipulation of the respective genes. An important question that has arisen concerns the relevance of performing and extrapolating data from toxicity experiments *in vitro* where a fixed tropic environment is defined as opposed to a heterogeneous one *in vivo*.

1.7.4 Bcl-2

The *bcl-2* gene codes for a 25-26 kDa protein. The C-terminal 21 amino acids encode a stretch of hydrophobic amino acids that are required for insertion into membranes. This ability to insert into membranes is closely associated with the regulation of apoptosis. Bcl-2 is found on the mitochondrial outer membrane, the nuclear membrane and the endoplasmic reticulum. Majority of the protein is found on the cytosolic face of the endoplasmic reticulum.

Gene deletion experiments have shown that *bcl-2* is important during development and in adults. Bcl-2 knockout mice survive embryonic development but die later as a result of massive involution of the thymus and the spleen and polycystic kidney disease (Veis *et al.*, 1993). Bcl-2 deficient mice however die during embryonic development. This death is attributable to massive apoptotic cell death in developing nervous and haematopoietic cells. Bax deletion does not result in embryonic death but is characterized by sterility in males and an increase in thymocytes and splenic B-cell numbers (Knudson *et al.*, 1995).

The *bcl-2* family can be defined by three or four regions with extensive amino acid sequence similarity (homology regions BH1-BH4) (Strasser *et al.*, 2000). Nine members

of the family have been identified in mammalian cells. One of the first bcl-2 homologues to be identified was the gene bax which contains the signature BH1, BH2 and BH3 domains in addition to the C-terminal transmembrane domain. Overall, bax is 45% homologous to bcl-2. Over expression of bax committed the cell to apoptosis and antagonizes the proteolytic effect of bcl-2. Formation of bcl-2/bax heterodimers are thought to be an important point of control in apoptosis. Another member of the family that commits the cell to apoptosis is bak (Brown, 1997).

Experiments have revealed that bcl-2 appears to prevent the signal that normally activates the apoptosis machinery after DNA damage from reaching its target. There are instances where bcl-2 is incapable of protecting the cell against apoptosis, such as apoptosis induced by the T-cell protease granzyme B (Brown, 1997).

1.7.5 Ionic regulation

Evidence exists that bcl-2 is capable of regulating intracellular Ca^{2+} levels. It has been shown to stabilize the calcium gradient between the cytoplasm and the endoplasmic reticulum. Apoptotic suppression by bcl-2 is correlated with the regulation of nuclear and cytosolic Ca^{2+} (Lam *et al.*, 1994).

1.7.6 Caspases

Most morphological changes that occur during apoptosis are caused by a set of proteases. These death proteases share a great degree of homology and are part of a large protein family known as the caspases (for cysteine-containing aspartases) (Hengartner, 2000). In mammals more than a dozen genes code for these caspases with a cysteine-containing active site and a predilection for cutting peptides on the carboxy-terminal side of an aspartic acid residue in a 4-amino acid motif (Wyllie, 1997).

The caspases are responsible for selectively cleaving a restricted set of target proteins, usually at one, or at most a few positions in the primary sequence (always after an aspartate residue). In addition to cleaving proteins and inactivating them, caspases can activate proteins directly by inactivating a regulatory domain (Fig 8). Caspases are responsible for activating the nuclease responsible for the formation of the famous nucleosomal ladder during apoptosis. It has been demonstrated that the DNA ladder nuclease known as caspase activated Dnase (CAD) pre-exists in living cells as an inactive complex with an inhibitory subunit, dubbed ICAD. Caspase activated Dnase activity is mediated by caspase-3-mediated cleavage of the inhibitory subunit, resulting in the release and activation of the catalytic subunit. Caspase cleavage of the nuclear lamins results in nuclear shrinking and budding (Buendia *et al.*, 1999). Disintegration of the overall cell shape is probably due to the cleavage of cytoskeletal proteins such as fodrin and gelsolin (Kothakota, 1997). The active blebbing that occurs in apoptotic cells is due to caspase mediated cleavage of PAK2, a member of the p21-activated kinase family (Rudel and Bokoch, 1997).

1.7.7 Caspase activation

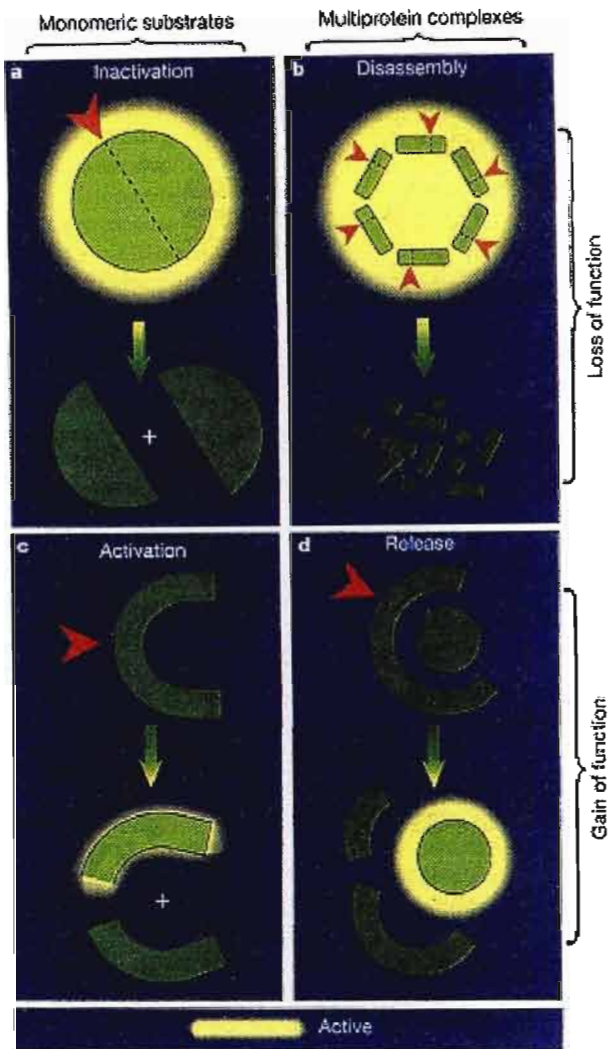


Figure 8 The nature of the substrate and the exact position of the cleavage site in the primary sequence can lead to diverse results by caspase action. The simplest or most common outcome is the loss of biological activity (panels a and b in the figure opposite). Limited proteolysis by caspases can also result in a gain of biological activity (panels c and d) (Hengartner, 2000).

Like most proteases, caspases are synthesized as inert zymogens. These zymogens are made up of three domains: an N-terminal prodomain, and the p20 and p10 domain, which are found in mature enzymes. Caspases exhibit three general modes of activation (Fig. 9). The simplest mode of procaspase activation is exposure to another previously activated caspase molecule. This so-called caspase activation is extensively utilized by cells for the activation of the three short prodomain caspases, caspase -3, -6 and -7. These are the

three main effector caspases and are regarded as the workhorses of the caspase family. Although the caspase cascade is a useful method to amplify and integrate pro-apoptotic signals, it does not explain how the initial most upstream caspases gets activated.

Caspase 8 is the key initiating caspase in the death receptor pathway. Once ligand binding occurs death receptors such as CD95 (Apo-1/Fas) aggregate and form membrane bound signalling complexes. The complexes formed then recruit using adapter proteins, several molecules of procaspase-8, resulting in a high local concentration of zymogen. The close proximity of these molecules mediates the low intrinsic protease activity of procaspase-8 the activity of which is sufficient to allow the various proenzyme molecules to mutually cleave and activate each other (Fig. 9) (Hengartner, 2000).

Caspase-9 represents a much more complex mechanism of activation. Its effect is exerted in association with a dedicated protein cofactor, Apaf-1 (Fig. 9). Effector caspases are usually activated proteolytically by an upstream caspase, whereas initiator caspases are activated through regulated protein-protein interactions. Along with cytochrome-c, Apaf-1 was identified biochemically as a protein required for caspase-9 activation (Hengartner, 2000).

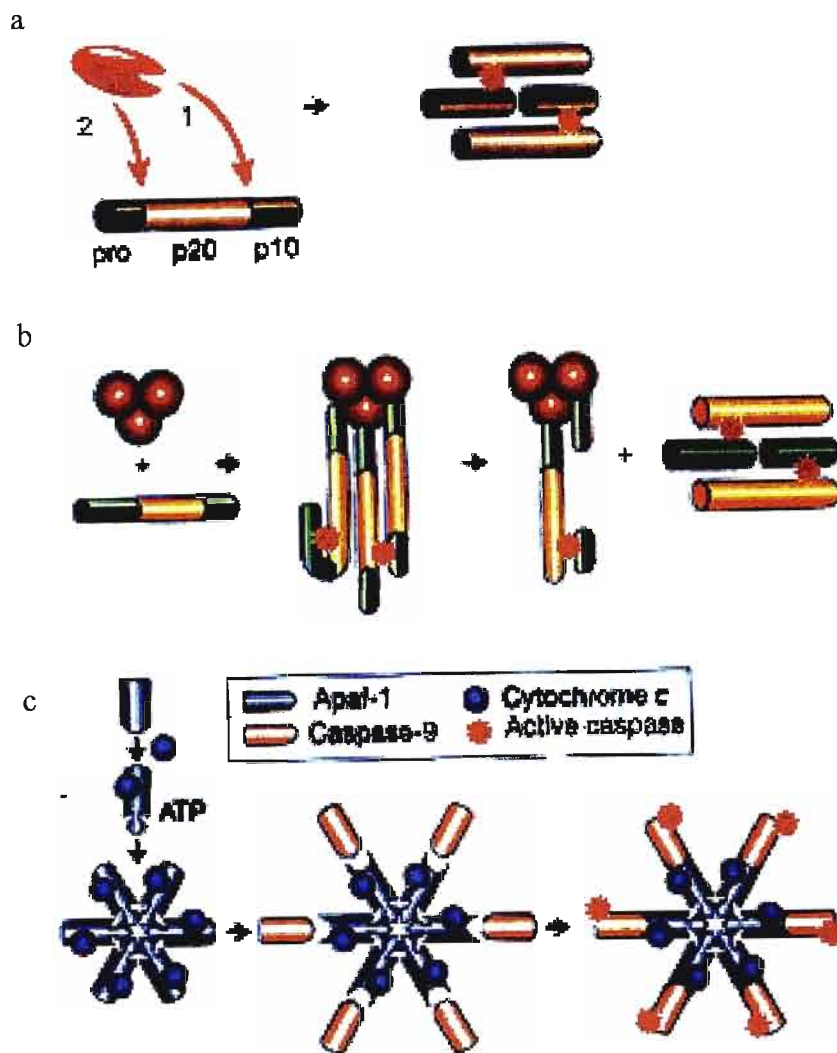


Figure 9 The three modes of caspase activation a) proteolytic cleavage by an upstream caspase which is straightforward and effective, b) induced proximity involves recruitment or aggregation of multiple procaspase-8 molecules into close proximity somehow causing cross-activation, and c) holoenzyme formation where cytochrome c and ATP-dependent

oligomerization of Apaf-1 allows recruitment of procaspase-9 into the apoptosome complex (Hengartner, 2000).

1.8 Apoptosis and the mitochondria

Several competing hypotheses have been proposed to explain the regulation of cytochrome c release by bcl-2 (Fig. 10). None of these have been proven. Three plausible models have been advanced (Hengartner, 2000).

1.8.1 The formation of channels by the Bcl-2 family to facilitate protein transport

It has been suggested that the bcl-2 proteins might act by inserting, following conformational change, into the outer mitochondrial membrane, forming channels or even large holes. Bcl-2 family members can insert into synthetic lipid bilayers, oligomerize, and form channels with discrete conductance's (Reed, 1997).

1.8.2 The interaction of Bcl-2 with other proteins to form channels

Proapoptotic bcl-2 family members may recruit other mitochondrial outer membrane proteins into forming a large pore channel. A key player in this regard is the voltage dependent anion channel (VDAC), as several bcl-2 family members can bind to it and regulate its channel activity. The channel formed by VDAC is small and therefore it is assumed that it undergoes significant conformational change upon binding to bcl-2 family members (Hengartner, 2000).

1.8.3 Bcl-2 family members may cause rupture of the mitochondrial membrane

Mitochondrial homeostasis may be under the control of bcl-2 family members. Apoptosis signals alter mitochondrial physiology such that the organelle swells resulting in the rupture of the outer membrane and the release of inter-membrane proteins into the cytosol. Bcl-2 members may influence mitochondrial homeostasis directly via the

proposed intrinsic ion-channel activity mentioned earlier or indirectly, through the modulation of other mitochondrial proteins. A key player in this regard is VDAC, as it is a subunit of the mitochondrial permeability transition pore (PTP), a large channel, the opening of which results in rapid loss of membrane potential and organelar swelling. Opening of PTP rapidly leads to cytochrome c release and apoptotic cell death.

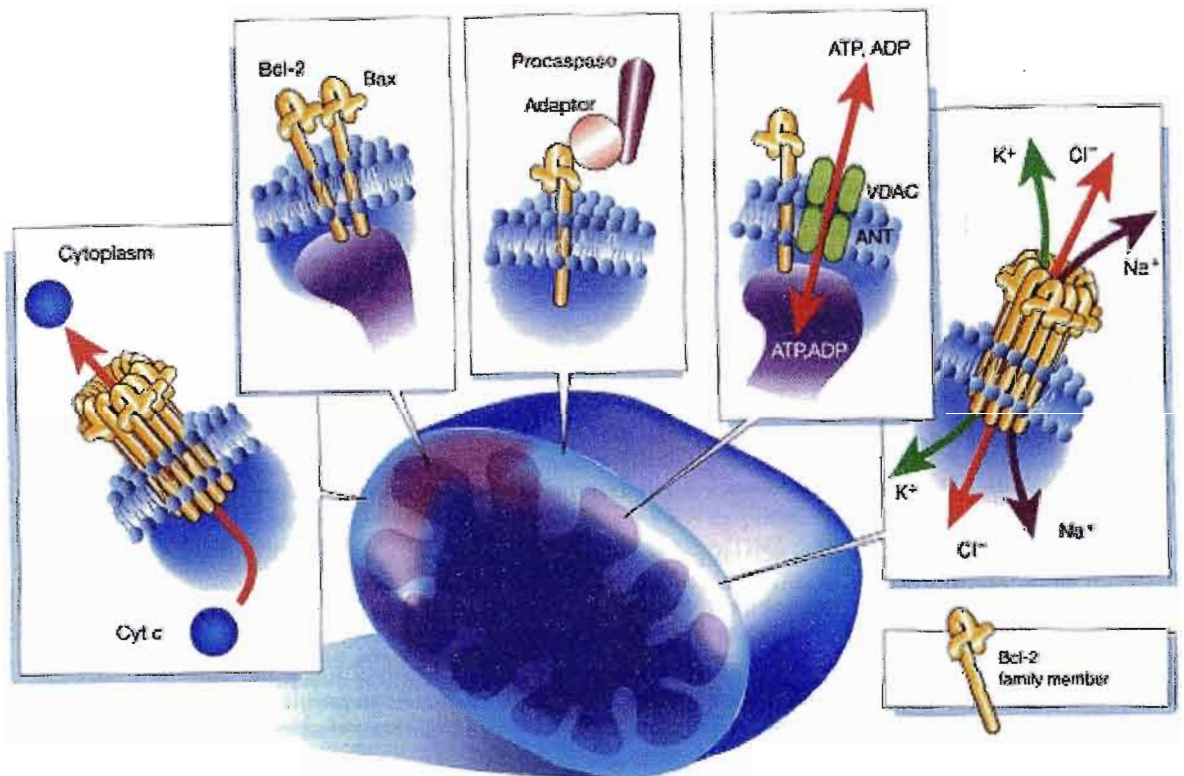


Figure 10 Various proposed mechanisms of bcl-2 action:

- The formation of a pore, through which cytochrome c and other proteins can escape.
- Heterodimerization between pro- and anti-apoptotic family members. Dimerization is achieved when the BH3 domain of one molecule binds into a hydrophobic pocket formed by the BH1, BH2 and BH3 domains of another family member.
- Direct regulation of caspases via adaptor molecules.
- Interaction of other mitochondrial proteins, such as VDAC to generate a pore for cytochrome c exit, or to modulate mitochondrial homeostasis.
- Oligomerization to form a weakly selective ion channel (Hengartner, 2000).

Apoptosis induced by death receptors bypass the mitochondrial pathway. In this case the apoptotic death is insensitive to bcl-2 protection and cytochrome c release into the cytosol is likely to be a result of caspase activation, rather than its cause.

The mitochondria actually possesses an arsenal of pro-death denizens. Amongst these are AIF (a flavoprotein with potent but relatively mysterious apoptotic activity), Smac/Diablo, and several procaspases. The induction of many of these death-promoting molecules might be necessary to insure swift and certain death (Loeffler and Kroemer, 2000).

The release of pro-apoptotic factors from the mitochondria does not necessarily result in apoptotic cell death. Cells can occasionally be rescued after this insult of pro-apoptotic death factors. Mammals, the fruit fly *Drosophila* and some viruses possess caspase inhibitors, known as the inhibitors-of-apoptosis (IAP) Smac (for second mitochondria-derived activator of caspases) or Diablo (for direct IAP-binding protein with p1) were recently identified IAP inhibitors. Smac/Diablo bind to IAP's and neutralize their anti-apoptotic activity. These anti-apoptotic bcl-2 family members can be seen as buffers that minimize accidental release of mitochondrial contents (Hengartner, 2000).

1.9 CD95 and apoptosis

Apoptosis is an important form of death in the immune system. In the immune system death involves the death receptor/death ligand system (Krammer, 2000).

The signalling transduction involved in death are part of a subset of tumour necrosis factor receptor (TNF-R). Members of this family are characterized by one to five cysteine-rich repeats in their extracellular domains, and a death domain in their cytoplasmic tail. The death domain is an integral part the transduction of the apoptotic

signal. CD95 is a glycosylated cell surface molecule of relative molecular mass 24 500-52 000 (335 amino acid residues). It is a type one transmembrane domain receptor. Apoptosis induced by CD95 occurs via its natural ligand CD95, which is a TNF related type two transmembrane molecule and expressed in a far more restricted way than the receptor. Cytotoxic T lymphocytes remove, for example, virus infected cells, and those that express CD95L can do so by interacting with the CD95 receptor on their targets (Fig 11). Some cytotoxic T lymphocytes kill target cells by activating the death receptor while others use perforin and granzyme-B (GrB) to eliminate infected cells. Perforin facilitates the path of GrB through the target cell allowing it to directly cleave and activate caspase-8 (Medema, 1997).

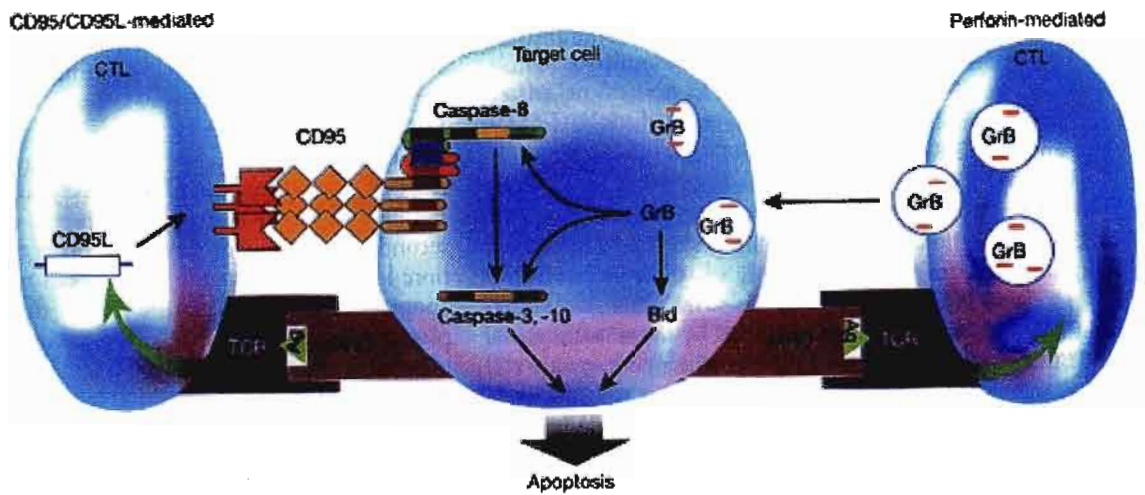


Figure 11 Cytotoxic T lymphocytes can kill target cells by the CD95 (yellow)/CD95L (red) system (left) or by the perforin/granzyme B (Grb) system (right). CD95 signalling involves a caspase cascade. GrB cleaves and activates caspases in target cells. The target cell dies by apoptosis through either a CD95 or a GrB signalling event (Hengartner, 2000).

1.9.1 CD95 Signal transduction

Oligomerization or most probably trimerization of CD95 is required for the transduction of the apoptotic signal. Numerous proteins associate with activated CD95. This so called death inducing signalling complex (DISC) forms within seconds of receptor engagement. Initially the receptor FADD (Fas-associated death domain protein, also known as Mort 1) binds via its own death domain to the death domain in CD95. One of the domains of FADD is the death effector domain (DED) and via a process of homologous interaction, employs the DED-containing procaspase-8 (also known as FLICE) into the DISC (Krammer, 2000).

Following this, procaspase-8 is activated proteolytically and active caspase -8 is released from the DISC into the cytoplasm in the form of a heterotetramer containing two small

subunits and two large subunits. One of the main targets of active caspase-8 is procaspase 3 which initiates the activation and execution of the complete cell death programme (Krammer, 2000).

CHAPTER 2

2. Cytotoxicity testing : Methyl thiazole tetrazolium assay

A requirement of most biological assays is the measurement of surviving and/or proliferating mammalian cells. Over the years numerous methods have been employed to achieve this, eg., counting cells that include/exclude vital dyes, measuring released Cr-labelled proteins after cell lysis, and measuring incorporation of radioactive nucleotides ([³H] iododeoxyuridine) during cell proliferation). The advantage of cytotoxicity assays that utilize multiwell scanning spectrophotometry is that they can measure large numbers of samples with a high degree of precision (Mosmann, 1983).

Colorimetric assays for living cells, usually utilize a colourless substrate that is modified to a coloured product by a living cell, but not by dead cells or tissue culture medium. A range of tetrazolium salts are useful for this purpose, because they measure the activity of various dehydrogenase enzymes (Slater *et al.*, 1963). The tetrazolium ring is cleaved in active mitochondria, and so the reaction occurs only in living cells (Fig 12).

This study made use of a modified version of the methylthiozol tetrazolium (MTT) assay first used by Mosmann (1983). The assay is based on the tetrazolium salt MTT (3-(4,5-dimethylthiozol-2-yl)-2,5-diphenyl tetrazolium bromide) that measure only living cells and can be read on a scanning multiwell spectrophotometer (ELISA reader). The MTT salt is yellow in aqueous solution at neutral pH and is reduced by mitochondrial dehydrogenases, such as succinate dehydrogenase, of metabolically active cells to insoluble blue formazan crystals. The resulting crystals are then solubilized with dimethyl sulphoxide (DMSO) and quantitated spectrophotometrically (595nm). The amount of formazan crystals generated by the cells gives an indication of the number of

metabolically active surviving cells. The absorbance is directly proportional to the number of viable cells.

The assay has proved to be useful in testing the toxicity of various mycotoxins on various cell lines. The technique makes use of 96 well plates that are useful in assessing a number of concentrations of mycotoxins simultaneously. The aim of this study was to evaluate the cytotoxic effect of FA on human lymphocytes.

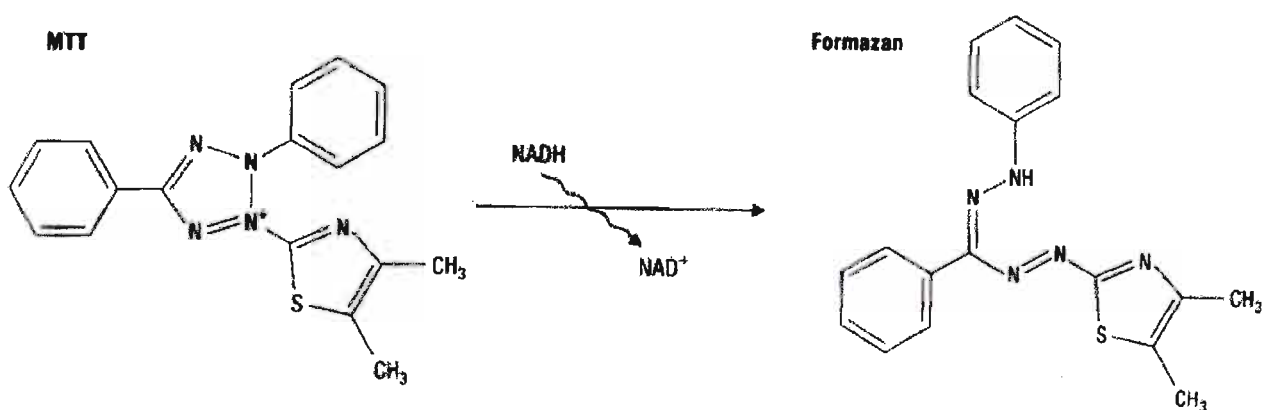


Figure 12 Cleavage of the tetrazolium ring in the MTT salt.

2.1 Materials and method

2.1.1 Materials

The chemicals were purchased from the following suppliers :

MTT salt from Sigma Chemical Co. Ltd., US; DMSO from Merck; Eagles minimum essential media, L-glutamine, penstrep fungizone and L-glutamine from Sterilab Laboratories, fusaric acid from Acros.

2.1.1.2 Cell culture media

RPMI 1640, (pH 7.2-7.4), containing L-glutamine and a combination of inorganic salts, glucose, amino acids and vitamins, was used to culture normal lymphocytes.

Foetal calf serum (FCS) (heat inactivated) was required as an additional nutrient source as RPMI was insufficient to sustain cells alone. Foetal calf serum (5-10%) (v/v) was added to RPMI (100ml) to make up complete culture media (CCM). To counteract the problem of microbial contamination of media penstrep fungizone (1ml) was added to the CCM.

Ethical approval (Ref. H030/02) was obtained for this study from the Faculty of Health Sciences, Nelson R. Mandela School of Medicine, University of Natal.

2.1.2 Methods

2.1.2.1 Lymphocyte isolation

All lymphocyte isolations were carried out in the laminar flow (Labotec) containing a UV light. The unit was swabbed with 70% alcohol before isolations were carried out. Sterile latex gloves were used at all times. Sterile conditions were maintained at all times. Whole blood 4ml was collected in lithium heparin Vacutainer tubes by venopuncture from a healthy donor. The 4ml of whole blood was diluted to 10ml using phosphate buffered saline (PBS). Diluted blood was then carefully layered horizontally onto 5ml of histopaque in a sterile 15ml Sterilin tube. Samples were then centrifuged for 30 minutes at 1500 rpm at 25°C. The resulting cell interface/buffy coat layer was separated using a sterile pasteur pipette. The buffy coat layer was then pipetted into a new Sterilin tube, topped up to 10ml with PBS and then centrifuged down at 1500 rpm at 4°C for 5

minutes (1st wash). The supernatant was then decanted and the pellet resuspended in the residual fluid of PBS. The tube was then topped up to 10ml with PBS and again centrifuged at 1500 rpm at 4°C for 5 minutes (2nd wash). The resultant supernatant was discarded and the pellet was resuspended in the residual fluid of PBS.

2.1.2.2 Cell counting and viability

Trypan blue was used as an exclusion dye for viable cell counting. Cell counts were carried out in disposable haemocytometers. An average of 4.5×10^6 lymphocytes was obtained for each 4ml of blood processed.

2.1.2.3 Preparation of the MTT salt

The MTT salt 5mg was dissolved in HBSS (1ml) to give a concentration of 5mg/ml. The suspension was filtered through a 0.45µm filter to remove insoluble residues of MTT salt.

2.1.2.4 Lymphocyte treatments

The lymphocytes (50 000 per well with CCM) were plated in a 96-well tissue culture plate (100µl cell suspension per well). Fusaric acid was dissolved in sterile distilled water and made up to a stock solution of a 2000µM in CCM. Cell suspensions were treated with a range of serial dilutions and made up to final concentrations ranging from 3-1000µM. Ten replicates were used for each concentration. After a 24 hour incubation period at 37°C the plates were spun down and the supernatants removed and replaced with 10µl of MTT (5mg/ml) and 100µl CCM and incubated for a further 4 hours at 37°C. After this incubation period the supernatant was removed and 100µl of DMSO was added to each well to solubilize the resulting formazan crystals. After an hour of incubation the optical density was determined spectrophotometrically using a Bio-Rad

plate reader at 595 nm and a reference wavelength of 655 nm. Absorbance was expressed as percentage cleavage activity as follows:

$$\% \text{ Cleavage activity} = \frac{\text{Mean of absorbance of toxin-treated cells}}{\text{Mean of absorbance of control}} \times 100$$

$$\% \text{ Mortality} = 100\% - \text{cleavage activity}$$

2.2 Results and Discussion

The cytotoxic effect of FA on healthy lymphocytes was evaluated. The various concentrations (3-1000 μ M) FA treated lymphocytes were all compared to the control values (Fig 13). Minimal cytotoxicity was observed at 3 μ M FA treatment with a 2% cell mortality ($p > 0.05$). Significant cytotoxicity did however occur at 6 μ M FA treatment with an 18% cell mortality ($p < 0.001$). Increases in the concentrations of FA treated lymphocytes caused substantial increases in cell mortality when compared to the controls. Table 1 indicates that the metabolic viability of lymphocytes was depressed in a dose dependant manner by FA. An increase in FA treatment of lymphocytes from 25-50 μ M caused no significant change in percentage cell mortality ($p > 0.05$). Similarly there was no significant change in percentage mortality between the 400 μ M and 1000 μ M concentrations ($p > 0.05$).

The principle mode of FA action is metal ion chelation. Apoptosis is modulated by intracellular excess or deficiency of Zn^{2+} . The major conclusions on Zn^{2+} metabolism are:

- i) Zinc deficiency, resulting from dietary deprivation or exposure of cells to membrane-permeable Zn^{2+} chelators induces apoptosis,

- ii) Cell cultures supplemented with Zn^{2+} can prevent apoptosis,
- iii) An intracellular pool of chelatable Zn^{2+} plays a critical role in apoptosis as it possibly modulates the activity of endonuclease (Fernandez Pol *et al.*, 2001).

Higher concentrations of FA treatments such as 400 μ M and 1000 μ M thus chelate more Zn^{2+} ions and increase cell death (ie. apoptosis).

TABLE 1 METABOLIC ACITVITY OF LYMPHOCYTES TREATED WITH FUSARIC ACID

Toxin	Mean absorbance	Mean cleavage activity	Mean % mortality
Control	0.188 - 0.001155		
3 μ M	0.184 - 0.001155 \otimes	98%	2%
6 μ M	0.155 - 0.0005774	82%	18%
25 μ M	0.145 - 0.0005774	77%	23%
50 μ M	0.140 - 0.001155	74%	26%
200 μ M	0.132 - 0.003215	70%	30%
400 μ M	0.108 - 0.006351	57%	43%
1000 μ M	0.105 - 0.006351	56%	44%

- Values are given as mean absorbance of three independent experiments with standard error of the mean. Mean cleavage and % mortality were calculated. All absorbance's of concentrations are significant at $P < 0.0001$ except those marked \otimes .

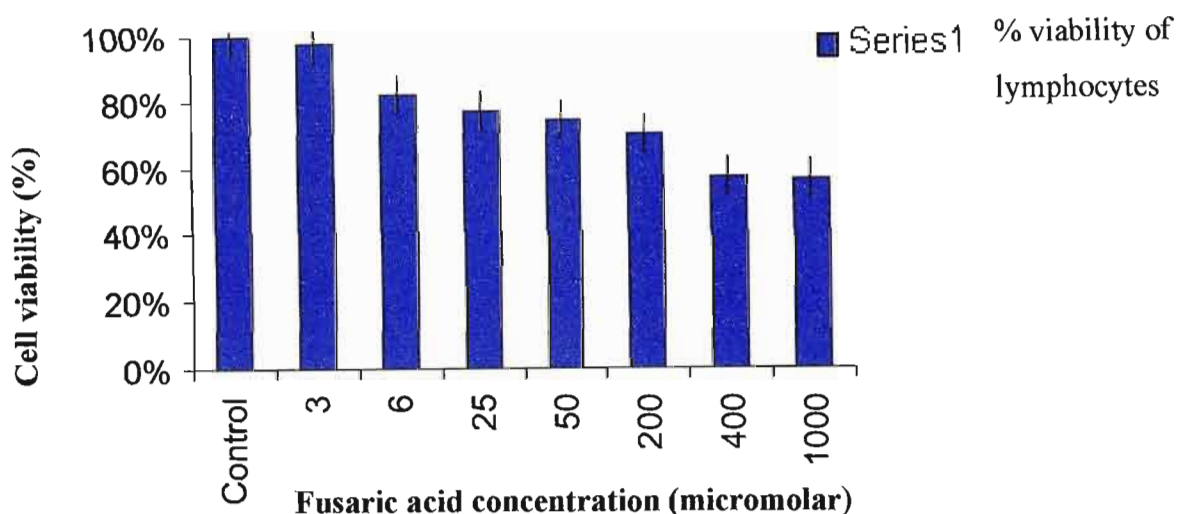


Figure 13 Mean percentage lymphocyte viability at various concentrations of FA.

In this study the cytotoxic effect of FA on healthy human lymphocytes was evaluated.

The use of the MTT salt is an efficient means for assaying cell survival and proliferation.

The MTT salt is cleaved by all living metabolically active cells but not dead cells or erythrocytes. The formazan derived from this cleavage is directly proportional to the cell number over a wide range using a homogenous cell population. Cells that are active produce more formazan than cells that are at rest. This allows the measurement of activation even in the absence of proliferation (Mosmann, 1983).

The MTT salt is cleaved to formazan by the "succinate tetrazolium reductase" system which belongs to the mitochondrial respiratory chain and is active only in viable cells. It has been noted that mitochondrial electron transport may play a minor role in the cellular reduction of MTT. This is since most cellular reduction occurs in the cytoplasm and probably involves the pyridine nucleotide cofactors NADH and NADPH. It has been

cofactors NADH and NADPH. It has been demonstrated that most cellular reduction of MTT was dependant on the reduced pyridine nucleotides NADH and NADPH and not on succinate as had been previously believed. Cellular reduction of MTT was associated with enzymes of the endoplasmic reticulum and was more related to NADH production through glycolysis than to respiration (Slater *et al.*, 1963).

Whatever the case, FA has been postulated to affect both these areas of cellular activity. *In vitro* this mycotoxin inhibits certain metal containing enzymes for example cytochrome oxidase depolarising the plasma membrane while decreasing cellular ATP levels. It is believed that the protonophore activity of FA can uncouple oxidative phosphorylation and this decreases ATP synthesis or mitochondrial electron transport is directly inhibited at the cytochrome oxidase level by the toxin. In this manner FA may directly exert its effect in the amount of MTT cleavage taking place.

It has been postulated that the effect of PA on NRK cell growth inhibition is not a direct one, and it is possible that it may be converted into another molecule. Numerous pyridine derivatives are known to undergo an exchange reaction catalysed by NAD^+ to form the corresponding NAD^+ analogue. It is therefore believed that a similar derivative of picolinic acid may be the active species (Johnson and Fernandez-Pol, 1977).

Fusaric acid could act by metal ion chelation or by interference with NAD^+ metabolism or functions. Fusaric acid could possibly bind to and activate a specific protein-metal iron complex in a manner similar to the binding of nicotinic acid to leghaemoglobin. Numerous pyridine derivatives undergo an exchange reaction with the nicotinamide moiety of NAD^+ to form NAD^+ analogues. It is possible that FA could be incorporated into a similar molecule that is an active species (Fernandez-Pol *et al.*, 1977).

It is well known that FA is toxic for many prokaryotes and eukaryotes (Marasas, 1993). Results obtained clearly indicate that FA affects the metabolic viability of human lymphocytes *in vitro*. Its effect is especially pronounced at higher concentrations.

Chapter 3

3. Single cell gel electrophoresis (Comet Assay)

Techniques which permit the sensitive detection of DNA damage in studies of environmental toxicology are constantly sought after. The effects of environmental toxicants are often tissue and cell type specific and therefore require detection of DNA damage in individual cells (Singh *et al.*, 1988). The single cell gel electrophoresis (SCGE) or comet assay is a sensitive technique used to detect DNA damage in biological systems (Abd-Allah *et al.*, 1999). The detection of the DNA breaks are facilitated by alkaline electrophoresis of cells embedded in agarose and lysis by detergents of high salt concentration (Vijayalaxmi *et al.*, 1992). DNA breaks migrate in the direction of the anode producing an image resembling that of a comet. Furthermore in addition to measuring DNA strand breakage the alkali comet assay measures alkali labile sites of intermediates in base or nucleotide - excision repair (Gedik *et al.*, 1992, Green *et al.*, 1992). The sensitivity of the comet assay in the evaluation of DNA damage depends on accurate and reproducible measurement of DNA in the comet head and tail regions. Various experimental factors may influence the assay (Fig 14) (Olive *et al.*, 1992).

Single cell gel electrophoresis (SCGE) is an adaptation of techniques such as nucleoid sedimentation and the halo assay (Mckelvey-Martin *et al.*, 1993). The use of alkaline conditions (Singh *et al.*, 1988) makes the relationship with single stranded breaks (SSB's) more apparent. Single stranded breaks are measured by procedures that include treatment with high pH alkaline unwinding, alkaline elution and alkaline sucrose sedimentation.

Single stranded breaks can only be detected if the DNA base pairing is disrupted by alkali. Neutral pH does not seem to affect the long duplex molecule.

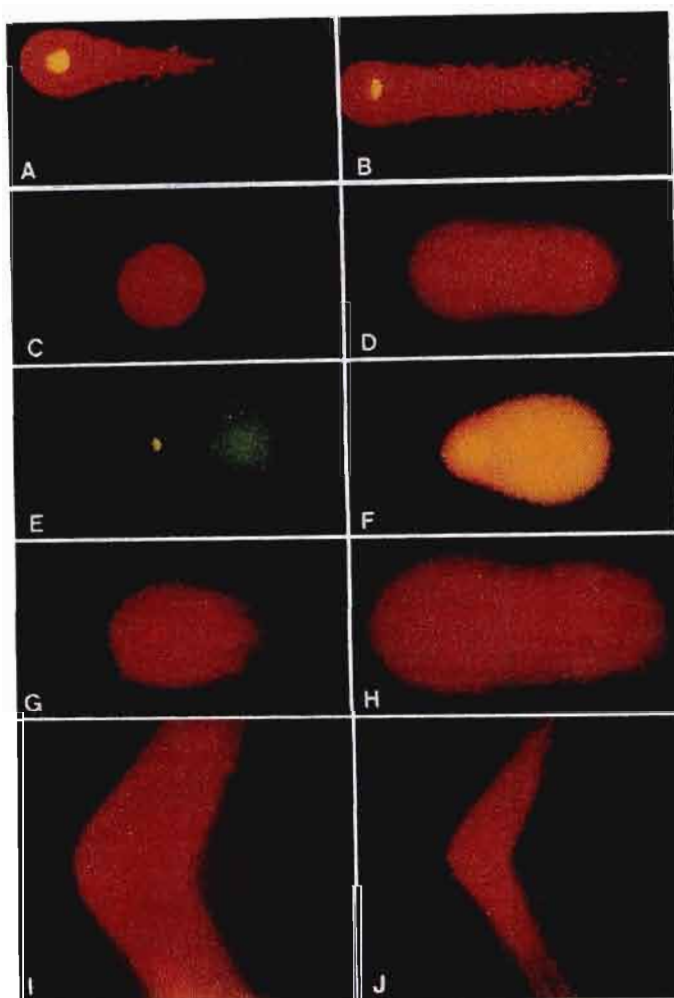


Figure 14 Fluorescence micrographs showing individual Chinese hamster V79 comets processed in the SCGE assay. (A, B) Alkaline lysis after 1 hour at room temperature in 0.03 M NaOH, 1M NaCl followed immediately by electrophoresis in TAE buffer at 4.5 V/cm for 12 minutes. Alkaline lysis after 1 hour at room temperature (0.03 M NaOH, 1M NaCl, 0.5% sarkosyl, pH 12.5) followed by rinsing for 1 hour and electrophoresis in 0.03M NaOH, 1mM EDTA at 0.6V/cm for 25 minutes. (E, F) Cells which were allowed to incorporate BrdUrd into DNA, then irradiated, lysed under alkaline conditions electrophoresed as in C and D, and incubated with fluorescein isothiocyanate-conjugated antibodies against BrdUrd alone (E) or with propidium iodide (F). (G, H) Neutral lysis at 50°C for 4 hours in 0.5% SDS, 30mM EDTA, pH 8.0, followed by rinsing and electrophoresis for 20 minutes at 0.6 V/cm. (I, J) Cells lysed under neutral conditions, then exposed to pulsed-field gel electrophoresis at 1.7 V/cm for 24 hours with a pulse time of 20 minutes. Each of the above frames is approximately 300µm wide and the anode is to the left for constant field gel electrophoresis (A-H) (Olive *et al.*, 1992).

DNA in the nucleus which is supercoiled and tightly packed can however be significantly influenced by SSB's occurring in the absence of alkaline treatment. Eukaryotic DNA (0.5-1m in length) has to be condensed 10^5 - fold to fit within a nucleus of 5-10 μ m diameter. Single stranded breaks induce a relaxed structure of DNA. The compromised DNA exhibit structural changes that are readily detected and quantitated by visual examination or by analysis of DNA sedimentation properties (Mckelvey-Martin *et al.*, 1993).

The SCGE assay offers many advantages in the detection of DNA damage. It allows the detection of intercellular differences in DNA damage and repair in virtually any eukaryote cell population obtainable in single cell suspension. The technique also gives an indication as to the degree of apoptosis occurring. The technique requires relatively small cell samples (between 1-10 000 cells) and results can be obtained rapidly (within a single day). The cost of performing the assay apart from image analysis is relatively low when compared to other assays (Mckelvey-Martin *et al.*, 1993).

The sensitivity of the SCGE assay in estimating damage in single cells is comparable to that of other methods which measure average damage to a population of cells (Olive *et al.*, 1992). The technique has been assessed by incubating permeable cells after UV irradiation with exogenous UV endonuclease and consequently examining the DNA breaks by alkaline SCGE and by alkaline unwinding. The sensitivity of the SCGE assay extends to the detection of less than 0.1 breaks per 10^9 daltons of DNA (Gedik *et al.*, 1992). The most frequently employed version of the SCGE assay is that of Singh *et al.*, (1988) in which the electrophoresis is performed at high pH. This serves to reveal alkali labile sites and frank breaks. Staining with ethidium bromide reveals increased extension

of the DNA from the nucleus in the direction of the anode in cells with increased DNA damage. Damaged cells thus have the appearance of comets, exhibiting brightly fluorescent heads and tails whose length and degree of fluorescence intensity are related to the number of DNA-strand breaks induced by respective test agents. Cells exhibiting no DNA damage appear as intact nuclei (comet heads) without tails.

3.1 Analysis of DNA breakage in the SCGE assay

Singh *et al.*, (1988) initially found that the tail length reflected the amount of breakage in a cell. Other researchers, however, found the tail length was constant over a range of DNA break frequencies of 1-14 per 10^{16} Daltons and the intensity of the fluorescence in the tail increases markedly with increased frequency of breaks (Gedik *et al.*, 1992). It was found that while length changes by only 2% over a 4-fold range of breakage, the fluorescence intensity in tails more than doubles (Olive *et al.*, 1992). In the neutral lysis method, and the optimized alkali method, voltage can be reduced 10-fold and the observable tail length is largely independent of radiation dose (Olive *et al.*, 1992).

3.2 Principles that determine the behaviour of DNA in the SCGE assay

High pH (pH 12 or above) provides conditions for the disruption of DNA base pairing and strands tend to separate. Unwinding of the DNA molecule occurs at the ends and also from SSB's.

The organization of DNA within the nucleus explains the behaviour of single cells undergoing electrophoresis. DNA exists as loops attached to a framework or nuclear matrix, and is negatively supercoiled by virtue of its organization in nucleosomes. Permeabilization of cells with detergent and extraction of nuclear proteins with high salt, leaves the DNA remaining within a residual nucleus-like structure, the nucleoid. Breaks

occurring in DNA leads to the relaxation of supercoiling and the loops. Instead of being constrained within the bounds of the nuclear matrix the DNA becomes free to extend outside. The key to DNA behaviour during electrophoresis is the release of supercoiling in a loop of DNA. That loop is then capable of extending towards the anode once an electrophoretic voltage is applied. Under alkaline conditions it is thought that DNA in the open loops denatures and becomes flexible, allowing fragments of higher order structure to be released from the nucleus, enabling the comet tail to develop (Mckelvey-Martin *et al.*, 1993).

3.3 Applications of the SCGE assay

The SCGE assay has found application in a number of *in vitro* and *in vivo* studies to assess DNA damage and repair induced by various agents in a variety of mammalian cells (Singh *et al.*, 1988, 1991; Olive *et al.*, 1992). The attributes of the SCGE assay highlight it as an assay of DNA breakage with widespread applications in DNA damage and repair studies, biomonitoring, genetic toxicology, and analysis of irradiated foods.

3.4 DNA damage and repair studies

The SCGE assay is particularly useful in the dissection of excision repair of DNA. Unlike seriously potent inducers of DNA damage, uv radiation does not induce significant DNA breakage. These DNA damaging agents producing bulky adducts are repaired by the process of nucleotide-excision repair. The use of the SCGE assay to measure incision breaks arising from UV irradiation have illustrated that human lymphocytes from xeroderma pigmentosum donors display very few breaks relative to normal donors and therefore suggest that this technique may offer a rapid diagnostic assay for xeroderma pigmentosum. The technique also lends insight into the repair defect in these cells

(Green *et al.*, 1992). For this latter purpose SCGE may also be used to study DNA damage and repair in repair deficient cell lines (Mckelvey-Martin *et al.*, 1993).

3.5 Biomonitoring

The SCGE assay has been successfully applied to biomonitoring studies. It has been used to screen lymphocyte samples from human populations for susceptibility to oxidative damage, UV and ionizing radiation (Singh *et al.*, 1988; Olive *et al.*, 1992; Green *et al.*, 1992). It has also been used in the evaluation of human lymphocytes to air pollutants (ozone and gasoline), contaminated water (arsenic and fluoride), and pesticides (Valverde *et al.*, 1999) and radiation induced damage in keratinocytes from primary and secondary cultures obtained from medium thickness skin biopsies and in epidermal cells, without culture, obtained from the same sample of skin biopsies of patients requiring skin grafts. These individuals were exposed to radiation accidents involving localized irradiations resulting mainly from improper handling of sealed sources of Co^{60} , Cs^{137} or Ir^{192} at workplaces for industrial gammagraphy and other radiation sources. The technique has been employed in the development of water pollution tests using the ciliated protozoan *Tetrahymena thermophila*. The work was modified for protozoan cells in order to perform genotoxicity tests biomonitoring of polluted surface waters and wastewater's in a simple reliable and economic manner (Fig 15a-d) (Lah *et al.*, 2001).

In the search of new human genotoxic biomarkers, the SCGE assay has been proposed as a sensible alternative. Human monitoring involves the use of biological or molecular markers as indicators to signal events in individuals exposed to environmental chemicals. Three specific types of biological markers are identified. The first type involves a biological marker of exposure. This may be the xenobiotic chemical itself, its metabolites or the product of an interaction between the chemical and its target biomolecule. The second is a marker of susceptibility, whether inherited or induced, which indicates that the individual is particularly sensitive to the effect of a xenobiotic or to the effects of a group of such

group of such compounds. The third type is a marker of effect, which may be an endogenous component, a measure of the functional capacity, or some other indicator of the organs, systems or body condition that might be affected by the exposure (Valverde *et al.*, 1999).

In this regard the SCGE assay has been successfully employed as a useful biomarker for early effects.

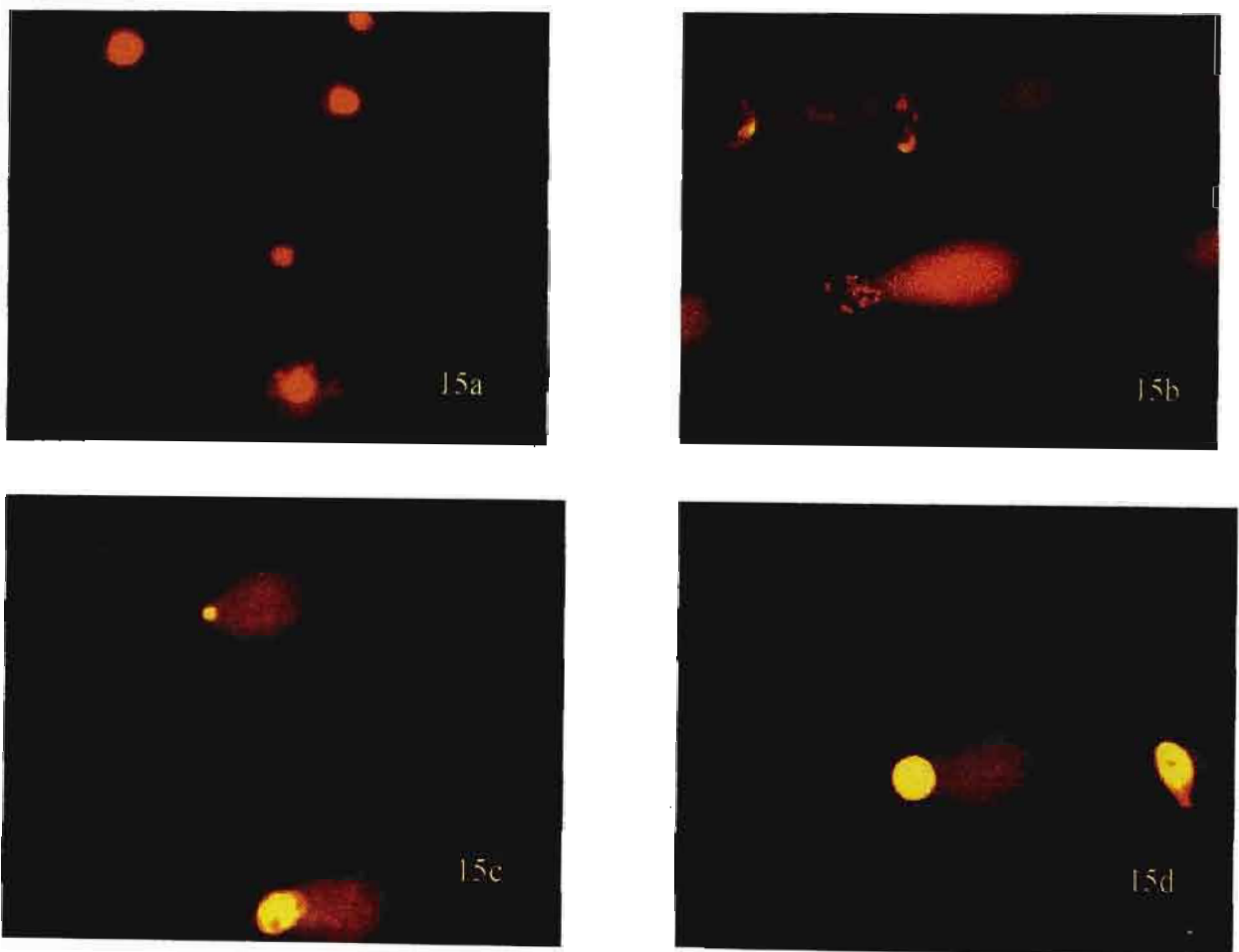


Figure 15a *Tetrahymena. thermophila* cells before cell lysis. 15b Cells centrifuged at $1000 \times g$ and then electrophoresed. 15c-d cells collected by natural sedimentation then electrophoresed (Lah *et al.*, 2001).

The SCGE assay has also been used to measure the DNA damage that occurs in human cells from individual and combined exposure to various recommended therapeutic AIDS

agents. Azidothymidine (AZT) has been noted to cause DNA damage in lymphocytes. Single cell gel electrophoresis detected these breaks and the concentration of AZT and time of exposure that was necessary to produce such damage (Fig 16 a-b).

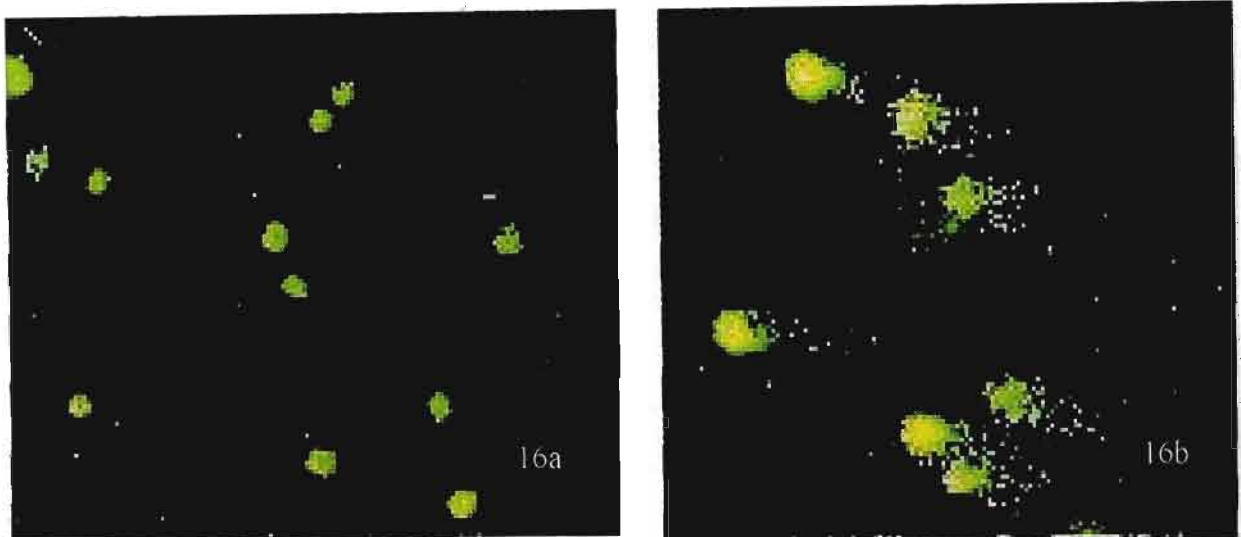


Figure 16a Untreated control cells. 16b Lymphocytes treated with AZT (Levin *et al.*, 1998).

3.6 Determination of Genotoxicity

The SCGE assay has proved to be sensitive in the assessment of genotoxic damage. Both cultivated cells in tissue culture as well as in primary cells in suspension culture can be studied for DNA damage. It is recommended that when performing the SCGE assay in genotoxicity, a few procedures for the evaluation of a test compound are required. Four doses, appropriate controls and two independent experiments should be performed. Viability measurements by trypan blue exclusion staining should be made (Mckelvey-Martin *et al.*, 1993).

The aim of this study was to evaluate the DNA damage caused by FA in healthy lymphocytes using the comet assay.

3.7 Materials and Method

3.7.1 Materials

The chemicals used in the experiments were purchased from the following suppliers :

Low melting point agarose (LMPA) and ethidium bromide from Roche biochemicals; Triton X from Sigma Chemicals USA; Tris and DMSO, EDTA, NaOH and NaCl from Merck.

3.7.2 Methods

3.7.2.1 Blood preparation and treatments

Whole blood 12ml was collected in EDTA Vacutainer tubes by venopuncture from 3 healthy donors. Volunteers (male) were age and sex matched. Lymphocytes were immediately isolated as before (described in chapter 2) and treated with various concentrations of FA (3 μ M, 6 μ M, 50 μ M and 100 μ M) and subsequently incubated at 37°C in a CO₂ water jacket incubator for 1 and 4 hours respectively.

3.7.2.2 Slide Preparation

The procedure described for the SCGE assay by Singh *et al* (1988) was followed with minor modifications (Fig 17) : 200 μ l of 0.75% LMPA at 37°C agarose was diluted in Ca²⁺ and Mg²⁺ free PBS buffer was added to frosted microscope slides, immediately covered with coverslips (18mm \times 18mm no.1 glass coverslip) and kept for 10 minutes in a refrigerator to solidify. Coverslips were subsequently removed and 10 μ l of lymphocytes (10⁴) mixed with 90 μ l of 0.5% LMPA at 37°C were added to the first layer. The slides were immediately covered with a coverslip and kept in the refrigerator 4°C for another 5 minutes to solidify the LMPA. The coverslips were again removed and a final top layer of 75 μ l of 0.5% LMPA at 37°C was added and again refrigerated for a further 5

minutes. Coverslips were then carefully removed and the slides were immersed in a trough of cold lysing solution (appendix 4) (2.5 M NaCl, 100mM EDTA, 1% Triton X-100, 1% Tris and 10% DMSO) which was freshly made up. Slides were kept at 4°C for 1 hour.

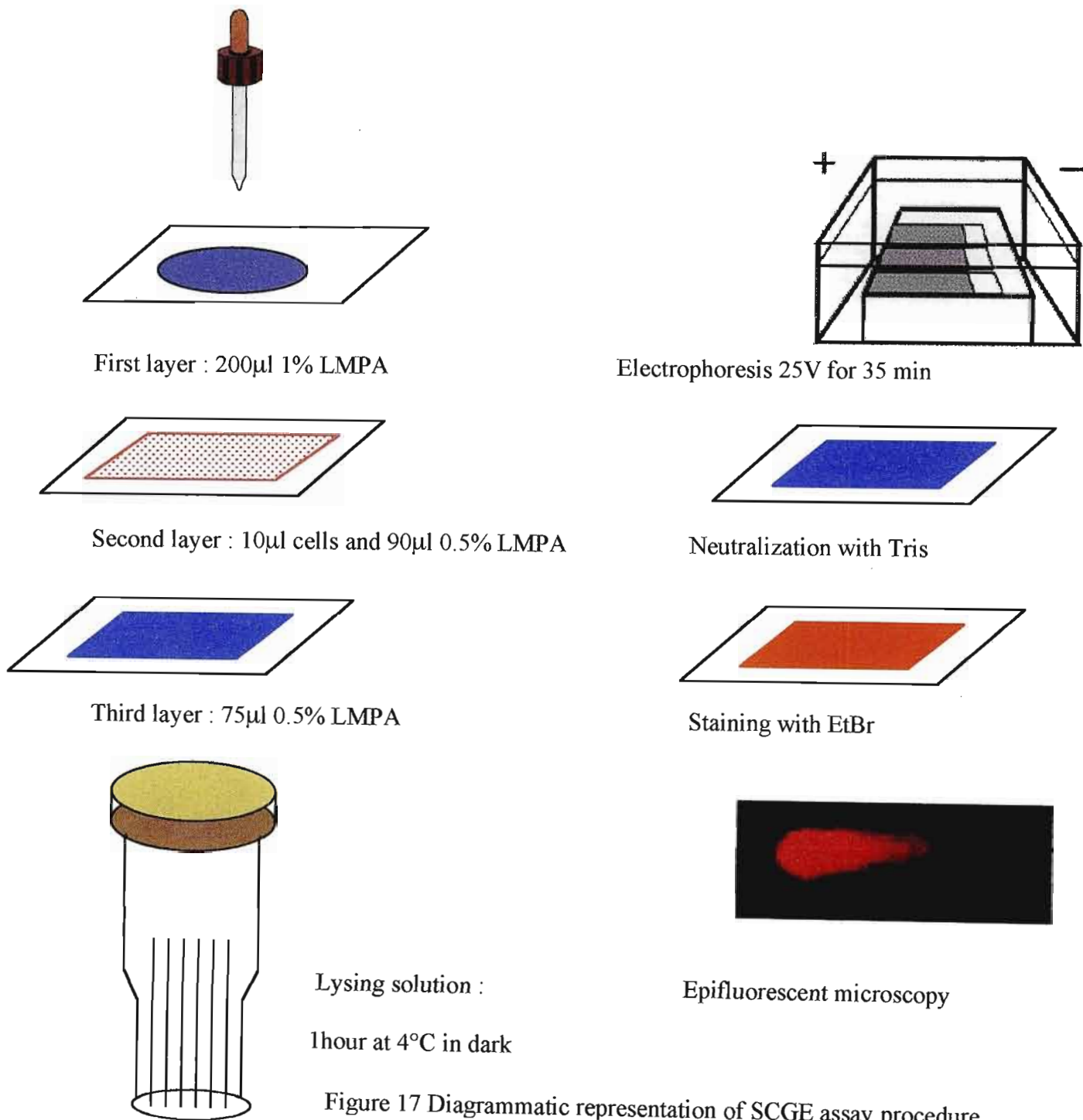


Figure 17 Diagrammatic representation of SCGE assay procedure.

3.7.2.3 Electrophoresis

After the lysis step the slides were removed and placed in an electrophoresis tank. The tank was carefully filled with freshly made alkaline buffer (appendix 5), 500ml (300mM NaOH and 1mM EDTA, pH 13.0) to a level of approximately 0.30 mm above the slides. Slides were allowed to stand in the electrophoresis buffer for 20 minutes to allow for DNA unwinding before electrophoresis. The slides were then electrophoresed at 300mA (25V) (Biorad compact power supplier) for 35 minutes at room temperature. The above steps were conducted in dim light to prevent any additional DNA damage.

3.7.2.4 Staining

After electrophoresis the slides were removed and washed with 0.4% Tris pH 7.5. This was done to remove alkali and detergents which would interfere with the ethidium bromide staining. The slides were allowed to stand in Tris 0.4 % for 5 minutes and this step was repeated thrice. Finally the slides were stained by placing 40 μ l of 20 μ g/ml ethidium bromide solution on each slide and then covering them with a coverslip.

3.7.2.5 Image analysis

Observations of cells were made using a Nikon E-400 fluorescent microscope, equipped with an excitation filter of 450-490nm and a barrier filter of 520nm. Images of single cells were taken at 200 \times magnification using Scion image software. DNA migration lengths were determined on a negative image by measuring the nuclear DNA and the migrating DNA in 50 randomly selected cells (25 from each replicate) for each concentration of FA.

3.7.2.6 Statistical analysis

Data were represented as the mean tail moment for the cells plus or minus the standard deviation within toxin treatments. A one way ANOVA was employed for statistical analysis with a value of $P < 0.001$ being used to determine the significance.

3.8 Results and Discussion

The DNA strand breaks that result after treatment of healthy lymphocytes with FA are readily detectable by the comet assay. This cytotoxic damage, as reflected by an increased DNA migration, is clearly the result of FA treatment of healthy lymphocytes as control untreated lymphocytes exhibited little or no DNA migration by comparison. Figures 18, 19a-c and 20a-e (lymphocytes from person 3) demonstrate the differences in DNA migration of lymphocytes treated with varying concentrations of FA. Diagrams accentuate the increase in DNA damage with an increase in FA concentration as compared to the untreated controls.

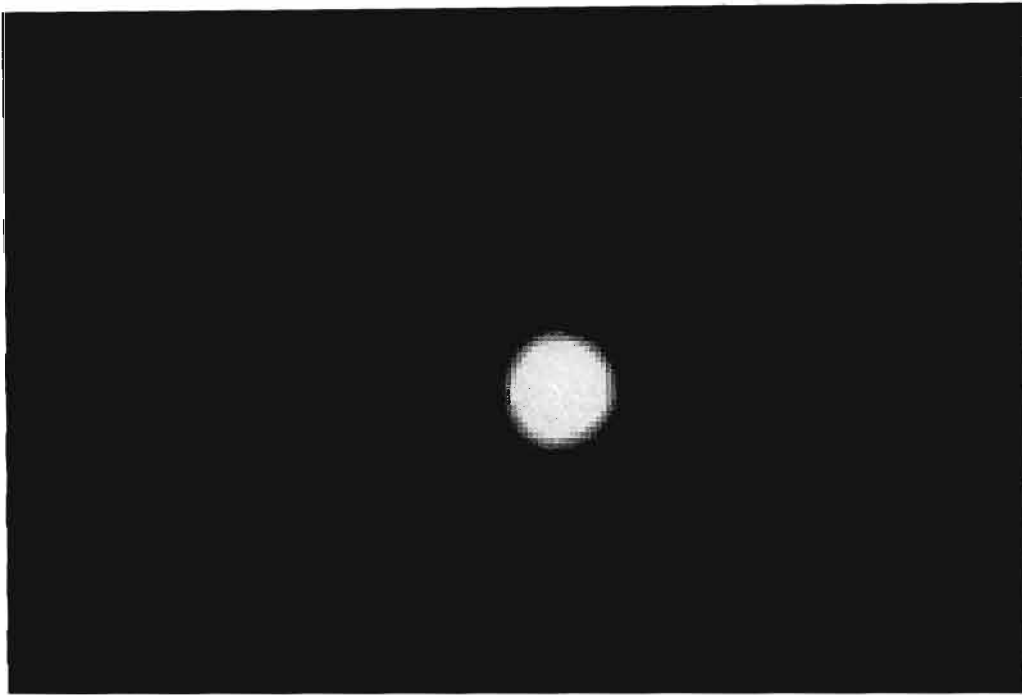


Figure 18 Control lymphocyte exhibiting no DNA damage (untreated) 32 microns.

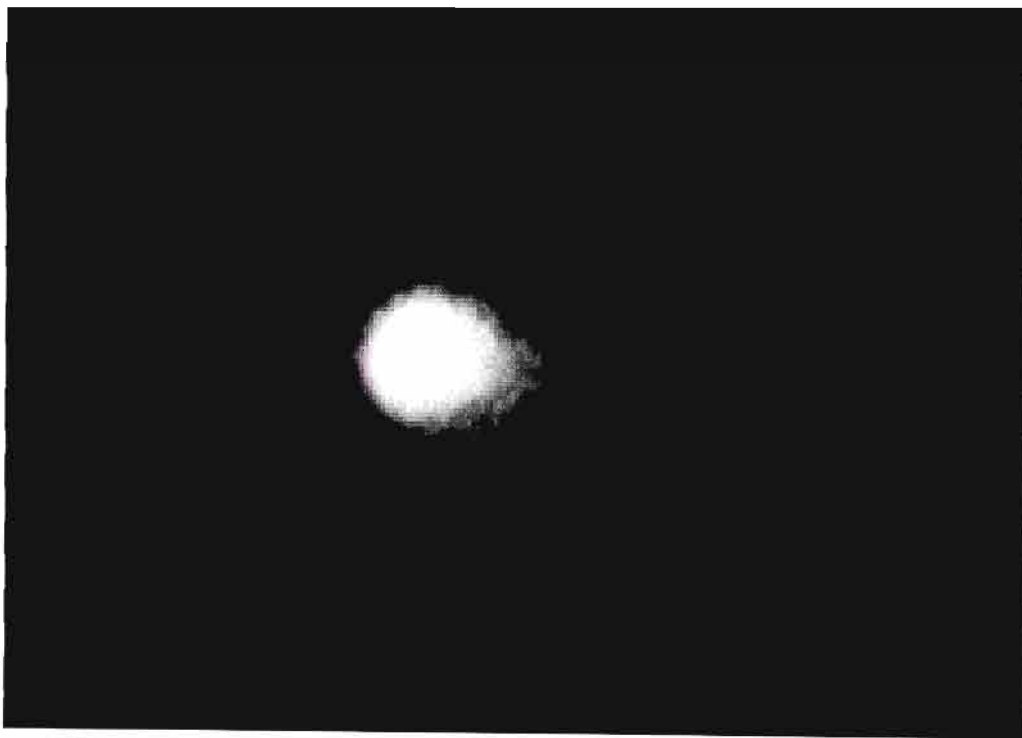


Figure 19a Mild degree of DNA damage exhibited by short migration of DNA (6 μ M FA) 81 microns.



Figure 19b Lymphocyte exhibiting moderate degree of DNA damage (50 μ M FA) 114 microns.



Figure 19c Lymphocyte exhibiting extreme DNA damage (100 μ M FA) 130 microns.

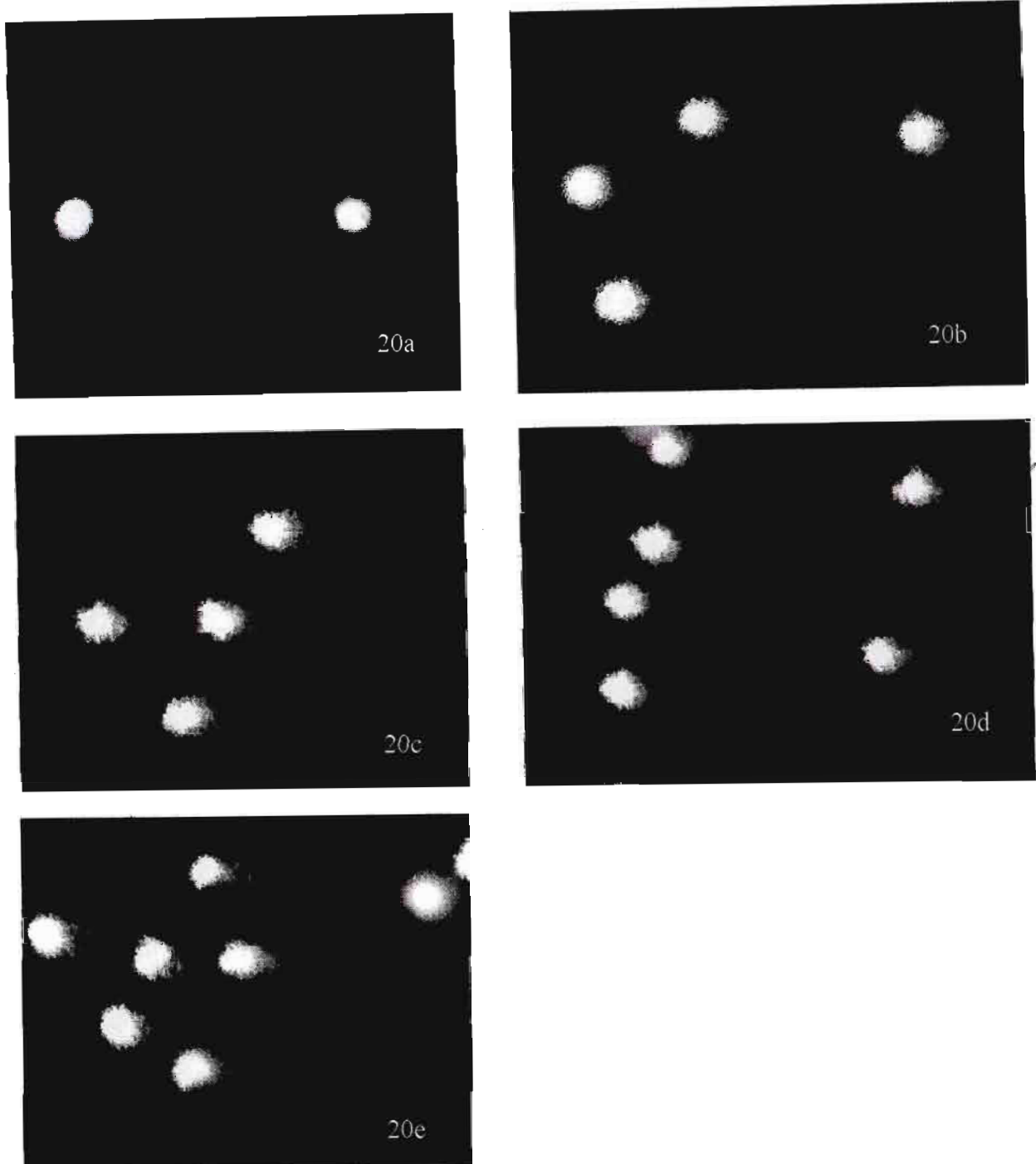


Figure 20 : Four hour treatments of lymphocytes with varying concentrations of FA (lymphocytes from person 3)
20a: Untreated control cells with no DNA damage.
20b: Cells treated with 3 μ M FA with little DNA damage.
20c: cells treated with 6 μ M FA with minor DNA damage.
20d: cells treated with 50 μ M FA with increased DNA damage.
20e: cells treated with 100 μ M FA with major DNA damage.

TABLE 2 DEMONSTRATION OF DNA DAMAGE INDUCED IN HUMAN LYMPHOCYTES BY FA USING THE SCGE TECHNIQUE

	<i>Length of DNA migration in (microns)</i>				
1 Hour	Control	3μM FA	6μM FA	50μM FA	100μM FA
Person 1	32.4 \pm 0.41	41.3 \pm 0.38	51.6 \pm 0.78	52.4 \pm 0.78	62.4 \pm 0.56
Person 2	32.3 \pm 0.42	37.3 \pm 0.41	39.2 \pm .042	46.1 \pm 0.51	57.1 \pm 0.65
Person 3	34.6 \pm 0.41	35.5 \pm 0.50	45.8 \pm 0.84	53.6 \pm 1.14	56.9 \pm 1.28
	<i>Length of DNA migration in (microns)</i>				
4 Hour	Control	3μM FA	6μM FA	50μM FA	100μM FA
Person 1	32.4 \pm 0.76	80.0 \pm 1.35	81.5 \pm 1.47	84.6 \pm 1.49	104 \pm 1.57
Person 2	34.9 \pm 1.26	109.3 \pm 2.6	118.2 \pm 1.8	120.1 \pm 1.52	121.3 \pm 1.6
Person 3	38.2 \pm 1.01	121.0 \pm 1.9	101.9 \pm 2.2	130.5 \pm 1.4	137.2 \pm 1.29

Values are given as the mean \pm the standard deviation of the mean. Data is based on 50 randomly counted cells (25 from each of two replicate slides) per sample concentration. For each experimental concentration, the values of all treated lymphocytes are significantly different from the controls at $p < 0.001$.

Bloods treated with varying concentrations of FA (3 μ M ,6 μ M, 50 μ M and 100 μ M) were assayed at 1 and 4 hours to observe the effects of FA on lymphocytes. Table 2 shows the mean values and standard deviations of the lymphocyte DNA tail moments (representing DNA damage). The results for the 1 hour incubation indicate substantially increased tail moment ($p < 0.001$) when compared to the control lymphocytes. The 1 hour incubations exhibit an almost dose dependant increase in DNA migration. Treated lymphocyte tail

moments at 1 hour for person 1 starts at 41.3 microns at 3 μ M FA, increases to 52.4 microns at 50 μ M FA and reaches 62.4 microns at 100 μ M FA. The 4 hour incubation indicates a considerable increase in DNA tail moments when compared to the 1 hour treatments. Treated lymphocyte tail moments at 4 hours incubation for person 1 starts at 80 microns at 3 μ M FA, increases to 84.6 microns at 50 μ M FA and reaches 104 microns at 100 μ M FA. The effect of FA on the subject bloods is significantly different as expected ($p < 0.001$). Images of typical lymphocytes in control samples or treated at various toxin concentrations are presented in figure 20. Under the experimental conditions carried out, no appreciable migration of DNA occurred among the majority of the control cells while an almost linear increase in the length of DNA migration was observed for the 1 hour incubations. The 4 hour incubations exhibit an almost two fold increase in the length of DNA migration as compared to the 1 hour concentrations. The results of DNA damage induced by FA in human lymphocytes is thus considerably different from that of the controls.

The focus of the present study was to demonstrate the utility of the comet assay for monitoring the genotoxicity of FA in the blood of healthy individuals. During the course of the electrophoresis in the comet assay, fragments of the DNA migrate away from the DNA core to form a fast moving "tail". Results obtained demonstrated increased tail moments as the concentration of FA treatment increased.

Fusaric acid is a known ion chelating agent that has low affinity for Ca²⁺ and Mg²⁺ and a high affinity for other essential metal ions such as Fe²⁺, Mn²⁺, Zn²⁺ and Cu²⁺. Its mode of action therefore may involve its interference with various transition metal ions and thus may be analogous to picolinic acid (PA) (Fernandez-Pol *et al.*, 1993). Radioisotopic

studies in PA have shown that it inhibits incorporation of radioiron into cells and possesses the ability to remove radioiron from cells (Fernandez-Pol *et al.*, 1993).

It is possible that FA chelates Zn^{2+} , Cu^{2+} and Mn^{2+} ions which are integral structural and functional compounds in numerous protein systems. These proteins are invariably associated with cell growth, differentiation, and protection against free radicals such as Cu^{2+} and Mn^{2+} containing superoxide dismutases (Fernandez-Pol *et al.*, 1993). It is possible, in an *in vivo* situation, that FA chelation to the prosthetic group of the ubiquitous haem protein catalase that catalyses the dismutation of hydrogen peroxide into water and molecular O_2 would invariably lead to an increase in spontaneously derived H_2O_2 from superoxide radicals. H_2O_2 along with many other chemicals are known to generate DNA damage through oxygen radical methods (Anderson *et al.*, 1999). Investigations have shown that eukaryotic cells are susceptible to the genotoxicity of H_2O_2 inducing chromosomal aberrations, gene mutations and DNA strand breaks (Mckelvey-Martin *et al.*, 1993).

DNA damage induced by H_2O_2 has been demonstrated in human lymphocytes (Mckelvey-Martin *et al.*, 1993, Singh *et al.*, 1991) and neonatal fibroblasts (Singh *et al.*, 1991).

Lymphocytes showed significant increase in DNA damage at all concentrations of FA after 1 hour incubation. The DNA damage is much more pronounced at 4 hour post toxin treatment. An increase in concentration of FA also led to a considerable increase in DNA damage at both 1 and 4 hour time intervals. This shows that FA influences healthy lymphocytes in a dose and time dependant manner.

Results obtained in each of the 3 volunteers is also significantly different although the general trend is an increase in DNA damage with increasing concentration and increasing time intervals. The variability of the individual DNA damage among the 3 volunteers is expected as each individual possessed different immune statuses at the time the assays were conducted. Each individual was in a healthy state at the time of the experiments and no external physical factors such as strenuous exercise viral infections or any other apoptosis inducing factors contributed to the increased apoptosis of the experiment. Person 3 however, exhibited a greater degree of DNA damage after 4 hours of treatment with FA. This can probably be attributed to the fact that person 3 is a smoker. Smoking constitutes a lifestyle factor that could compromise the immune status of person 3 and thus account for the increased DNA damage. The results obtained otherwise are thus attributable to the various FA treatments and increased time intervals.

The use of the SCGE assay has yielded several advantages intrinsic to the assay. These include the measurement of DNA damage at the level of the individual cell, the need for extremely small numbers of cells, the relative ease of obtaining data (results can be obtained within a few hours) and the fact that the assay is extremely cost effective when compared to assays that yield similar information. These advantages will no doubt provide the necessary impetus for increasingly widespread use of the SCGE technique in studies dealing with basic mechanisms of DNA damage and repairs, in radiation biology, in clinical applications and in genetic toxicology. In the future comparative and validative experiments must be performed in each area of application to enable this potentially valuable tool to achieve its full potential.

The results of the comet data on DNA damage induced by FA are novel as this assay has not been previously used to assess DNA damage in lymphocytes in healthy individuals. The DNA damage induced by FA whether endogenous or exogenous is readily detectable by the SCGE assay. We have successfully demonstrated the genotoxicity of FA in the lymphocytes of healthy individuals.

Chapter 4

4. DNA Fragmentation analysis

Wyllie A.H. (1980) showed that glucocorticoids induced extensive DNA degradation in rat thymocytes *in vitro* during the onset of cell death. The resulting DNA was of a specific pattern producing fragments that were multiples of 180-200 base pairs. The length of these base pairs corresponded with that of DNA wrapped around the histone octamer in a nucleosome, indicating that the chromatin was being cleaved at the linker DNA between nucleosomes, producing oligonucleosomal fragments. At that time this became known as the only significant biochemical event that occurred during the apoptotic process. Since this initial discovery internucleosomal DNA cleavage has been observed in almost all of the instances of apoptosis that have been studied. These include isolated leukaemia cells (Distelhorst, 1988), macrophages (Waring, 1990), erythroid progenitor cells (Koury and Bondurant, 1990), prostate (Kyprianou and Issacs, 1988), uterine epithelium and the targets of cytotoxic T lymphocytes and natural killer cells (Duke *et al.*, 1986). The fact that this DNA fragmentation occurs in almost all apoptotic cells suggests that there may be a common mechanism by which apoptosis occurs in different cell types.

A general tendency in literature has followed equating this internucleosomal DNA cleavage with apoptosis. Cohen and Duke, (1984) reported that the key morphological features of apoptosis may occur in the absence of internucleosomal DNA fragmentation.

4.1 The role of endonuclease in DNA fragmentation

In all circumstances concerning DNA fragmentation there is a series of strikingly similar morphologic changes, most of which occur mainly in the nucleus (Arends *et al.*, 1990).

It is widely assumed that DNA cleavage is the result of endogenous endonuclease activity. Studies have elucidated a Ca^{2+} and Mg^{2+} dependant endonuclease activity capable of cleaving chromatin at internucleosomal sites in nuclear preparations from normal (but apoptosis-prone) cells. Micrococcal nuclease exhibits this specificity and it seems that the enzyme is sterically hindered from hydrolysing the DNA that is wrapped around the core histones. Nuclei isolated from thymocytes and incubated with Mg^{2+} and Ca^{2+} produced DNA fragmentation comparable to cells exposed to dexamethasone (causes extensive DNA damage). This led to the deduction that a calcium and magnesium-dependant endonuclease was endogenously situated in the nuclei of thymocytes. The enzyme is presumably inactive when the cell is not exposed to glucocorticoids because the intranuclear availability of a suitable form of calcium is low. It has been suggested that glucocorticoids might induce the synthesis of a calcium transport mechanism which causes calcium to migrate into the nucleus in such a form as to activate the endogenous endonuclease (Cohen and Duke, 1984). It is possible that many other cytolytic enzymes may be involved co-ordinately, but this probability has not been adequately addressed. Certain studies have however provided strong evidence that the structural changes in the nucleus in apoptosis are the direct result of a selective nuclease activation within the dying cells.

Endonuclease activity does not seem to be accompanied by indiscriminate proteolytic digestion of chromatin. Protein constituents of the nuclear matrix and the ultrastructure of

its recovered fragments are substantially the same as those of morphologically normal cells (Arends *et al.*, 1990). The enzyme responsible for chromatin cleavage during apoptosis may be a neutral endonuclease dependant upon the coincident presence of calcium and magnesium ions and alteration of the ionic environment in the nucleus may be sufficient to activate this enzyme (Allbriton *et al.*, 1988). Endonuclease exhibiting these features have been found to be present within the nuclei of many cell types (Nakamura *et al.*, 1981). They have been isolated and purified from the nuclei of normal thymocytes and certain lymphoid cell lines.

4.2 DNA Digestion is influenced by pre- existing chromatin organization

Chromatin configuration occurs at multiple levels. DNA is wrapped twice around histone octamers (two each of H3, H2A, H2B and H4) to form nucleosomes separated by linker DNA in a 110 angstrom (\AA)- diameter beads on string structure (Richmond *et al.*, 1984).

This structure may be further assembled into a 300\AA filament believed to be formed by winding of the chain of nucleosomes into a solenoid containing six nucleosomes per turn with the linker DNA and histone H1 on the inside. Interactions occurring between H1 molecules possibly mediate formation of the solenoid, although other models have been suggested (Finch and Klug, 1976).

The induction of apoptosis as a result of activation of an endogenous endonuclease results in oligonucleosome chains with different properties, presumably reflecting the configuration of the chromatin from which they were derived. Some chromatin remains attached to the nuclear structure, is incompletely digested and contain long oligonucleosomal chains. These structures are associated with histone H1 and little HMG 1 or 2 proteins. This is consistent with the theory of origin from transcriptionally inactive

heterochromatin, packaged as the 300A° solenoid (Finch and Klug, 1976). Chromatin not attached to the nuclear structure contains a high percentage of mononucleosomes. These have relatively little histone H1 but are enriched in HMG 1 and 2 proteins, and represents about 30% of the total chromatin DNA. HMG 1 and 2 proteins are believed to replace H1 at the junction of linker and nucleosome-wrapped DNA. This increases the accessibility of chromatin to polymerases and other enzymes (Arends *et al.*, 1990).

Chromatin fibres of normal nuclei are anchored to the nuclear matrix by virtue of binding of certain consensus DNA sequences. Chromatin anchorage to the nuclear matrix is the basis of supercoiled DNA loops that becomes apparent on removal of histones from normal nuclei and are visualized as the diffuse halo around the nucleus in preparations (nucleoids) treated with high salt solution or dilute acid. The partial loss of this DNA halo in apoptotic nuclei is the result of multiple cleavage events between anchorage sites (Arends *et al.*, 1990).

Condensed chromatin may remain as aggregates of 300A° filaments, even after cleavage of DNA at internucleosomal sites, through protein protein interactions between adjacent coils of the solenoid (Warrant and Kim, 1978). The amount of DNA remaining attached to the nuclear structure is thus estimated at being 70% despite numerous onslaughts of multiple DNA cleavage events.

The aim of this study was to evaluate the DNA fragmentation profiles caused by FA in healthy lymphocytes.

4.3 Materials and Method

4.3.1 Materials

The chemicals used in the experiments were purchased from the following suppliers :

Tris, HCl, Mercaptoethanol from Merck; Phenyl methane sulphonyl fluoride, sodium N-lauroyl sarcosinate, proteinase K from Sigma Chemicals Co. Ltd., USA; MgCl₂ EDTA from Saarchem; RNase and ethidium bromide and DNA molecular marker 7 from Boehringer Mannheim.

4.3.2 Methods

4.3.2.1 Preparation of lymphocyte samples

Whole blood 4ml (6 tubes of 4ml each) was collected in lithium heparin Vacutainer tubes by venopuncture from a healthy donor. Lymphocyte isolations were carried out as in chapter 2. The lymphocyte suspensions (10^6 cells/ml) were treated in a sterile environment as in chapter 2 and incubated for 4, 24 and 48 hours. Fusaric acid was dissolved in sterile distilled water and made up to a stock solution of a 2000 μ M in CCM. Cell suspensions were treated with a range of serial dilutions and made up to final concentrations of 200, 400 and 1000 μ M. Positive control cells were treated with 4 and 20 μ M camptothecin. Control lymphocytes were untreated. After each respective time interval the lymphocytes (10^6 cells/ml) were collected by centrifugation at 400 \times g for 5 minutes. Cells were then washed with buffer A (appendix 1) (10 mM Tris-HCL, pH 5.8, 3mM MgCl₂, 2mM mercaptoethanol, and 0.3mM phenylmethane sulphonyl fluoride). The lymphocytes were further centrifuged at 400 \times g for 5 minutes. The supernatants were then discarded and the lymphocytes were then lysed in lysis buffer (appendix 2) (50mM Tris-HCL buffer, pH 7.8, 0.5% sodium N-lauroyl sarcosinate, and 10mM EDTA). The

lysed cell suspension was incubated sequentially with 200µg/ml of RNase A (Roche Biochemicals) and 0.5µg/ml proteinase K (Sigma) (60 minutes at 50°C).

4.3.2.2 Electrophoresis

Electrophoresis of the fragmented DNA was carried out in 2% agarose gels in TBE buffer (Appendix 3) containing 0.5µg/ml ethidium bromide. Agarose, a polysaccharide, is a common gel forming material used in the separation of DNA. Ethidium bromide is a fluorescent dye that intercalates into DNA and permits the visualisation of the DNA under ultra violet light. DNA molecular weight markers (marker 7, 857 bp-81 bp) (Boehringer Mannheim) were used for the calibration of fragmented chromosomal DNA size.

The molten agarose gel (50°C) was poured into a horizontal plastic plate with preset combs. The gels were left to solidify at room temperature for approximately 30 minutes. When the gels were fully set, the combs were carefully removed and the gel was carefully placed in a horizontal electrophoresis tank, with the wells closest to the cathode. The tank was subsequently filled with 800ml of electrophoresis buffer (TBE) which completely submerged the gel. Samples of extracted DNA (10µl) were loaded into separate wells by submerging a clean pipette tip of a micropipette about three quarters of the way into each well, but not touching the gel. The loaded gels were electrophoresed at 100 volts (V) for 45 minutes.

The DNA fragmentation patterns were visualized under UV illumination and thermal prints and scanned images of the results were prepared. All experiments were performed in duplicate on three different occasions.

4.4 Results and Discussion

Fragmentation of treated lymphocytes was observed after 24 hours of incubation at various concentrations of FA. The fragmentation was evident from the smear of the DNA along the length of the gel. Control samples exhibited little or no fragmentation as most of the DNA did not migrate beyond the well indicating that the DNA was not cleaved.

Figure 21 illustrates the 2% agarose gel of the different fragmentation profiles at different incubation times and FA concentrations. No fragmentation occurred at 4 hours incubation while there is a marked increase in the 24 hours incubation. This means that DNA fragmentation is not an early process for FA induced cellular injury. Significant fragmentation also occurred in the 48 hour incubations (Fig 22). Figure 21 and 22 two are representative experiments of three which confirm these results.

Maximal DNA cleavage occurred at 1000 μ M FA treatment after 24 hours. This is consistent with the maximal percentage mortality of lymphocytes that was demonstrated by the MTT assay when lymphocytes were treated with 1000 μ M FA for 24 hours. The DNA fragmentation that occurred with 200 μ M FA treatment of lymphocytes after 24 hours was minimal. The amount of DNA fragmentation increased at 400 μ M treatment of lymphocytes with FA after 24 hours but was less pronounced when compared to the 1000 μ M FA treatment at the same time. Similarly the amount of DNA fragmentation that resulted at 48 hours of incubation, when compared to the 24 hour incubation, increased with an increase in FA concentration.

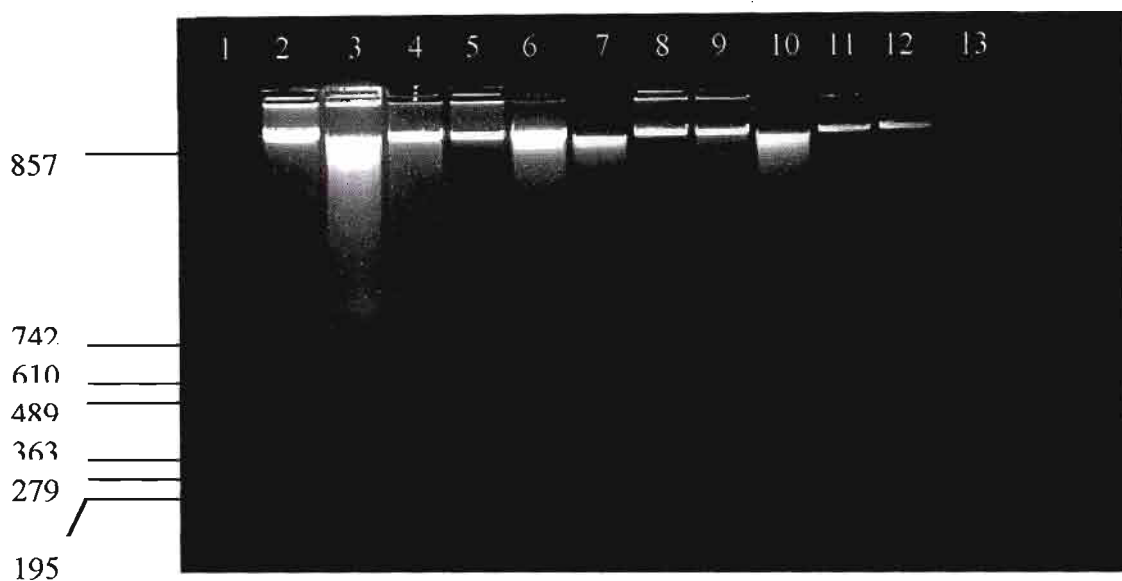


Figure 21 Fragmentation profiles of FA treated lymphocytes at various concentrations after 4 and 24 hours.

Key : Lane 1 Molecular weight marker 7
 Lane 2 control
 Lane 3 20 μ M camptothecin 4 hours
 Lane 4 4 μ M camptothecin 24 hours
 Lane 5 200 μ M FA 24 hours
 Lane 6 400 μ M FA 24 hours
 Lane 7 1000 μ M FA 24 hours
 Lane 8 200 μ M FA 24 hours
 Lane 9 400 μ M FA 24 hours
 Lane 10 1000 μ M FA 24 hours
 Lane 11 200 μ M FA 4 hours
 Lane 12 400 μ M FA 4 hours
 Lane 13 1000 μ M FA 4 hours

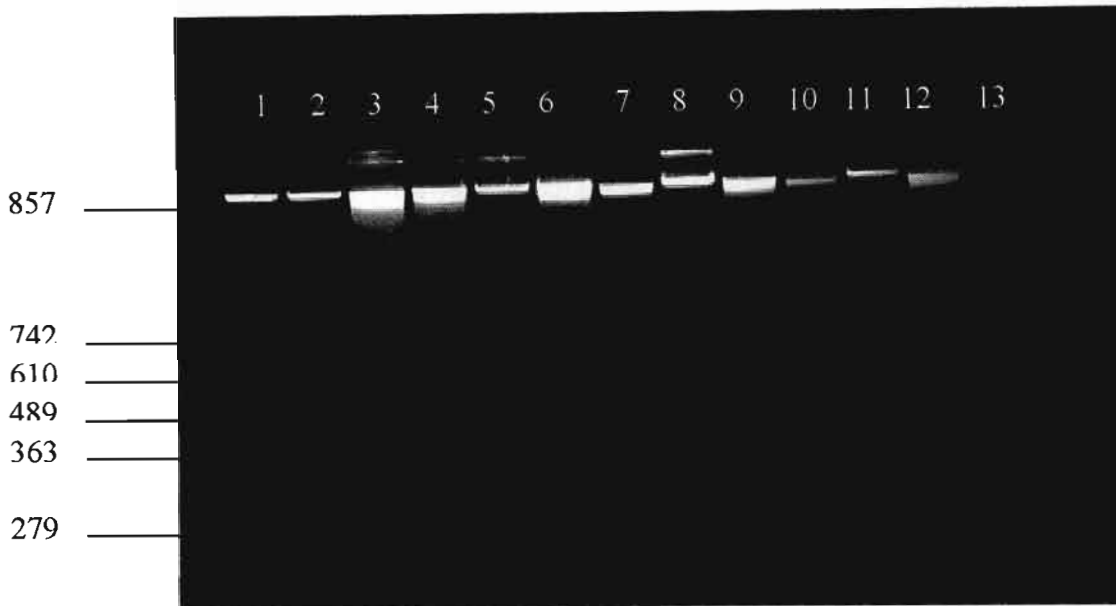


Figure 22 Fragmentation profiles of FA treated lymphocytes at various concentrations after 4 and 48 hours.

Key : Lane 1 Molecular weight marker 7
 Lane 2 control
 Lane 3 20μM camptothecin 48 hours
 Lane 4 4μM camptothecin 48 hours
 Lane 5 200μM FA 48 hours
 Lane 6 400 μM FA 48 hours
 Lane 7 1000 μM FA 48 hours
 Lane 8 200μM FA 48 hours
 Lane 9 400 μM FA 48 hours
 Lane 10 1000 μM FA 48 hours
 Lane 11 200μM FA 4 hours
 Lane 12 400 μM FA 4 hours
 Lane 13 1000 μM FA 4 hours

During the process of apoptosis several striking morphological changes occur in a cell many of which occur in the nucleus. One of the most important changes is the widespread cleavage of nuclear DNA at internucleosomal sites. It is now widely accepted that DNA cleavage is the result of endogenous endonuclease activity. A Ca^{2+} and Mg^{2+} dependant endonuclease capable of cleaving chromatin at internucleosomal sites has been identified in normal (but apoptosis prone) cells. This neutral endonuclease is highly dependant upon the coincident presence of Ca^{2+} and Mg^{2+} ions and alteration of the ionic environment in the nucleus may be sufficient to activate this enzyme (Allbriton *et al.*, 1988). A Ca^{2+} and Mg^{2+} dependant endonuclease capable of cleaving chromatin at internucleosomal sites has been identified in normal (but apoptotic prone) cells (Ishida *et al.*, 1974). There is little evidence to substantiate whether apoptosis involves appearance of new intranuclear nuclease activity or rearrangement of chromatin proteins permit DNA cleavage by pre-existing enzyme. At best analysis of cleavage products can be performed to define some of the properties of the cleavage reaction.

The DNA fragmentation induced by FA after 24 and 48 hours although quite significant when compared with the controls did not migrate beyond a certain fragment length. This length of fragments corresponded with the first band of the molecular weight DNA marker (857 bps). This is considerably large when compared to the fragments expected such as those produced during apoptosis (180 bps or multiples thereof).

A possible explanation for this lies in the fact that FA is a chelating agent and is capable of chelating both Ca^{2+} and Mg^{2+} . These ions are instrumental in activating the

endonuclease responsible for cleaving DNA during apoptosis. The chelating effect of FA would thus render this enzyme inactive. This however does not explain why the DNA was incompletely cleaved. The possibility that other cytolytic enzymes may be involved co-ordinately has not been directly addressed (Arends *et al.*, 1990). It is possible that other unidentified enzymes, that are unaffected by the chelating properties of FA, do exist which account for the cleavage profiles seen in figure 21 and 22.

Chapter 5

5. Ultrastructural evaluations using transmission electron microscopy (TEM)

Transmission electron microscopy analysis has been considered a milestone of the research in the field of apoptosis. A plethora of findings contributing to the knowledge of the process, e.g. the role of subcellular structures and organelles, have been widely published (Erenpreisa *et al.*, 1997).

5.1 Normal lymphocytes

DNA in the nucleus is combined with histones and other proteins and this arrangement collectively constitutes the chromatin. There are two forms of chromatin in the interphase nucleus, a condensed presumably inactive form referred to as the heterochromatin. This heterochromatin usually presents as collections of rounded or irregular-shaped electron-dense granules in ultrathin sections. The active form is called euchromatin and is dispersed in the nuclear matrix and does not stain very effectively (Ghadially, 1982).

Chromatin tends to aggregate in certain preferred sites within the nucleus and it is this configuration which forms the characteristic familiar chromatin pattern. Chromatin may be peripheral or marginal in which irregular shaped masses of chromatin are found adjacent to the nuclear envelope, between the nuclear pores. There exists a characteristic clear area devoid of heterochromatin immediately behind the nuclear pores.

Chromatin centres involve randomly distributed chromatin aggregates within the nucleus matrix. Nucleolus associated chromatin has focal aggregates of chromatin granules along the periphery of the nucleolus. Although intranucleolar chromatin contains mainly protein and RNA, studies have revealed that it contains small amounts of DNA (Ghadially, 1982).

5.2 Apoptotic lymphocytes

Morphologically the cell shrinks and becomes denser. The chromatin becomes pyknotic and packed into smooth masses applied against the nuclear membrane. This margination of chromatin may create curved profiles that have led to descriptive terms such as half moon, horse-shoe, sickle, lancet and ship like nuclei. Hence nuclei of apoptotic cells lack diffuse chromatin, while the compact chromatin with a supranucleosomal structure extends evenly throughout the nuclear interior (Fig 23 and 24a). These cells retain the supranucleosomal organisation of chromatin up to the late phase of apoptosis. Late apoptotic cells appear very small possessing dense non transparent chromatin, which sometimes segregates into crescents and caps (Fig 23). The nucleus may break up (karyorrhexis), and the cell may emit processes that often contain pyknotic nuclear fragments. These processes break off and become apoptotic bodies, which may be phagocytosed by macrophages or neighbouring cells. At high power transmission electron microscopy, the chromatin of apoptotic cells display very dense altered texture (Fig 24b) (Erenpreisa *et al.*, 1997).

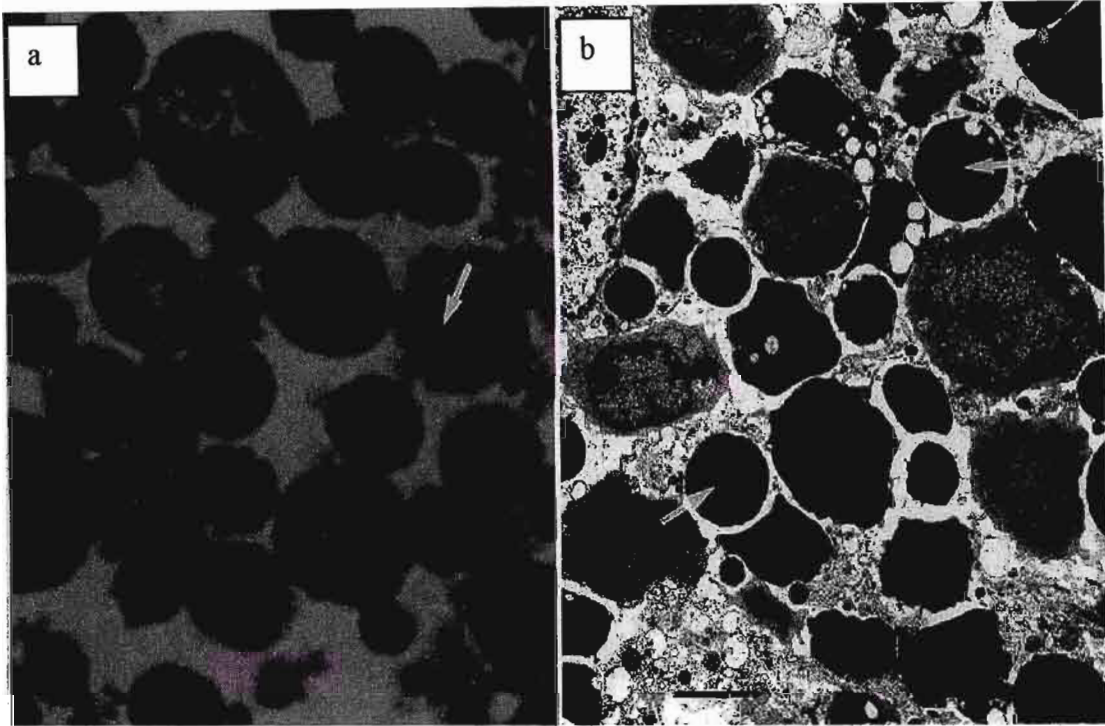


Figure 23 Semithin section (**a**) and low power transmission electron micrograph (TEM); **b** of prednisolone-treated rat thymus. (*Asterisk* T-lymphoblast, *stars* early apoptotic cells, *arrows* late apoptotic cells) Magnification for **ax2000**, bars 4.5 micrometers (Erenpreisa *et al.*, 1997).

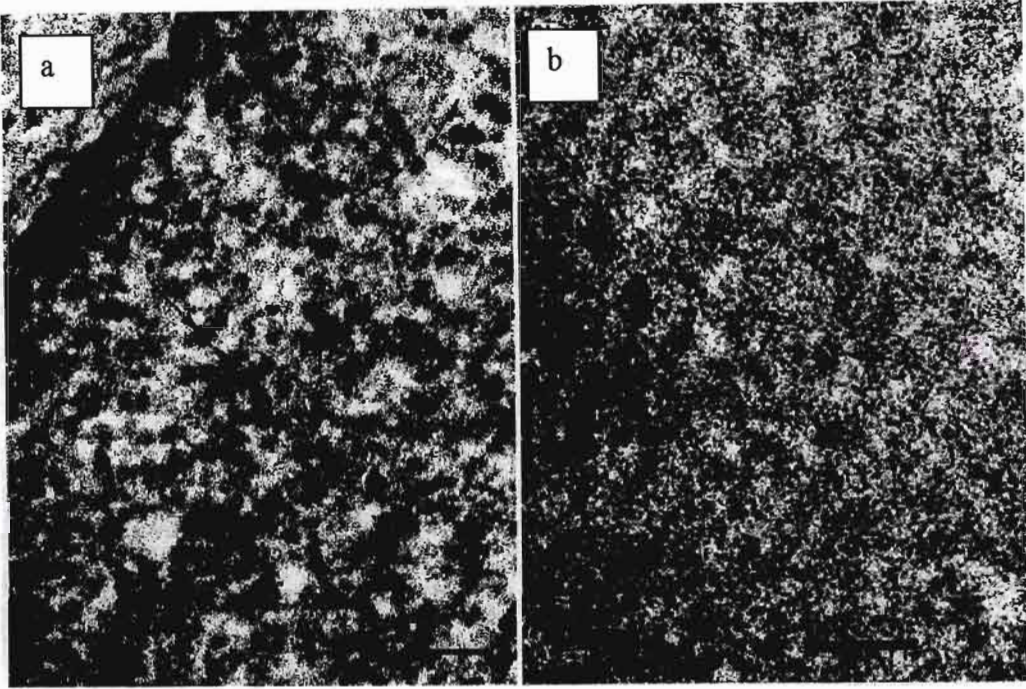


Figure 24 High power TEM showing the texture of apoptotic chromatin. a The nucleus of an early apoptotic cell. The coiled chromatin threads of the supranucleosomal level of organisation, textured as 30-nm globules, are seen (*arrows*). *Bar* 100 nm. b The nucleus of a late apoptotic cell. The chromatin is degraded and very dense. Contours of deteriorating (fuzzy) nucleosomes can only be assessed (*arrows*). *Bar* 50 nm (Erenpreisa *et al.*, 1997).

5.3 Mitochondria

This organelle is bound by two membranes, an external limiting membrane and an inner membrane from which arise the cristae. These membranes enclose two chambers which are not connected to each other. The outer chamber represents the space between the two membranes. The inner chamber is bound by the internal membrane and contains the matrix which is more electron dense than the contents of the outer chamber.

The cristae mitochondriales appear as membranous laminae or plate-like structures lying within the mitochondrion. They are derived from the inner membrane and traverse a variable distance across the width of the organelle. Cristae are infoldings of the inner membrane, enclosing a cleft-like space which is continuous with the outer chamber.

Mitochondrial studies have shown that most of the Krebs cycle enzymes are located in the matrix and the electron transport and oxidative phosphorylation enzymes form molecular assemblies in or on the inner mitochondrial membrane covering the wall cristae (Ghadially, 1982).

In ultrathin sections not all the cristae within the mitochondria are visible as some of them are cut obliquely or tangentially. This is often the case in long thin mitochondria which are slightly bent and sometimes quite tortuous. In such cases it is often difficult to ascertain whether cristae are actually missing or not present in a particular segment of the mitochondrial section (Ghadially, 1982).

The aim of this study was to evaluate the ultrastructural changes caused by FA in normal healthy lymphocytes.

5.4 Materials and Method

5.4.1 Materials

The chemicals used in the experiments were purchased from the following suppliers :

Hanks balanced salt solution (HBSS) from Sterilab suppliers, ethanol from Merck, Spurr's resin, glutaraldehyde, osmium tetroxide, copper grids, and Eppendorf tubes from Sigma.

5.4.2 Methods

5.4.2.1 Lymphocyte treatments

Whole blood 4ml (6 tubes of 4ml each) was collected in lithium heparin Vacutainer tubes by venopuncture from a healthy donor. Lymphocyte isolations were carried out as in chapter 2. Lymphocytes were immediately treated in sterile 12 well plates with various concentrations of FA (ie. 200 μ M, 400 μ M and 1000 μ M) and subsequently incubated at 37°C in a CO₂ water jacket incubator for 1, 4 and 24 hours respectively.

5.4.2.2 Processing, sectioning and staining of samples for transmission electron microscopy

After each incubation time, the control and FA treated lymphocytes were aspirated separately from their wells with a sterile pasteur pipette and placed in separate sterile eppendorf tubes. Each sample was centrifuged at 300 \times g for 3 minutes at room temperature. The supernatants were discarded and the pellet was resuspended in HBSS (1ml) for washing. After washing, the pellet was centrifuged at (300 \times g, 3 minutes, room temperature) and the supernatant discarded as before taking care not to dislodge the pellet. The pellet was washed twice in HBSS. The lymphocytes were then processed for TEM as outlined in table 3.

Each step of the processing except for the embedding medium required the centrifugation of the samples at 300×g for 3 minutes. This was necessary because the lymphocytes were in suspension. Pelleting allowed the discarding of the supernatant only. Embedded samples were removed from eppendorfs using a heated wire. Ultrathin sections were cut on a Reichart Jung Ultracut microtome. Ultrathin sections (0.5µM) were mounted on 200 mesh copper grids, stained with uranyl acetate and lead citrate and viewed using the Jeol JEM 1010 electron microscope (Department of Biology, University of Natal).

TABLE 3 : *IN VITRO* PROCESSING OF LYMPHOCYTES FOR TRANSMISSION ELECTRON MICROSCOPY

TIME	PROCEDURE
1 hour	Fix in 1% gluteraldehyde in HBSS
2×10 minutes	Rinse in PBS
1 hour	1% osmium tetroxide (4°C)
2×10 minutes	Rinse in HBSS (1ml)
20 minutes	Dehydrate- 70% ethanol
20 minutes	Dehydrate- 90% ethanol
2×30 minutes	Dehydrate- 100% ethanol
30 minutes	1:1 100% ethanol: Spurr's resin
1 hour	100% Spurr's resin (60°C)
24-48 hours	100% Spurr's resin (60°C) - Polymerization

5.5 Results and Discussion

Control lymphocytes exhibited a lack of most cellular organelles. They did however demonstrate nuclei and these exhibited the characteristic clockwise or cartwheel distribution of heterochromatin aggregates. The nucleolus (Fig 25) (white arrow), marginal chromatin (black arrow), chromatin centres and nucleolus-associated chromatin (grey arrow) are readily discernable. The thin layer of cytoplasm characteristically contained numerous polyribosomes. The control lymphocytes at 1, 4 and 24 hour periods exhibited normal healthy lymphocyte morphology (Fig 25).

Fusaric acid treated lymphocytes (ie. 200 μ M, 400 μ M and 1000 μ M) exhibited significantly different morphologies predominantly in the nuclear chromatin (Fig 26 and Fig. 27) and mitochondria (Fig 29). The lymphocytes treated at 1, 4 and 24 hours displayed numerous cellular organelles that were absent in the controls and the number of organelles increased with increasing time intervals.

Compared with the control lymphocytes, lymphocytes treated with 200 μ M, 400 μ M and 1000 μ M FA all displayed characteristic apoptotic morphologies at different stages (Fig 31). Damage to the lymphocytes was more evident at 24 hours than at 1 and 4 hours treatment. Treated lymphocytes exhibited a decrease in secretory vesicles (Fig 26) as opposed to untreated lymphocytes. Fusaric acid treated lymphocytes also displayed a large percentage of mitochondria that had slightly to moderately swollen cristae. Mitochondria of treated lymphocytes seemed to develop relatively electron-lucent matrices. This most probably represented mitochondrial matrix lysis. This is the most characteristic form of swelling, ie., the swelling of the inner chamber containing the mitochondrial matrix (Fig 29) (Ghadially, 1982).

Fusaric acid treated lymphocytes also contained vacuoles of various sizes (Fig 32 and Fig 33). Vacuoles seemed larger and more numerous with an increase in time intervals. These are possibly the result of transformed endoplasmic reticulum that hypertrophy. Control endoplasmic reticulum can be seen in figure 36.

It is apparent from ultrastructural analysis that FA induces death in lymphocytes by apoptosis. Certain lymphocytes exhibited the hallmarks of necrosis, but these were few and occurred only after 24 hours at 1000 μ M FA treatment. Cells treated with 200 μ M, 400 μ M and 1000 μ M FA all displayed condensation of chromatin at the nuclear periphery, nucleolar disintegration, and reduction in nucleolar size. There is a decrease in cell volume compaction of cellular organelles and dilatation of endoplasmic reticulum. Lymphocytes treated for 24 hours exhibit budding and separation of both nucleus and cytoplasm into multiple, small, membrane bound apoptotic bodies (Fig 30).

5.5.1 Nuclear envelope and nuclear pores

Electron micrographs of the nuclear envelope characteristically consist of two membranes separated by a perinuclear cistern, generally about 20-30nm wide. The outer membrane of the nuclear envelope is often studded with few or many ribosomes. A common occurrence is the fusion of two membranes of the nuclear envelope producing 'fenestrations' called the nuclear pores (Fig 34). The diameter of the nuclear pore is usually in the region of 55-70nm. Nuclear pores cannot be regarded as simple holes through which material small enough can pass unimpeded. It is possible in some sections to visualize a thin lamina extending across the nuclear pore (Fig 35).

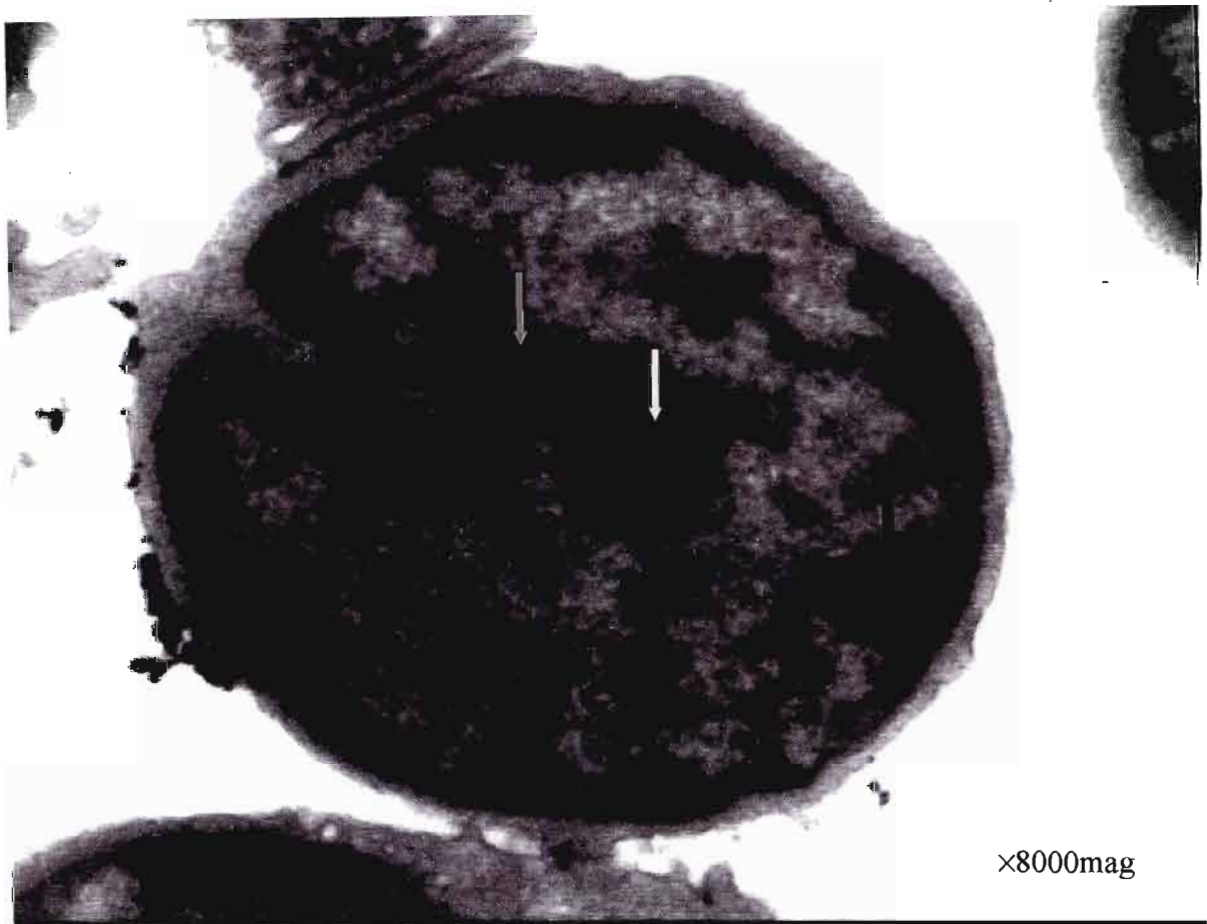


Figure 25 Typical control lymphocyte (24 Hours). Control cells are characteristically large round cells with a thin ring of cytoplasm and a single large nucleus. Organelles are not clearly distinguished in control lymphocytes. Nucleoli are distinguishable in some cells (arrow).

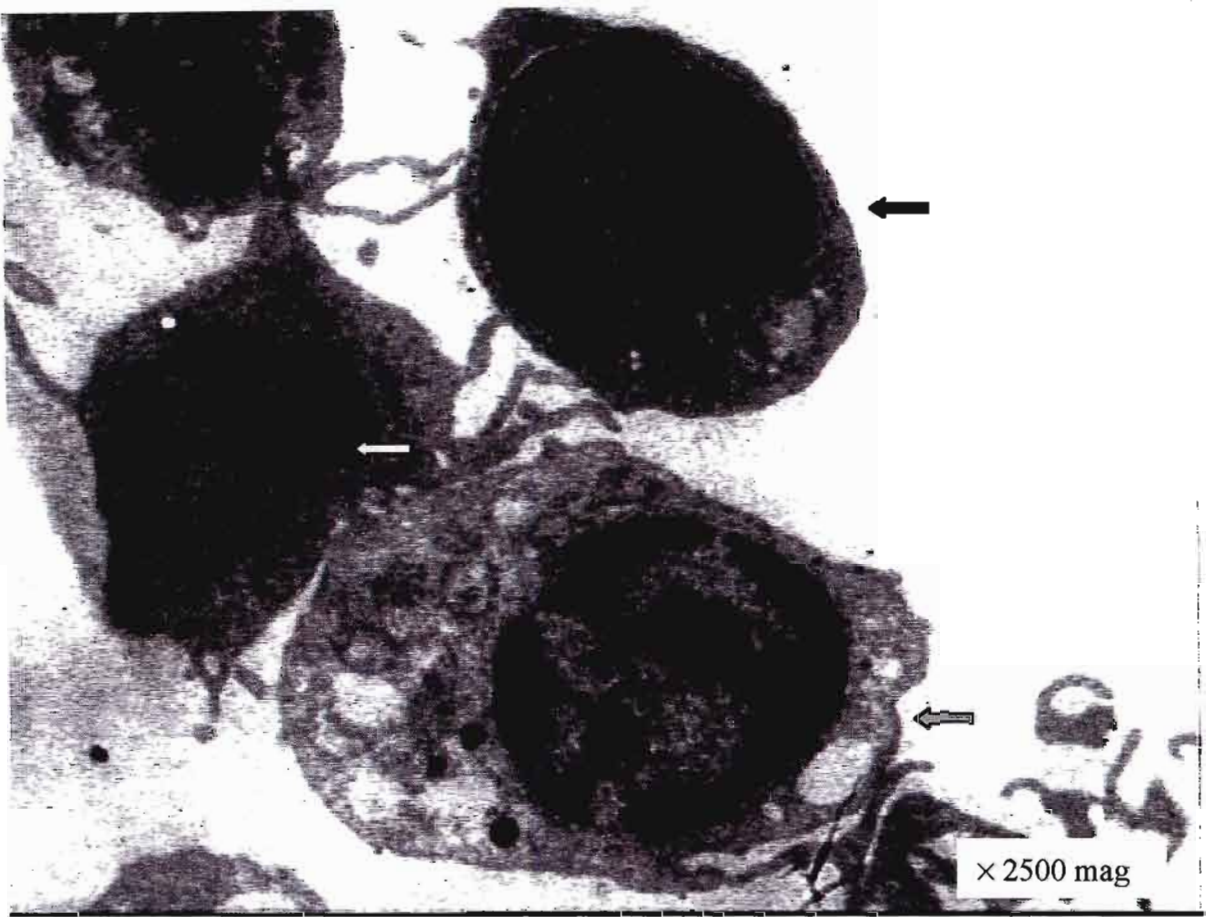


Figure 26 FA treated lymphocytes (24 hours). These three cells show three different phases of nuclear damage characterising apoptotic cells. Cell 1 (grey arrow) depicts the early phase of nuclear damage. Cell 2 (black arrow) shows a cell in a slightly more advanced stage of apoptosis where the chromatin material exhibits a higher degree of dissociation. Cell 3 (white arrow) exhibits nuclear damage in its later phase as the chromatin has predominantly migrated to the periphery of the nucleus.

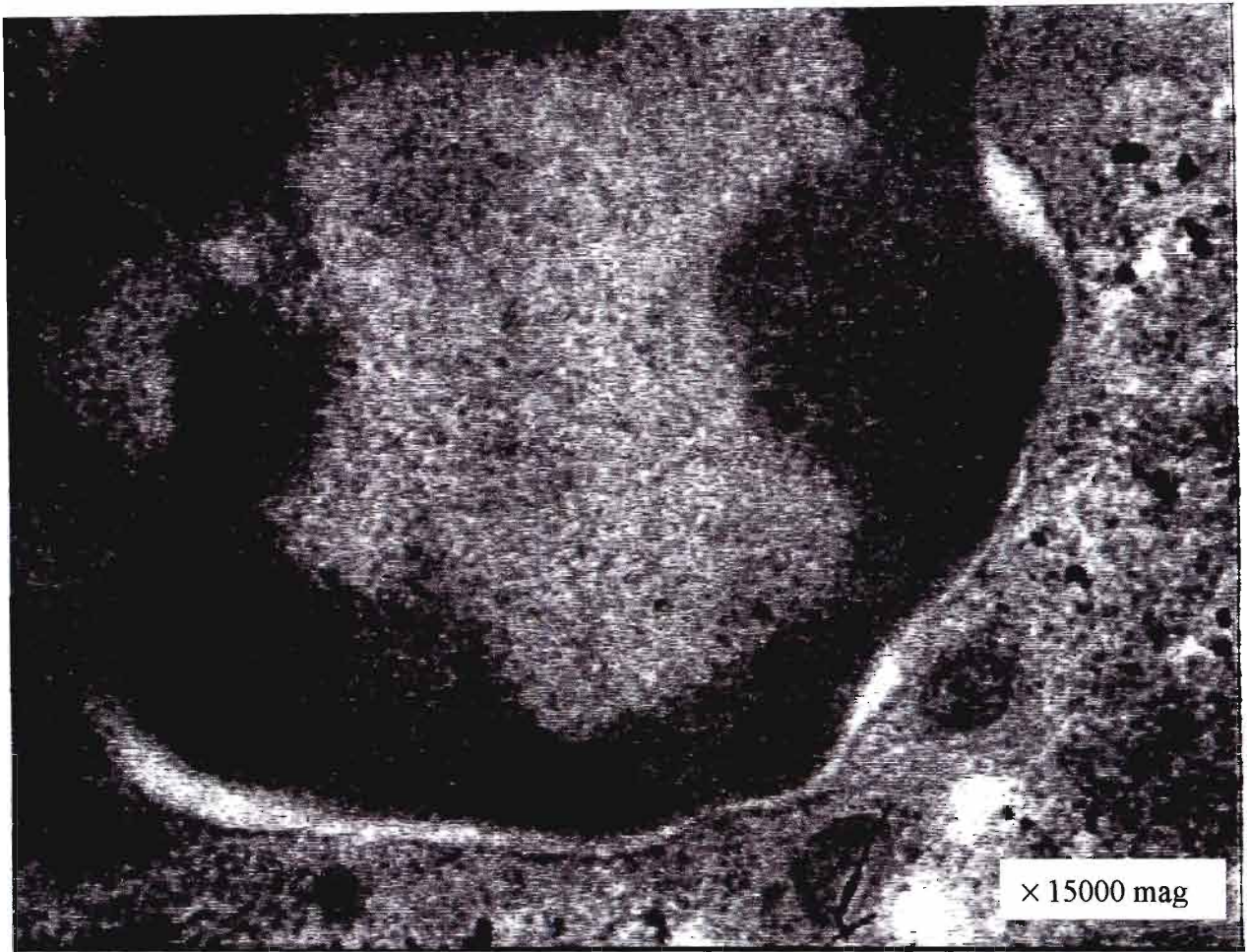


Figure 27 400 μ M FA treated lymphocyte (24 hours) exhibiting nuclear migration to the periphery of the nucleus which is characteristic of apoptosing cells.

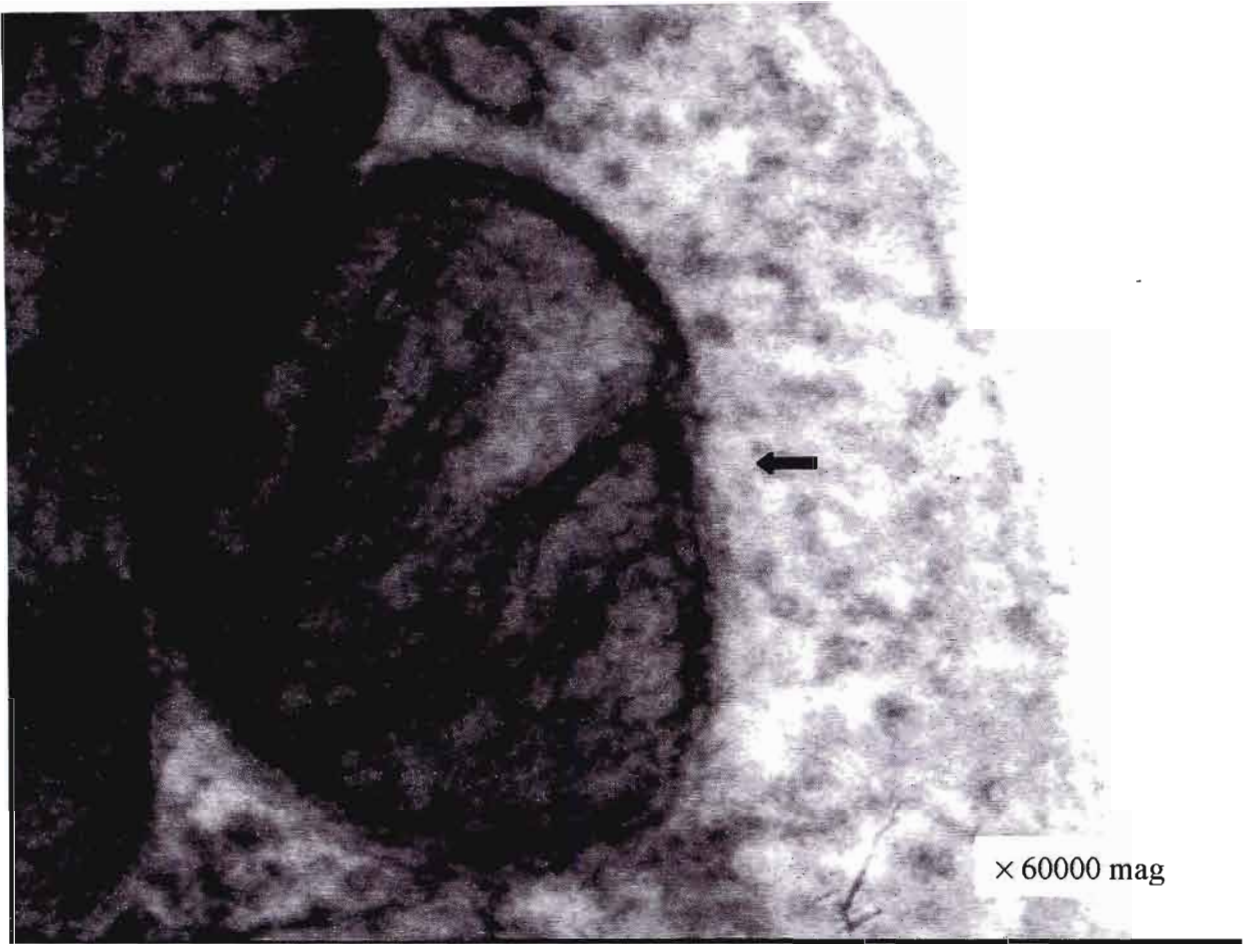


Figure 28 Mitochondria of control lymphocyte (24 hours) associated with normal parallel arrays of cristae (black arrow).

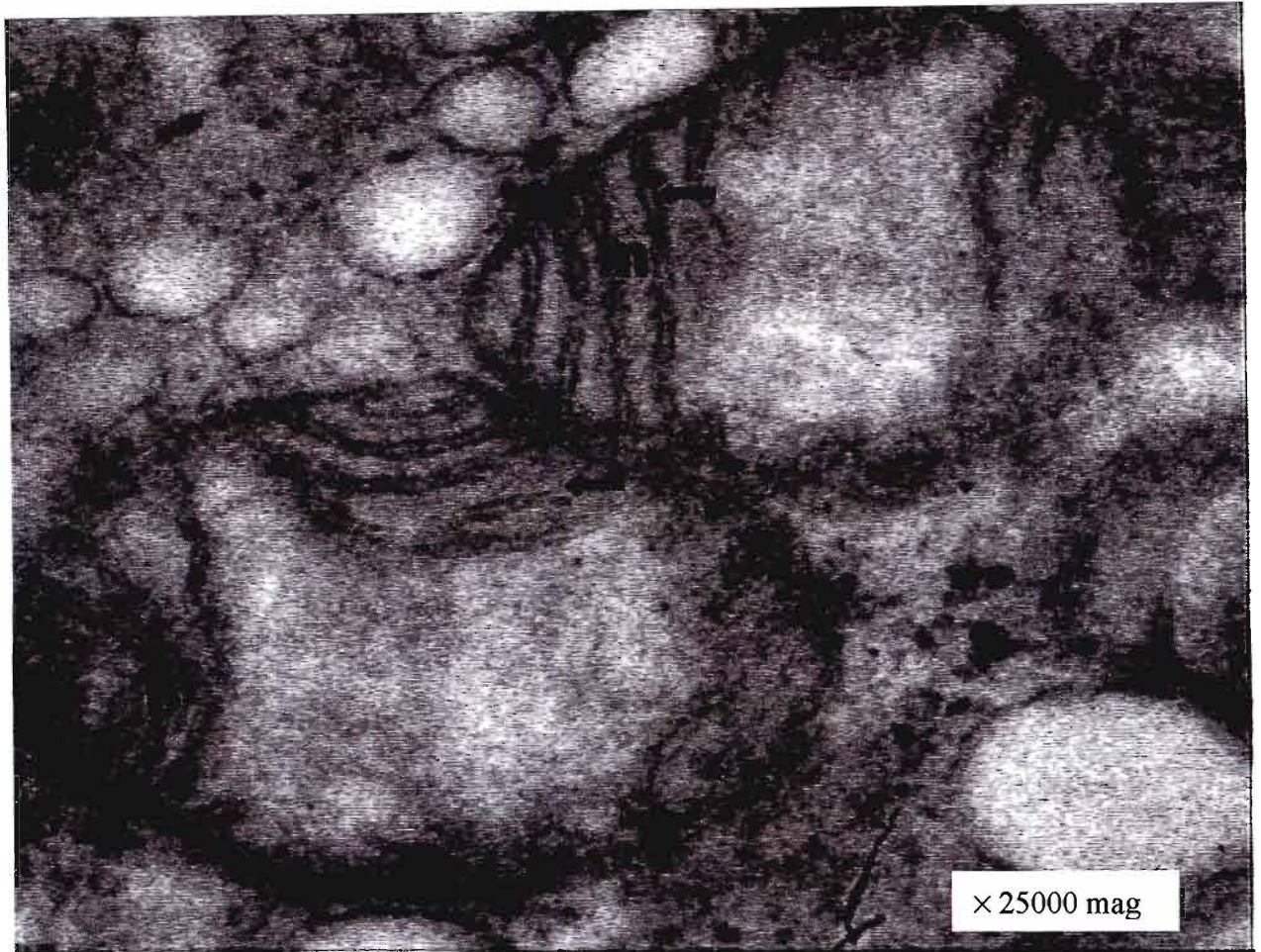


Figure 29 1000µM FA treated lymphocytes (24 hours). Mitochondria (m) are characteristically swollen. There is substantial clearing in the centre of the mitochondria. The cristae (black arrows) are displaced and almost exclusively located on the periphery of the mitochondria.

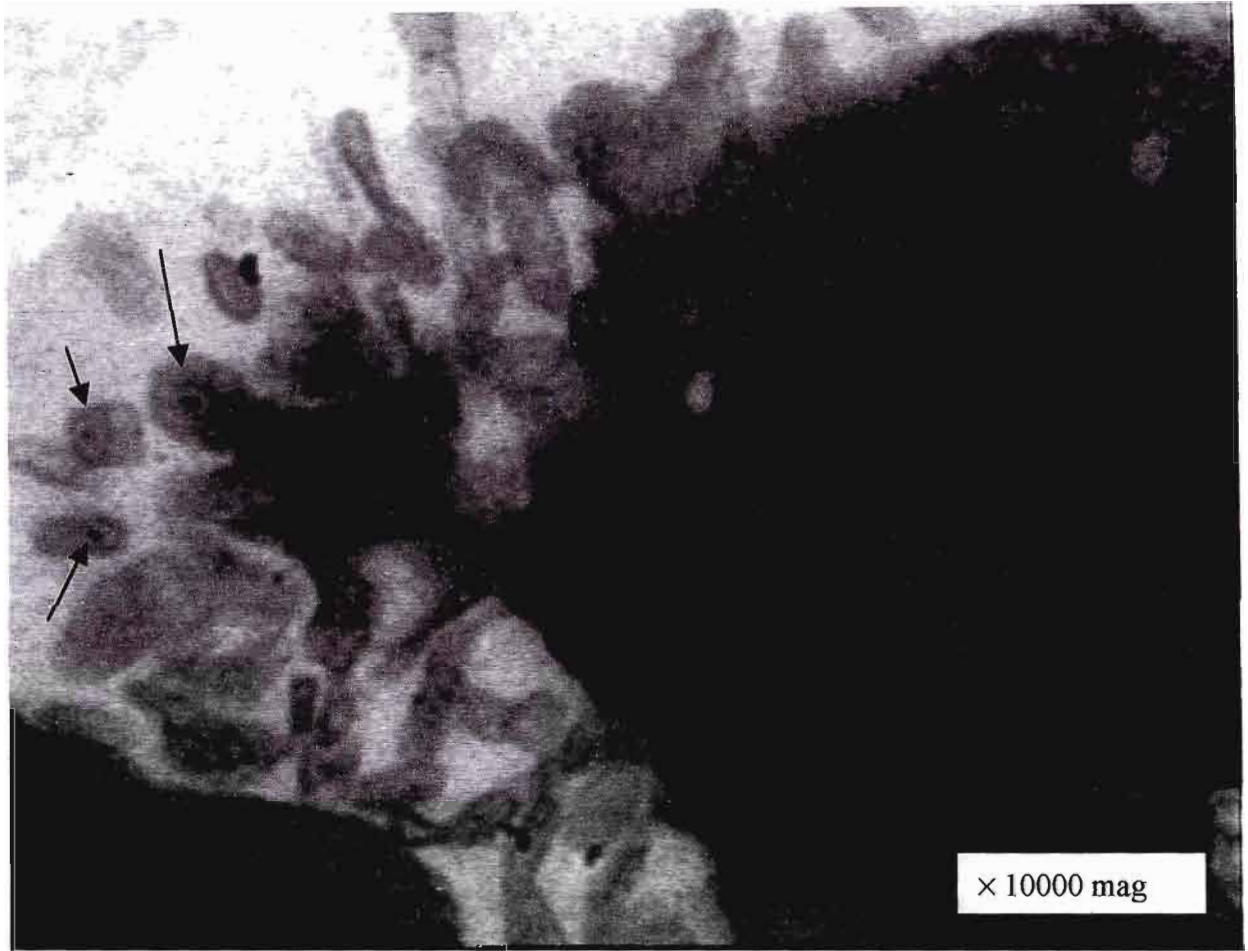


Figure 30 200µl FA treated lymphocyte exhibiting budding of numerous membrane bound vesicles from the apoptotic cell. Membrane bound organelles are clearly distinguishable (arrows).

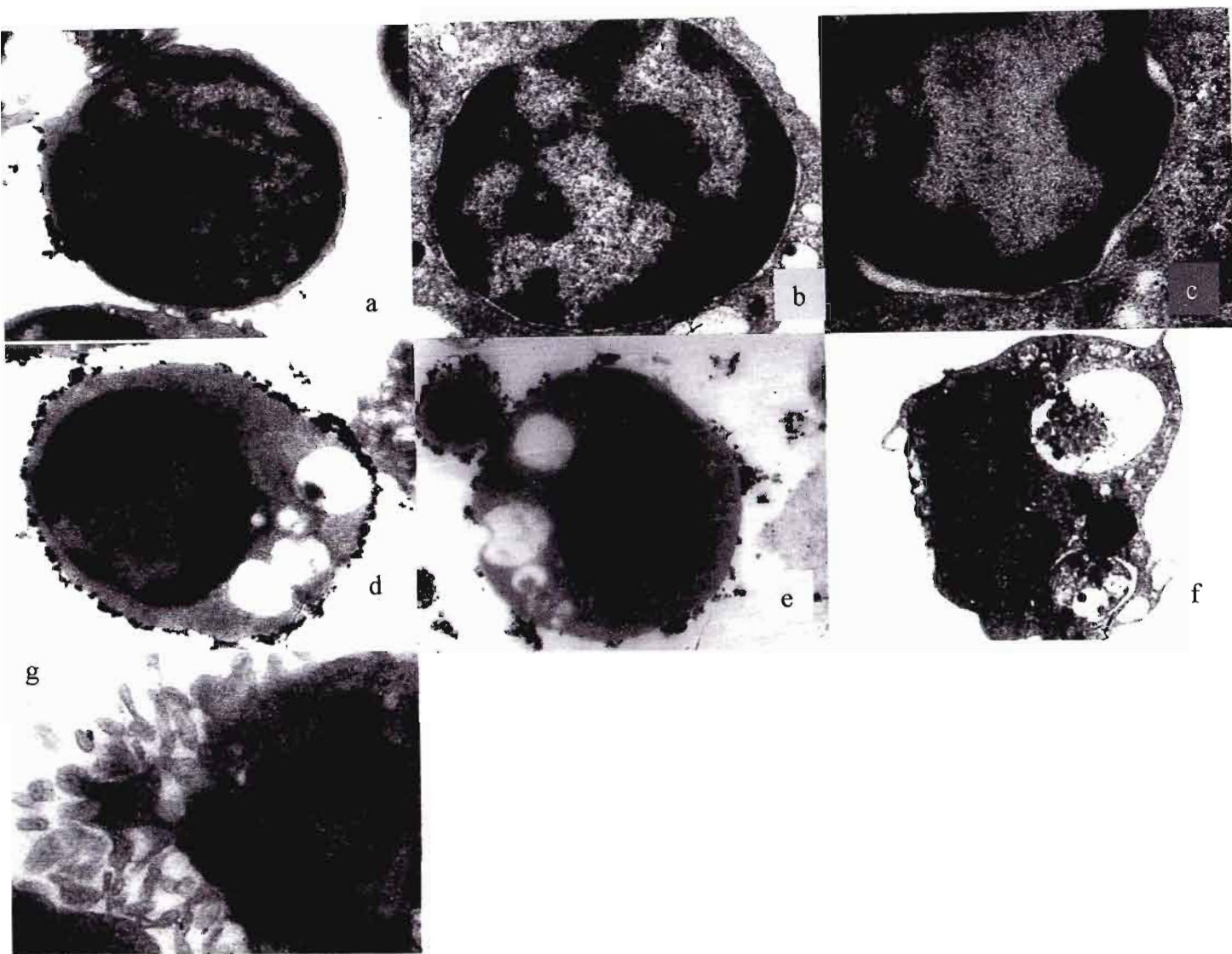


Figure 31 The stages of apoptosis in fusaric acid treated lymphocytes. a) The normal cell has a sparse cytoplasm and heterogeneous nuclear chromatin. b) The cell has lost some volume and its cytoplasmic organelles are not tightly packed. Clumping of chromatin occurs. Membrane changes occur that can lead to phagocytosis. c) Chromatin withdraws towards the periphery of the nucleus. The cell usually exhibits zeiosis at this stage. d) The chromatin begins to collapse down into crescents along the nuclear envelope. e) The nucleus at this stage collapses into a black hole. f) The collapsed nucleus breaks down into spheres. g) The cell fragments into apoptotic bodies which continues to exclude vital dyes for some time.

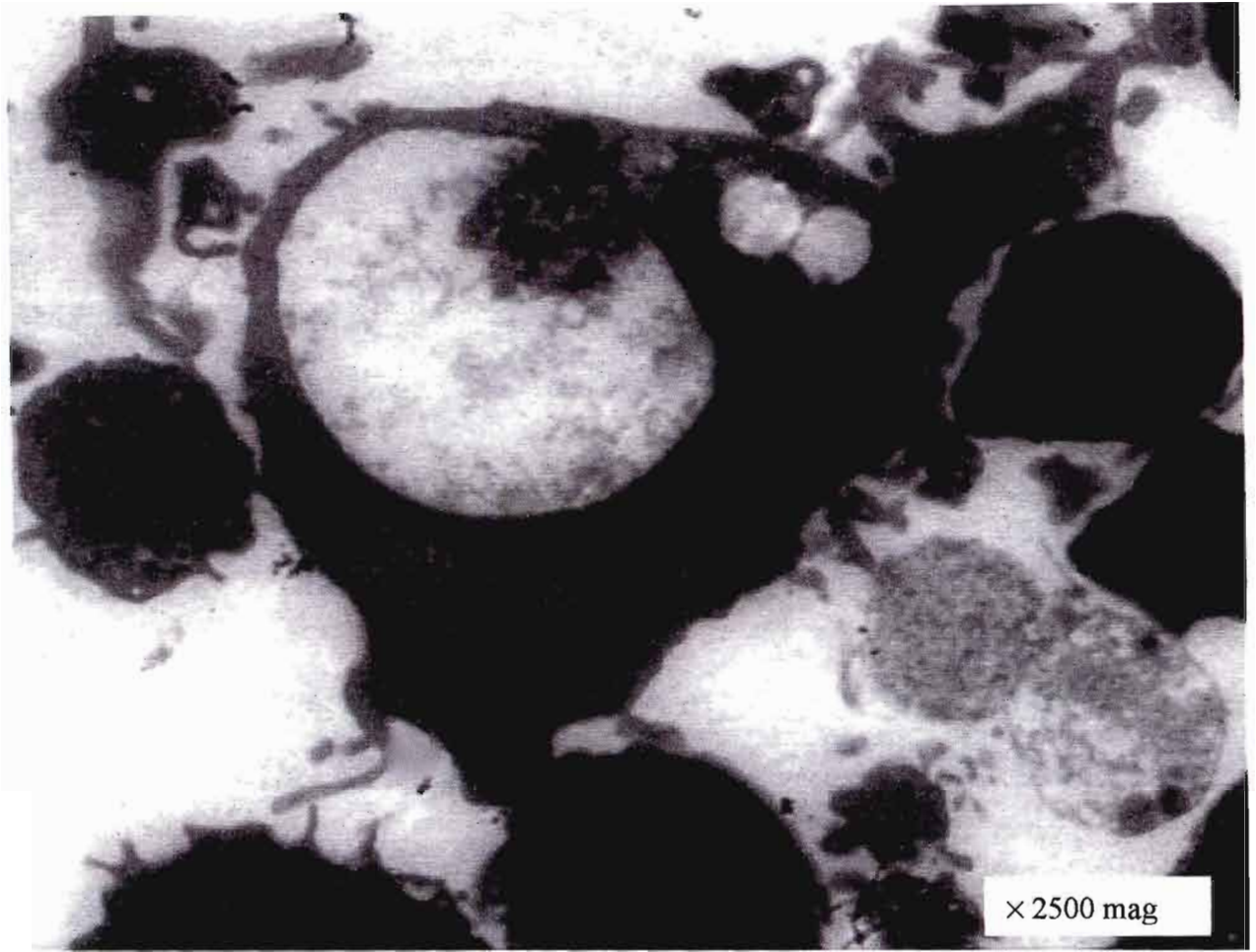
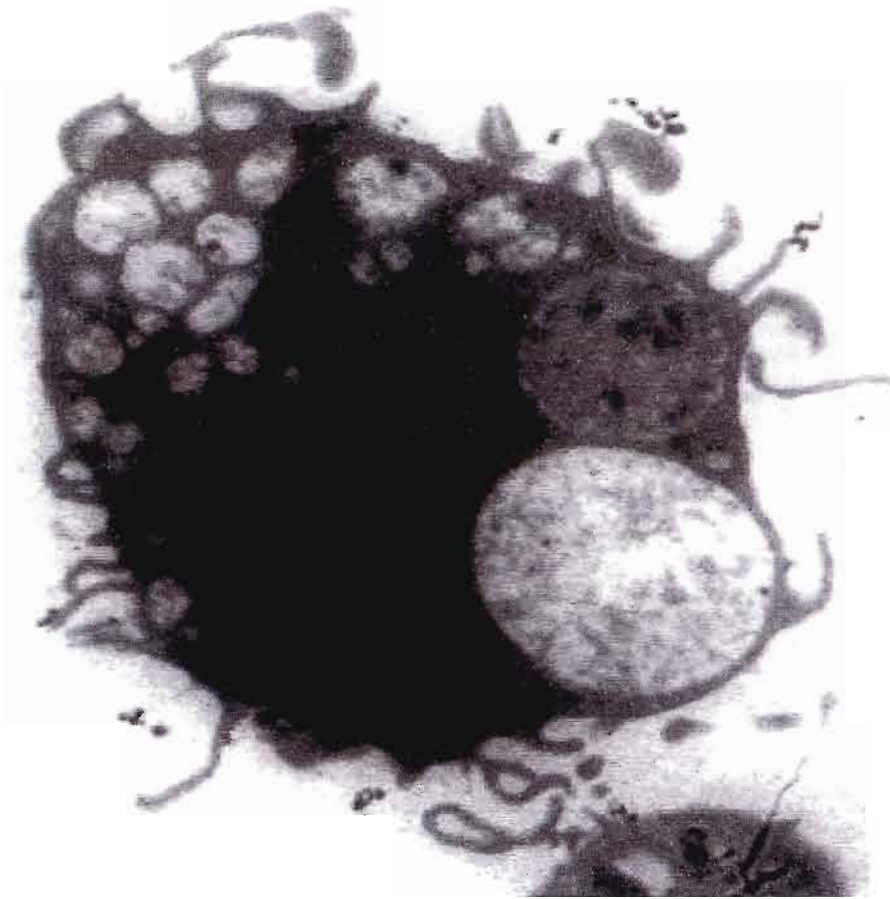


Figure 32 Lymphocyte treated with 200 μ M fusaric acid for 24 hours exhibiting large vacuole.



× 2500 mag

Figure 33 Lymphocyte treated with 200 μ M fusaric acid for 24 hours exhibiting numerous vacuoles of different sizes.

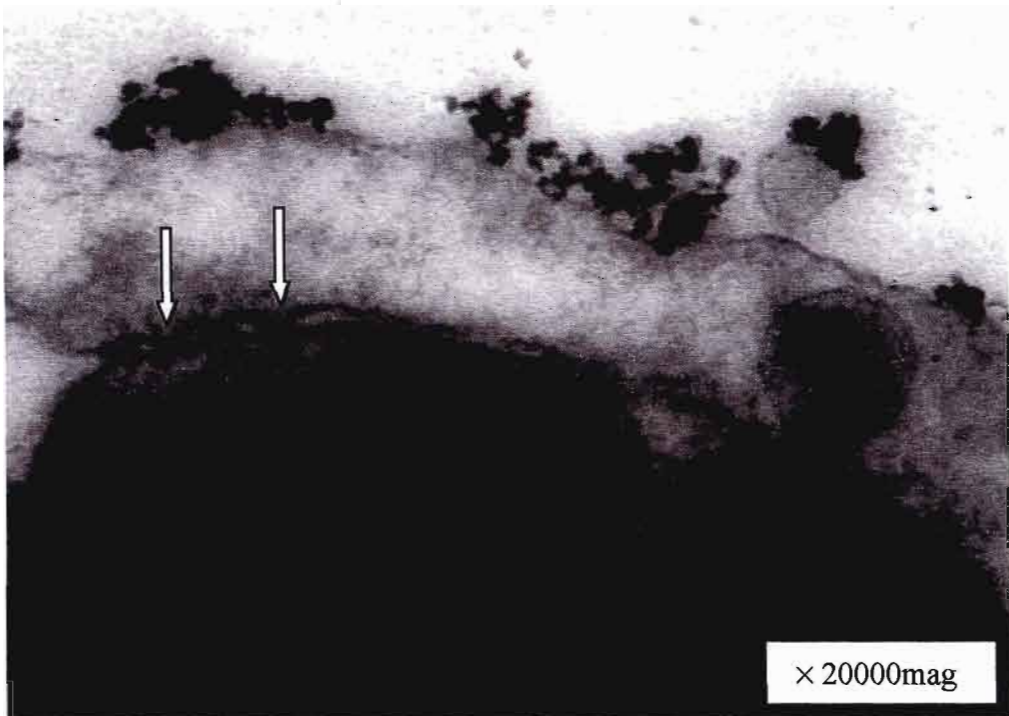


Figure 34 Nucleus of control lymphocyte exhibiting distinct nuclear pores (arrows).

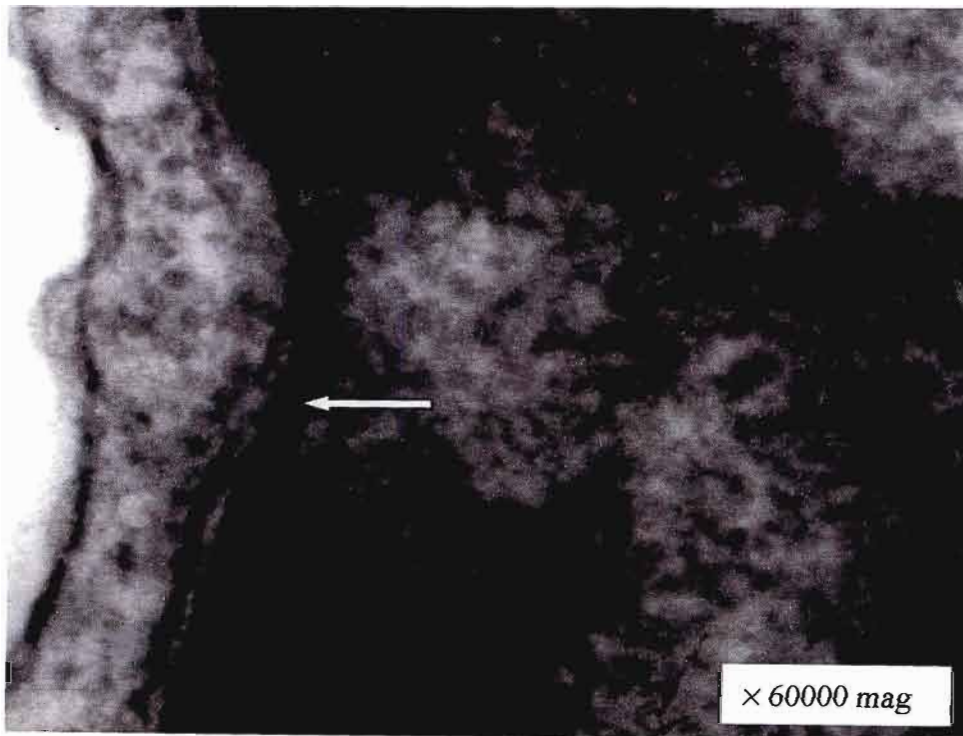


Figure 35 Nucleus of control cell displaying lamina across nuclear pore.

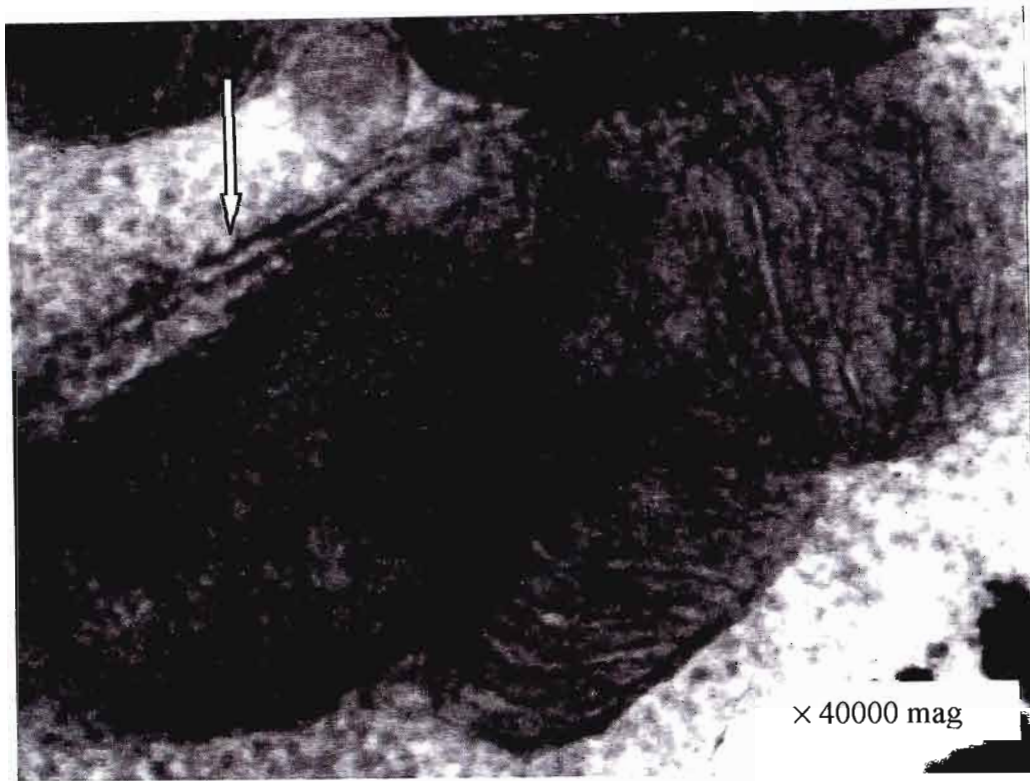


Figure 36 Endoplasmic reticulum of control cell (arrow).

The mechanism via which FA exerts its effect on cells is currently unknown although theories have been put forth. Mitochondria of treated lymphocytes exhibited relatively electron-lucent matrices which may be due to mitochondrial matrix lysis. This was the most characteristic form of swelling, ie., that of the inner chamber containing the mitochondrial matrix (Fig 29) (Ghadially, 1982).

Swollen or hydropic mitochondria occur due to the influx of water and solutes into the organelle, and can be caused by numerous agents that produce cell damage. Two types of swelling are distinguishable:

- 1) a passive swelling, which can be produced by altering the osmolarity of the medium

2) an active swelling, which is dependant on electron transport and can be brought about in isotonic solutions by adding minute amounts of various swelling inducing agents, such as phosphorus, calcium, vasopressin, insulin and hydrocortisone.

The swelling of mitochondria together with the swelling and vesiculation of the rough endoplasmic reticulum, constitutes the change called cloudy swelling by pathologists.

The commonest form of swelling is that due to the involvement of the matrix or inner chamber. Mild degrees of swelling are characterized by a modest increase in the size of the mitochondria, and dilution of the matrix evidenced by a decreased density, is barely discernible. The cristae are however commonly displaced to the periphery and show varying degrees of disorientation, shortening and reduction in numbers. During this period, although appearing somewhat paler, it retains its homogeneous character. Advancing hydration causes a patchy appearance due to development of multiple electron-lucent foci and in time frank cavitation of the mitochondrial matrix occurs. Matrix density is initially lost due to dilution but later there is also a loss of matrix substance. Grossly swollen mitochondria also exhibit breaks in the mitochondrial-limiting membranes (Ghadially, 1982).

The term 'cloudy swelling' was coined to describe intracellular water accumulation in cells subject to toxic stress. The pathogenesis underlying cloudy swelling is still not fully understood, but it is believed to involve a failure of cellular osmotic control mechanisms. It seems that damage and swelling of mitochondria suppresses ATP production, which in turn leads to a failure of the ATP-dependant sodium potassium pump at the cell membrane, resulting in the cellular compartments becoming flooded with water (Ghadially, 1982).

It is believed that its protonophore activity can uncouple oxidative phosphorylation and thus alter ATP synthesis. It is also possible that mitochondrial electron transport is directly inhibited at the cytochrome oxidase level by the toxin and depolarization of the plasma membrane decreases cellular ATP levels (Arias, 1985). This decrease in cellular ATP could lead to a failure of the ATP-dependant sodium potassium pump at the cell membrane, thus leading to an influx of water into cellular compartments (Ghadially, 1982).

The mitochondria of all aerobic cells produce superoxide anions and other reactive oxygen species (ROS) as normal by-products of electron transfer. The excessive production of ROS has long been known induce cellular death by causing massive oxidative damage to cellular components. Cells employ antioxidants and other safeguards to keep these potentially dangerous chemicals in check. Recent data suggests that ROS may play a role in apoptotic as well as necrotic cell death (Thress *et al.*, 1999).

While the roles of ROS and electron transport disruption in apoptosis cannot be ignored, mitochondria do participate actively in apoptotic cell death through the release of proapoptotic (apoptogenic) factors. The most common of these factors is cytochrome c. It was shown in a variety of different systems that cytochrome c is released from the mitochondria following propagation of a "death" signal. It is possible that FA provides this death signal that initiates the process of apoptosis.

Respiration of cells is inhibited by FA within as little as an hour. Secretory organelle alterations induced by respiratory inhibitors possibly results from inhibition of specific energy-dependant steps in endomembrane flow between secretory organelles (Arias, 1985).

Ultrastructural evaluations of FA treated lymphocytes have thus demonstrated that FA kills these cells by apoptosis and that its mode of action predominantly involves the mitochondria.

Chapter 6

6. Detection of apoptotic cells by light scatter analysis

The intersection of a cell with the light of a laser beam in a flow cytometer results in light scatter. Analysis of this scattered light provides information on the cell size and structure (Fig 37) (Omerod *et al.*, 1995).

The forward light scatter is associated with cell size while light measured at right angle to the laser beam ("side scatter") correlates with granularity, refractiveness and the ability of the intracellular structures to reflect light. During the process of death this inherent ability of the cell to scatter light is altered. This is reflected in the morphological changes such as cell swelling or shrinkage, rupture of the plasma membrane, chromatin condensation nuclear fragmentation and shedding of apoptotic bodies (Gorczyca *et al.*, 1997).

Necrosis is characterized by a rapid initial increase in the cells ability to scatter light simultaneously in the forward and right angle direction which is indicative of cell swelling. By contrast especially in the later stages of apoptosis the intensity of light scattered at both forward and right angles decreases (Gorczyca *et al.*, 1997). A change in light scatter alone does not imply the occurrence of apoptosis and necrosis. It is possible that mechanically broken cells, isolated nuclei, or cell debris may exhibit similar light scatter properties to apoptotic or necrotic cells. Other methods need to be employed to enhance measurements and provide a more definite identification of these phenomena (Gorczyca *et al.*, 1997).

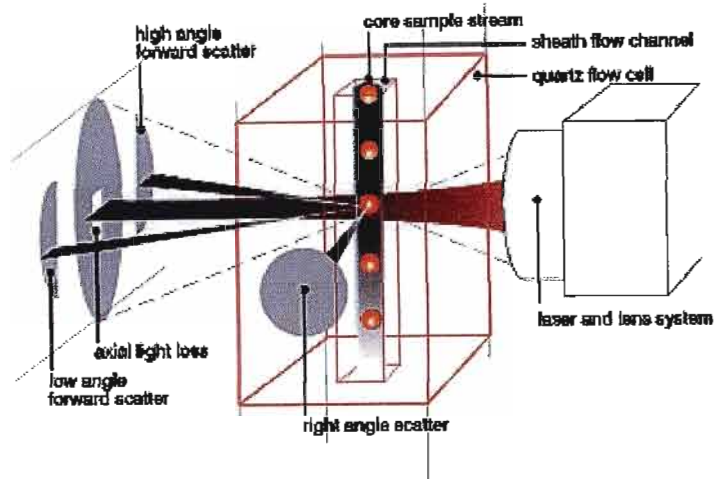


Figure 37 Diagrammatic representation of functional components and light scatter in a flow cytometer
www.idexx.com/.../InClinic/Catalog/lasergraphics.cfm.

6.1 Apoptotic assessment/quantification by detection of phosphatidylserine with Annexin V-FITC conjugate

Apoptotic cells possess the ability to trigger their own engulfment by phagocytic cells prior to cell lysis in order to avoid tissue damage and inflammation associated with necrosis. Timely generation of recognition signals on the surface of apoptosing cells is therefore a key event in the apoptotic program (Verhoeven *et al.*, 1995).

Phospholipids found within the plasma membrane are asymmetrically distributed between the inner and outer leaflets of the plasma membrane. In live cells phosphatidylserine (PS) is almost exclusively observed on the inner surface of the membrane. It has recently been shown that loss of phosphatidyl asymmetry leading to exposure of PS on the outside of the plasma membrane is an early event in apoptosis. Annexin V, a Ca^{2+} -dependant phospholipid-binding protein, has high affinity for negatively charged phospholipids like PS (Vermes *et al.*, 1995, Koopman *et al.*, 1994).

Annexin when conjugated with a fluorochrome can be used as a sensitive probe for the presence of PS on the outside of the plasma membrane (Fig 38). The relocation of PS to the outer membrane is not exclusive to apoptosis but also occurs during necrosis. A combination of Annexin V-FITC conjugate and propidium iodide (PI) alleviates this problem. During apoptosis, the cells take up Annexin V after the onset of chromatin condensation but prior to the loss of the plasma membrane's ability to exclude cationic dyes, such as PI (Vermes *et al.*, 1995, Koopman *et al.*, 1994).

Nonapoptotic cells are Annexin V and PI negative, early apoptotic cells are Annexin

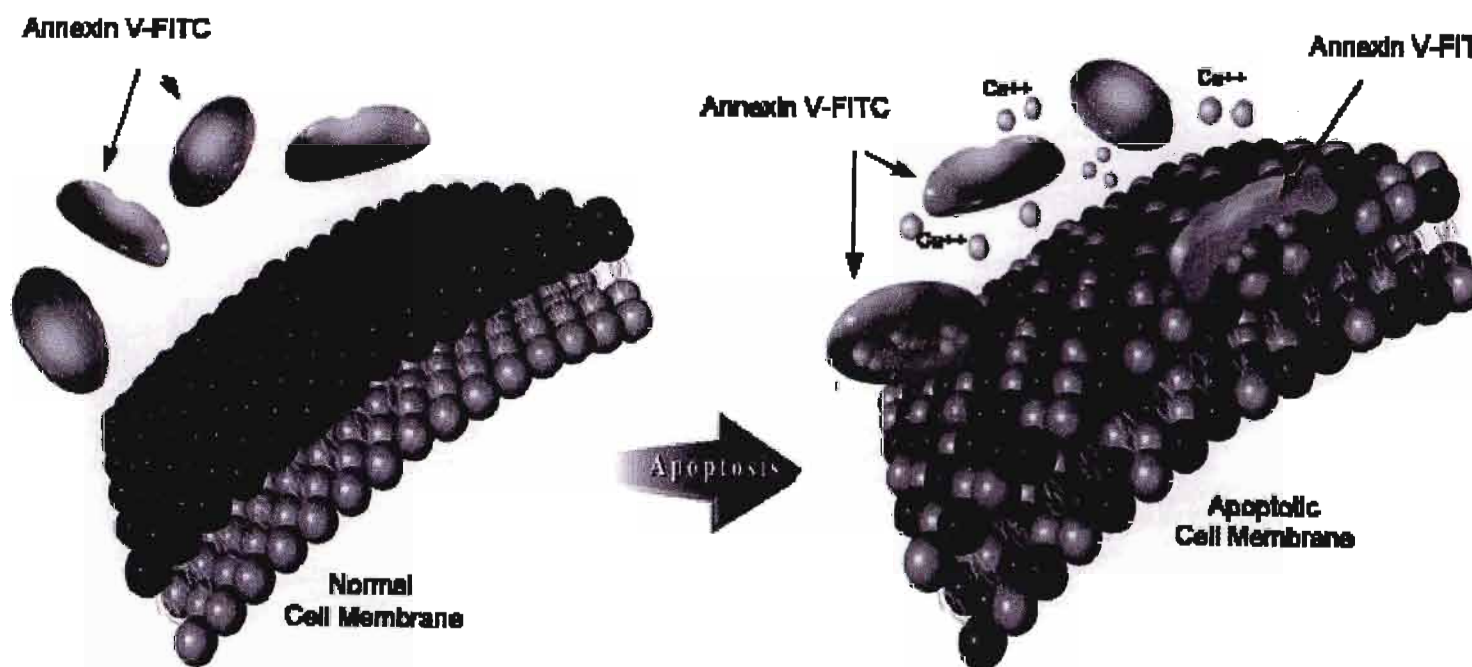


Figure 38 Annexin V-FITC can be used as a sensitive probe for the presence of PS on the outside of the plasma membrane of apoptosing cells (www.southernbiotech.com/techbul/10010.pdf).

positive and PI negative, and late apoptotic cells as well as necrotic cells are stained intensely with PI. Results obtained are best interpreted from three dimensional contour plots (Fig 39) or density plots (Fig 40).

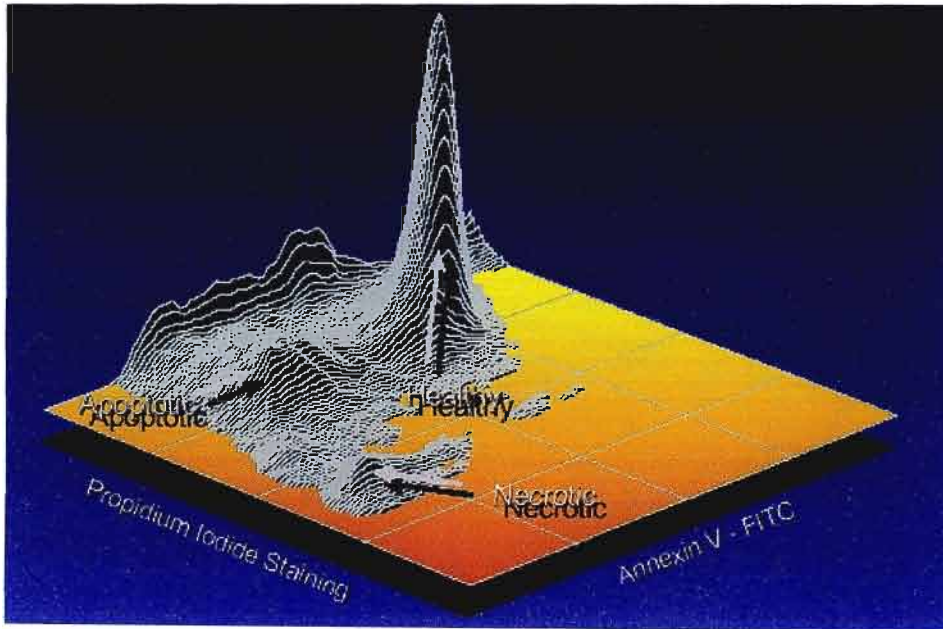


Figure 39 Dual parameter three dimensional contour plot exhibiting healthy apoptotic and necrotic cells (www.fcm-ntsrvr01.utmb.edu/apo.pdf).

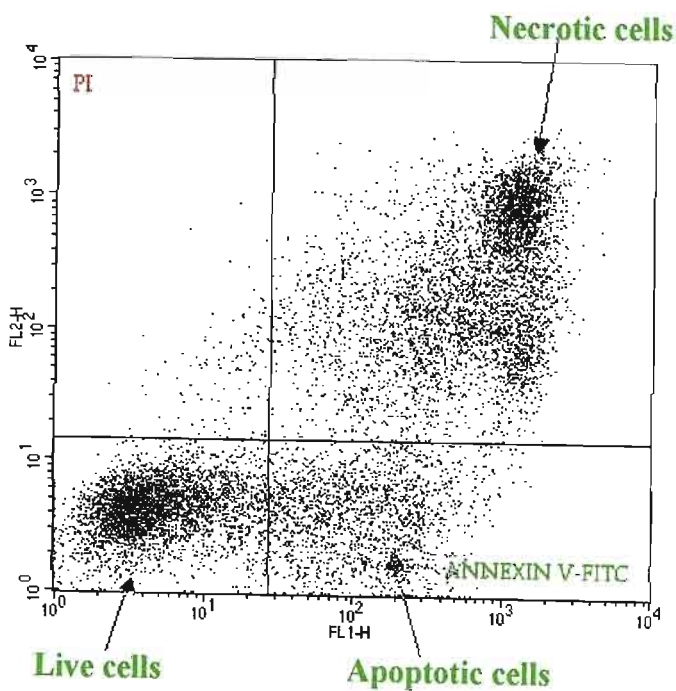


Figure 40 Dot plot exhibiting live, apoptotic and necrotic cells.

6.2 The role of phosphatidylserine in apoptosis

Membrane phospholipid asymmetry is ubiquitous. The outer membrane of the eukaryotic cell predominantly contains cholinephospholipids (sphingomyelin and phosphatidylcholine [PC]), whereas the majority of the aminophospholipids (phosphatidylserine [PS] phosphatidylethanolamine [PE]) are confined to the membranes inner leaflet. This means that asymmetric biomembranes are assembled and maintained by specific mechanisms that control transbilayer lipid sidedness. Asymmetry is generated by the activity of an adenosine triphosphate (ATP)-dependant aminophospholipid translocase that specifically transports PS and PE between bilayer leaflets. Loss of membrane asymmetry is associated with many physiologic and pathologic phenomena. Three mechanisms are thought to regulate membrane lipid asymmetry. Two of these are energy-requiring activities that seem to work together to maintain a non-random transbilayer phospholipid orientation. Calcium influx into the cytoplasm activates a scramblase activity that leads to phospholipid asymmetry across the membrane bilayer (Fig 41).

6.2.1 Aminophospholipid translocase.

The discovery of an ATP-dependant aminophospholipid translocase in red blood cells yielded evidence for the existence of mechanisms that generate and maintain membrane asymmetry through the transport of specific lipids across the cell's membrane (Seigneuret and Devaux, 1984). Aminophospholipid translocase transports PS and PE from the outer to inner leaflet of plasma membranes against the concentration gradient. Cholinephospholipids are not moved.

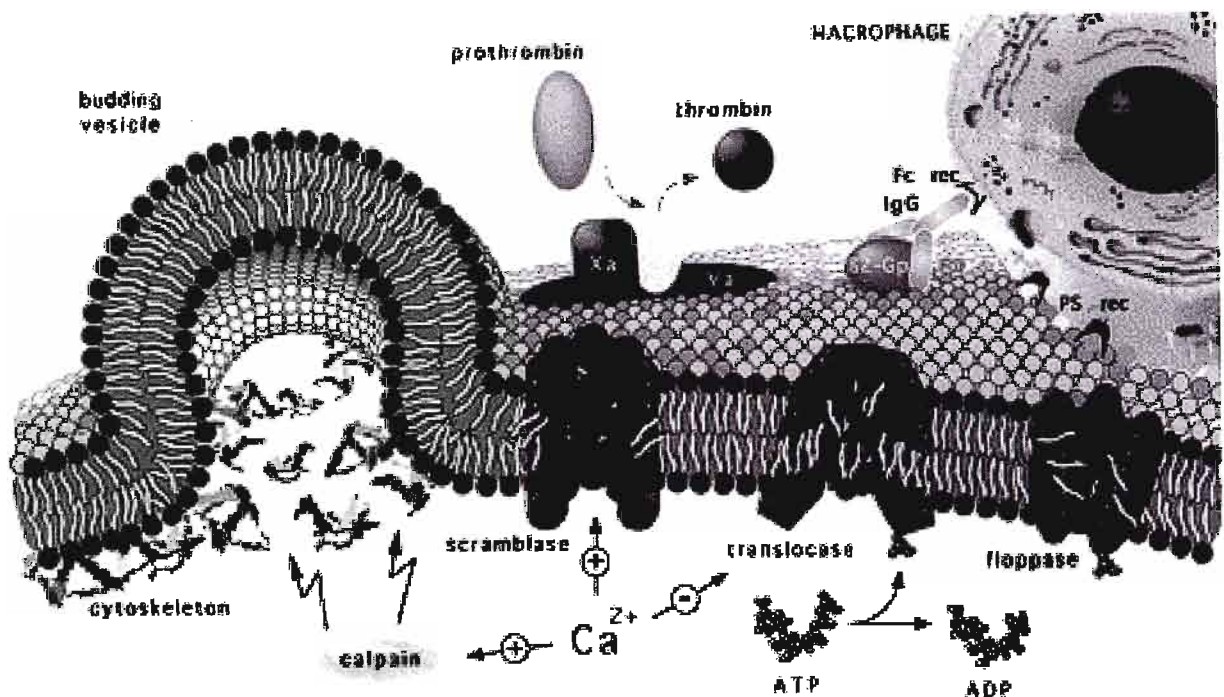


Figure 41 The regulation and physiology of membrane phospholipid asymmetry. Membrane lipid asymmetry is regulated by the cooperative activities of three transporters. The ATP-dependent aminophospholipid-specific translocase, which rapidly transports PS and PE from the cell's outer-to-inner leaflet; the ATP-dependent non-specific lipid floppase, which slowly transports lipids from the cell's inner-to-outer leaflet; and the Ca^{2+} -dependent non-specific lipid scramblase, which allows lipids to move randomly between both leaflets (Zwaal and Schroit, 1997).

Competition experiments have demonstrated that the same protein transports both PS and PE, although PS is transported much faster, with half-times of 5 to 10 minutes (Morrot *et al.*, 1989; Connor *et al.*, 1992). This process consumes one molecule of ATP per molecule of lipid transported (Beleznay *et al.*, 1993). The identity of this translocase was initially unknown. An ATPase was initially isolated and reconstituted into artificial lipid vesicles with at least a fraction of its active centre at the outer face.

It was found that these vesicles were capable of translocating a spin-labelled PS analogue from the inner to outer leaflet of the membrane upon addition of Mg^{2+} -ATP. It was later found that the isolated fraction was not homogenous and that it consisted of numerous proteins ranging from 35 kD to 120 kD. These observations meant that the transporter was in all likelihood not a single protein and are consistent with studies implicating the involvement of a 30-kD to 32-kD band 7 transmembrane polypeptide in aminophospholipid transport (Connor and Schroit, 1988). Aminophospholipid translocase activity has been observed in other membranes, including intracellular chromaffin granule membranes (Zachowski *et al.*, 1989), and endoplasmic reticulum (Hermann *et al.*, 1990). Activity has also been shown in various cells, including endothelial cells, in which its expression is regulated by basic fibroblast growth factor (Tilly *et al.*, 1990).

6.2.2 ATP-dependent floppase

In addition to aminophospholipid translocase another ATP-dependent translocating activity has been observed. This factor apparently regulates the differential transbilayer orientation of phospholipids in complex biologic membranes. This less specific ATP-requiring floppase, transports both aminophospholipids and cholinephospholipids from the inner to the outer leaflet with half-times about 10 times longer than those of the translocase-mediated inward movement of PS and PE. In a similar manner to the inward transport of aminophospholipids, outward movement was found to be cancelled by ATP depletion, sulfhydryl oxidation, and histidine modification indicating that this process is also energy and protein-dependent (Connor *et al.*, 1992). Both lipid-transporting processes seem to act together and establish a dynamic asymmetric steady-state in which all phospholipids are slowly but continuously moved to the outer membrane surface,

whereas the aminophospholipids are shuttled directly back to the inner leaflet. Translocase and floppase thus seem to furnish the cell with a mechanism that corrects against any alterations in lipid distributions to avoid any pathological situations. Although cells may be resistant to lipid asymmetry changes in the peripheral circulation, changes in lipid asymmetry could be coincident with different membrane fusion processes linked with endocytosis and exocytosis (Tilly *et al.*, 1990).

6.2.3 Lipid Scramblase

A Ca^{2+} -dependent mechanism existing in platelet plasma membranes can rapidly move phospholipids back and forth between the two membrane leaflets, leading within minutes to a loss of membrane lipid asymmetry. An influx of calcium in this instance means a loss of function of the translocase system and thus a lack of a correctional system for membrane asymmetry. Unless aminophospholipid translocase is not irreversibly inactivated by intracellular calpain, Ca^{2+} efflux can lead to restoration of lipid asymmetry. Scramblase by contrast to the other energy requiring activities does not require hydrolysable ATP. It is believed that a 37 kDA protein is responsible for the scrambling activity (Basse' *et al.*, 1996). Lipid scrambling could also possibly be the result of a complex between phosphatidylinositol 4,5-bisphosphate and calcium (Sulpice *et al.*, 1994).

Basically, the synchronous and cooperative action of the aminophospholipid translocase and the non-specific floppase contribute to the generation and maintenance of membrane phospholipid asymmetry, whereas lipid scramblase activity results in its collapse.

6.3 Annexins

The annexins are a group of homologous proteins that bind phospholipids in the presence of calcium. They are instrumental in providing a major pathway for communication between cellular membranes and their cytoplasmic environment. These proteins may be involved in intracellular membrane trafficking as well as in the regulation of a wide array of calcium-dependant events on membrane surfaces (Creutz, 1992). Annexins are characterized by a "bivalent" activity in the sense that they possess the ability to draw two membranes together (Creutz, 1992).

6.3.1 Annexin structure

The basic structure of the annexins consist of four or eight repeats of 70 amino acids in length. The repeats are approximately 40-60% identical in sequence. The "endonexin fold" is a highly conserved 17 amino acid sequence. The annexins possess different sequences at their amino termini. These termini serve as regulatory regions, providing attachment sites for additional subunits (p10 or calyculin) (Glenney *et al.*, 1986; Towle and Treadwell, 1992) and sites for phosphorylation by protein kinase C (Schlaepfer and Haigler, 1988).

Proteolytic cleavage at these termini alters the calcium sensitivities of these proteins. High resolution structures have been obtained for conformations of annexin V (Fig 42). Each of the 70 amino acid domains in the annexin protein forms a bundle of five, almost parallel (or anti parallel), alpha helices wound into a right handed superhelix. The path existing between these polypeptide chains serves to stitch them into a tight protein domain.

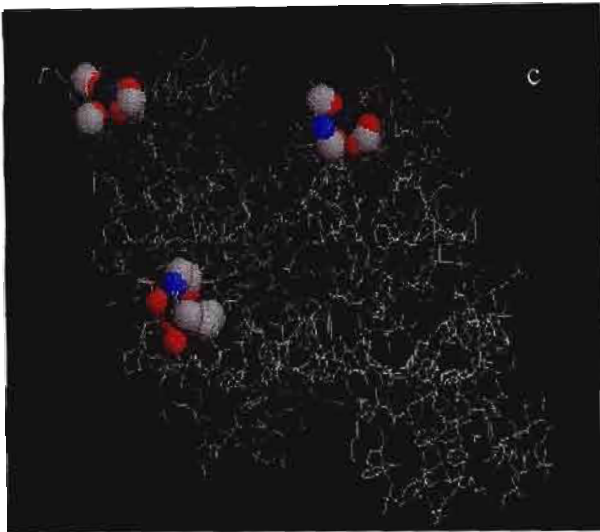
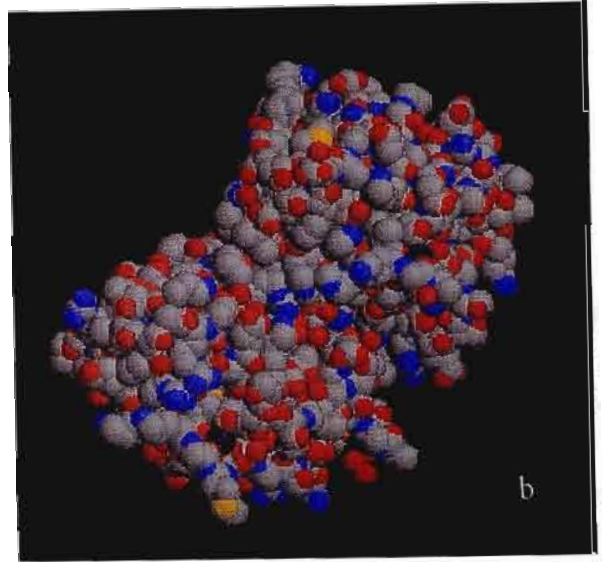


Figure 42 a)The alpha helices of annexin V.
b) The three dimensional structure of annexin V.
c) The three binding sites of annexin V
(www.bssv01.lancs.ac.uk/StuWork/BIOS316/Bios31697/annexin.htm).

The four domains are orientated about a central hydrophilic channel in an approximately planar manner. The calcium binding sites are all found on one side of the planar annexin molecule. This also forms the membrane binding face. Three high affinity and two lower affinity binding sites exist. The first few residues of the endonexin fold and, unexpectedly, amino acid residues in a second loop, 39 residues downstream, form an integral part of each high affinity calcium binding site. The overall structure of the annexin calcium binding site bears remarkable resemblance to that of the calcium-binding site found in secreted phospholipase. There exists however, no extended sequence similarity between these protein families (Verheij *et al.*, 1980).

Annexin V possesses a particularly short regulatory amino-terminal tail. This amino terminal tail is present on the slightly concave face (the "cytoplasmic face") opposite the membrane-binding face. It forms a cinch which attaches the first domain to the fourth domain and thus maintains the circular arrangement of the 70 amino acid domains (Verheij *et al.*, 1980).

6.3.2 Implications of the annexin structure

Annexins are similar but not identical. Different domains may therefore be specific for different lipid head groups. Annexins possess the ability to distinguish different organelle membranes. This stems from the fact that four or eight repeats are present in each annexin enabling them to integrate information about the lipid composition of membranes (Creutz, 1992).

Annexins differ quite significantly in structure. The presence of an array of annexins within a single cell might provide a complex system for sensing, or modulating, local membrane lipid compositions (Creutz, 1992).

The question arises as to how these proteins can express a "bivalent" character and pull two membranes together when the localization of all the calcium and phospholipid-binding sites occur on one face of the annexin molecule. With regard to annexin ii, in which the p10 binding site near the amino terminus of the heavy chain presumably faces the cytoplasm, as does the annexin V amino terminus, it is possible that the two heavy chains have opposite orientations and can therefore bind two approaching membranes simultaneously. A protein self association event seems to be the most likely explanation for the other annexins (Creutz, 1992).

Annexin V possess a hydrophilic central channel and bundles of α helices orientated perpendicular to the membrane surface. This makes it very similar to the predicted structure of transmembrane ion channels. Annexin V forms voltage dependant ion channels across synthetic lipid bilayers on the tip of a patch pipet. A high degree of ion selectivity is provided by a pathway for ion permeation through the hydrophilic central channel of the protein (Pollard and Rojas, 1988).

The aim of this study was to quantitate the amount of lymphocyte apoptosis induced by FA using a flow cytometric procedure.

6.4 Materials and Method

6.4.1 Materials

The chemicals used in this experiment were purchased from the following suppliers : Phosphate buffered saline tablets (PBS), Ficoll Histopaque 1077, Sterilin tubes (15ml) and Pasteur pipettes (3ml) from Sigma. The Annexin V Fluos staining kit from Roche Diagnostics.

6.4.2 Methods

6.4.2.1 Preparation of lymphocyte samples for flow cytometry

Whole blood 4ml (6 tubes of 4ml each) was collected in lithium heparin Vacutainer tubes by venopuncture from a healthy donor. Lymphocyte isolations were carried out as described in chapter 2. The lymphocyte suspensions (10^6 cells/ml) were prepared and treated in a sterile environment as in chapter 2 and incubated for 1, 4 and 24 hours. Lymphocyte suspensions were treated with a range of serial dilutions and made up to final concentrations of $3\mu\text{M}$, $6\mu\text{M}$, $25\mu\text{M}$, $50\mu\text{M}$, $200\mu\text{M}$ and $400\mu\text{M}$ FA. Positive control cells were treated with $4\mu\text{M}$ camptothecin. Control lymphocytes were untreated. After each respective time interval the lymphocytes (10^6 cells/ml) were collected by centrifugation at $400\times g$ for 5 minutes.

Staining solution was made up by adding $20\mu\text{l}$ of both annexin V-FITC and propidium iodide to $1000\mu\text{l}$ of incubation buffer (Hepes buffer). The lymphocytes were then treated with $100\mu\text{l}$ of staining solution and incubated for 15 minutes at 22°C to allow the cells to take up the respective stains.

6.4.2.2 Flow cytometric analysis

After incubation, $400\mu\text{l}$ of incubation buffer was then added to the stained lymphocytes. The lymphocytes were then analysed on a Becton Dickenson FACS Calibur flow cytometer using a 488 nm excitation and 515 nm bandpass filter for fluorescein detection and a filter greater than 560 nm for PI detection.

Electronic compensation of the instrument was performed to exclude overlapping of the two emission spectra (appendix 6).

6.4.2.3 Data analysis

Acquisition of data was followed by analysis which was performed using Apple Macintosh Cellquest software for flow cytometry. For each concentration at each respective time interval, 100 000 cells were analysed altogether for levels of apoptosis and necrosis.

6.5 Results and Discussion

Annexin V was used to detect PS exposure on the membrane of FA induced apoptotic lymphocytes. It was found that FA induced apoptosis of healthy lymphocytes was easily quantifiable with fluorescein isothiocyanate (FITC)-labelled annexin V (table 4). The first hour of incubation with the various concentrations of FA yielded a substantial increase in the population of apoptotic lymphocytes. The percentage of apoptosis at 400 μ M FA treatment after one hour was almost nine fold greater than that of the control. The population of necrotic cells had also significantly increased with an increase in FA concentration from 3.49 % for the control lymphocytes to 24.42 % for the 400 μ M FA treated lymphocytes ($p < 0.001$).

The 1 and 4 hour incubations did not show a change in forward and side scatter profiles (Fig 43). However, after 24 hours of incubation with all concentrations of FA, a separate population was formed with a lower forward scatter and a higher side scatter profile than the normal lymphocyte population. This is characteristic of apoptotic cells (Gorczyca *et al.*, 1997) (Fig 43). The size of the population increased with an increase in FA concentration. Simultaneously an increasing proportion of the lymphocytes stained positive for annexin V. At 24 hours both single annexin V positive lymphocytes and annexin V /PI double positive lymphocytes were found to have increased (Fig 43). The

double stained necrotic population after 24 hours had increased substantially for all concentrations of FA treated lymphocytes. Lymphocytes in the "apoptotic" low FSC/high SSC subpopulation were all found to be annexin V- positive. At the highest FA concentration ie. 400 μ M, almost all the lymphocytes were double stained with annexin V and PI indicating that PI can only enter the apoptotic cell at a later stage when damage to the cell membrane has occurred. Figures 44a-i show three dimensional contour plots and annexin V/PI density plots that illustrate the change in lymphocyte populations with increasing FA concentrations and time intervals.

TABLE 4 PERCENTAGES OF APOPTOSIS AND NECROSIS IN LYMPHOCYTES AT VARIOUS TIME INTERVALS

	1 hour		4 hours		24 hours	
	Apoptosis	Necrosis	Apoptosis	Necrosis	Apoptosis	Necrosis
Control	5.26 ± 3.8	2.94 ± 2.7	12.96 ± 6.22	7.98 ± 6.74	14.32 ± 6.13	27.94 ± 11.57
4µg/ml *	34.26 ± 10.8	17.38 ± 13.2	45.07 ± 13.3	14.06 ± 0.24	33.43 ± 11.5	23.91 ± 2.26
3µM FA	20.98 ± 9.0	3.47 ± 2.87	21.67 ± 10.3	4.33 ± 0.77	17.27 ± 5.32	17.37 ± 2.79
6µM FA	27.94 ± 9.7	4.74 ± 3.78	19.87 ± 9.6	2.69 ± .08	43.56 ± 7.63	22.57 ± 3.33
25µM FA	48.04 ± 12.9	13.72 ± 8.4	23.51 ± 10.5	5.23 ± 0.84	39.53 ± 8.87	18.6 ± 1.44
50µM FA	37.34 ± 10.4	13.18 ± 8.8	24.15 ± 10.1	4.65 ± .68	35.53 ± 11.08	28.33 ± 2.17
200µM FA	38.23 ± 10.3	19.17 ± 10.5	25.71 ± 10.5	4.29 ± .58	36.87 ± 0.48	50.05 ± 4.43
400µM FA	43.58 ± 14.1	17.02 ± 8.0	31.81 ± 14.1	7.87 ± .60	15.7 ± 12.57	81.75 ± 11.22

*** Postive control : Camptothecin**

Values are given as the mean percentages of three experiments ± the standard deviation of the mean. For each experimental concentration, the values of all treated lymphocytes are significantly different from the controls at $p < 0.001$.

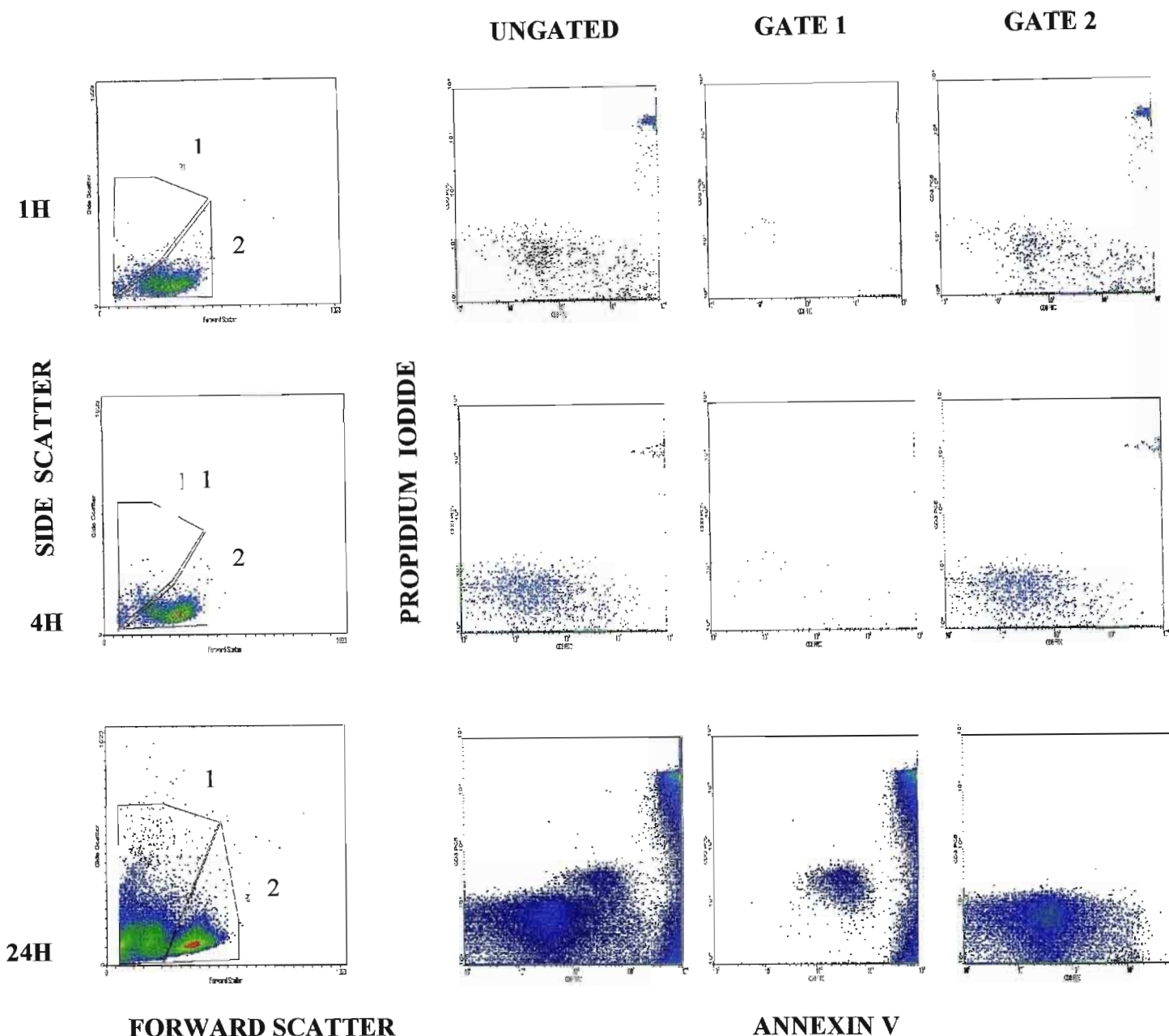


Figure 43 Flow cytometric analysis of apoptosis in FA (50 μ M) treated lymphocytes. Lymphocytes were treated at various concentrations of FA and incubated for 1, 4 and 24 hours. Cells were stained with annexin V and PI. FSC (forward scatter)/ SCC (side scatter) patterns (column 1) and annexin V/EB staining of ungated cells or of cells gated for low FSC/ high SSC profile (gate 1) or high FSC/low SSC profile (gate 2) are shown in columns 2 and 4, respectively. Representative experiment out of three is shown.

One hour contour and density plots of lymphocytes

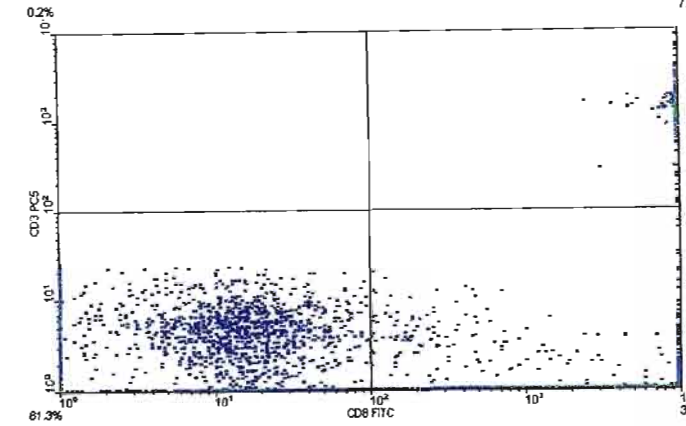
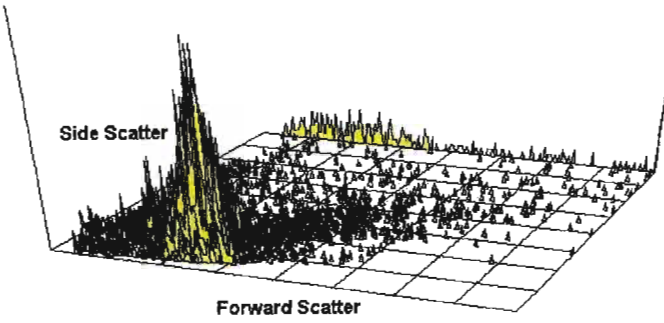


Figure 44a Control 3D contour and density plots at 1 hour incubation.

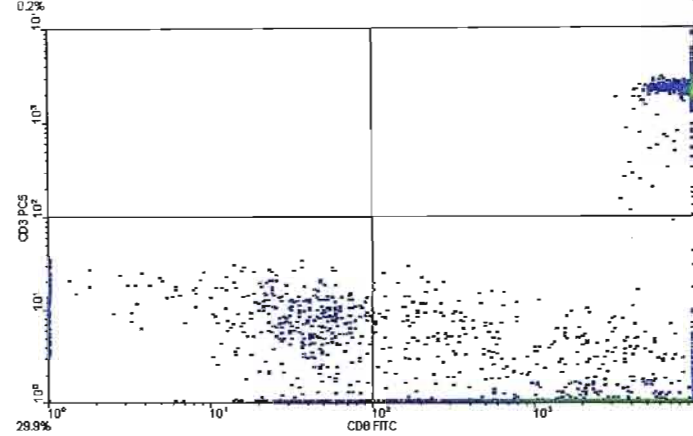
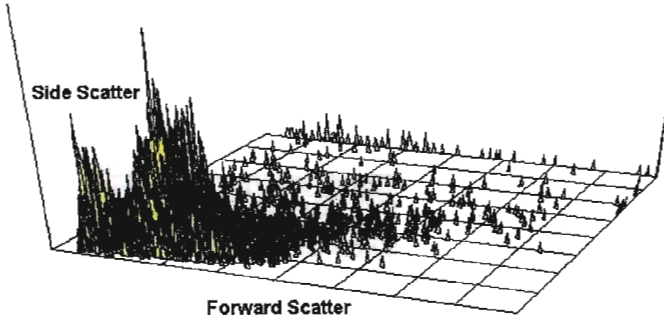


Figure 44b 50µM FA 3D contour and density plots at 1 hour incubation.

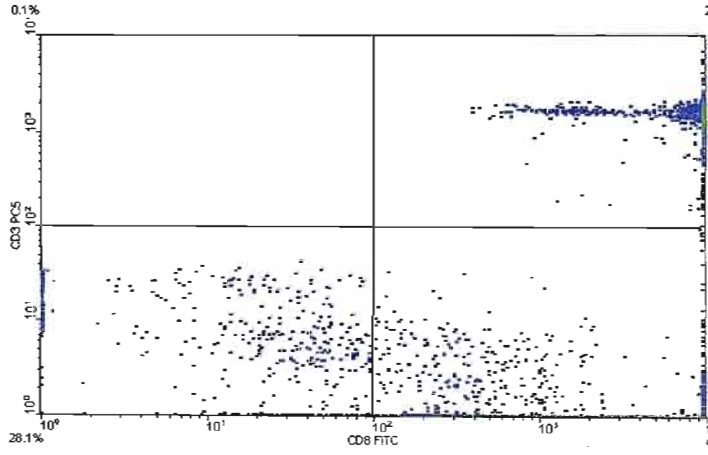
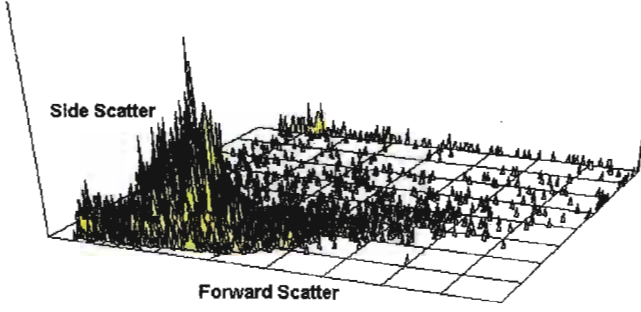


Figure 44c 200µM FA 3D contour and density plots at 1 hour incubation.

Four hour contour and density plots of lymphocytes

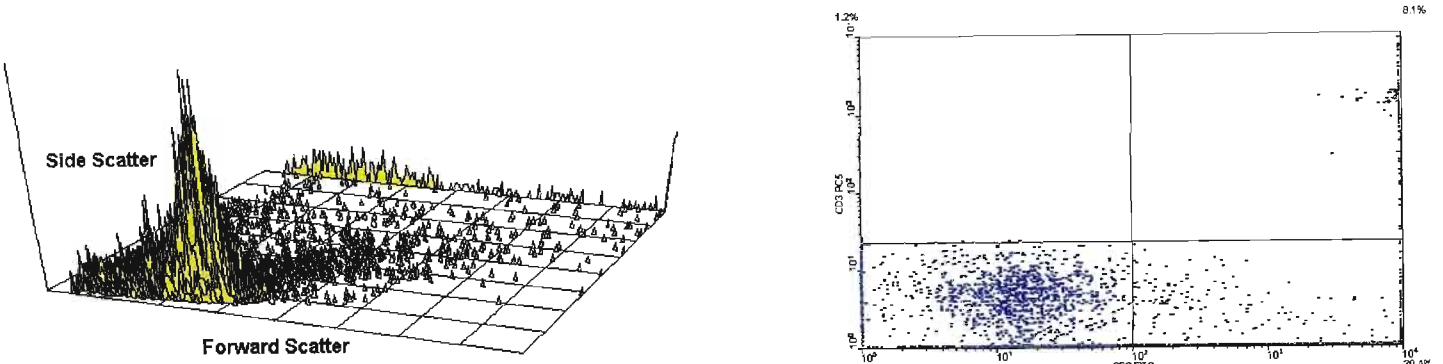


Figure 44d Control 3D contour and density plots at 4 hour incubation.

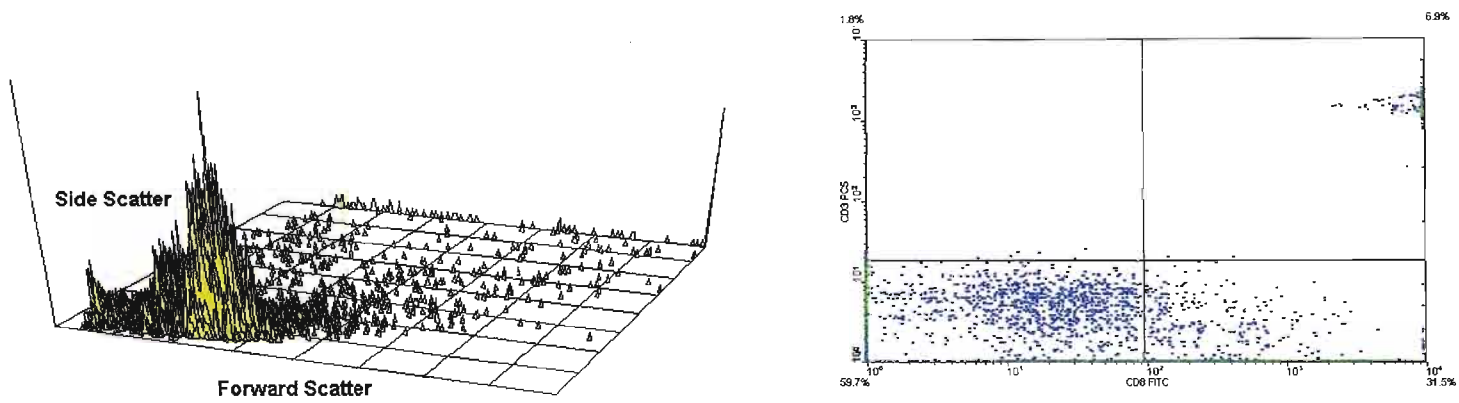


Figure 44e 50µM FA 3D contour and density plots at 4 hour incubation.

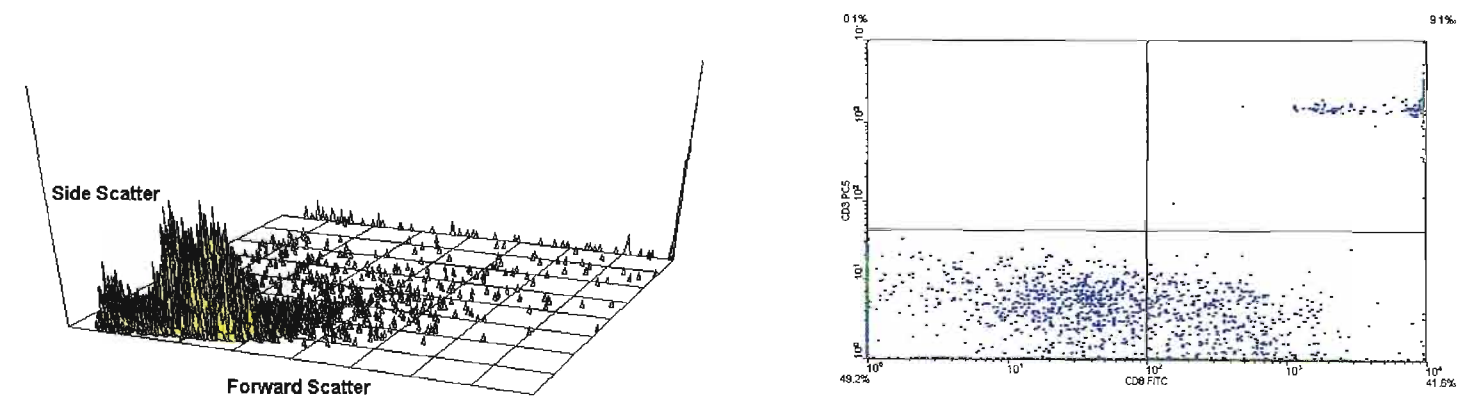


Figure 44f 200µM FA 3D contour and density plots at 4 hour incubation.

Twenty four hour contour and density plots of lymphocytes

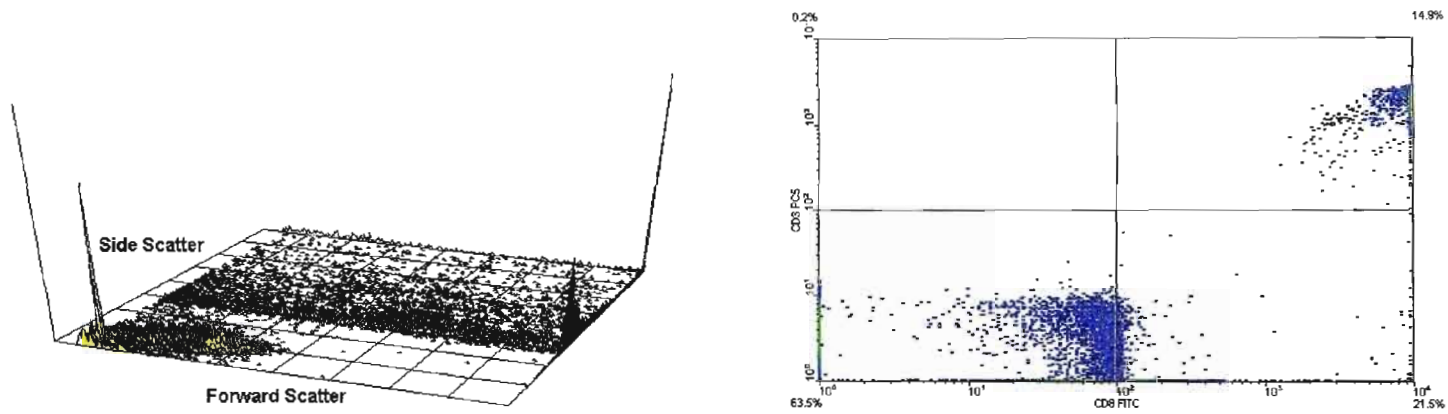


Figure 44g Control 3D contour and density plots at 24 hour incubation.

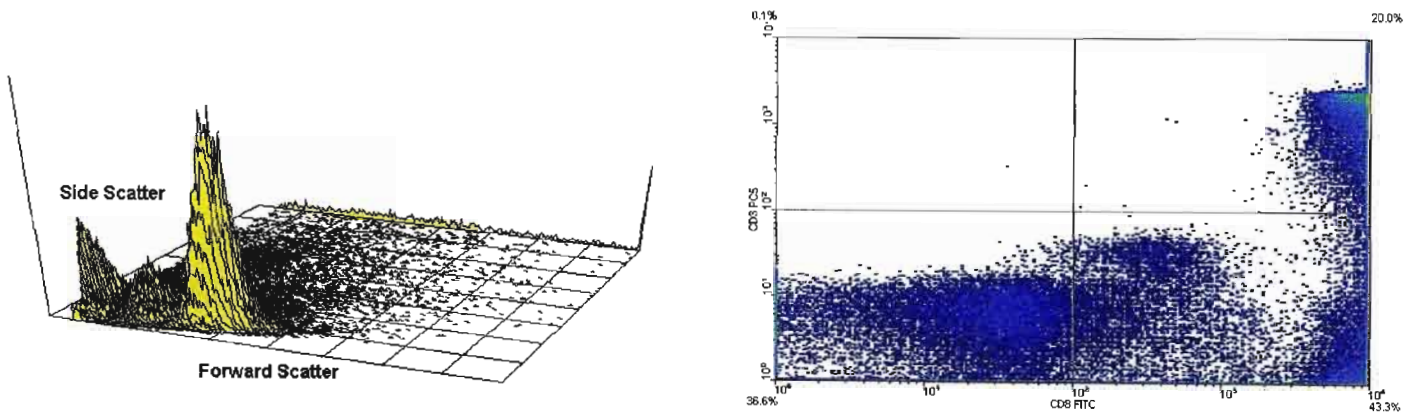


Figure 44h 50µM FA 3D contour and density plots at 24 hour incubation.

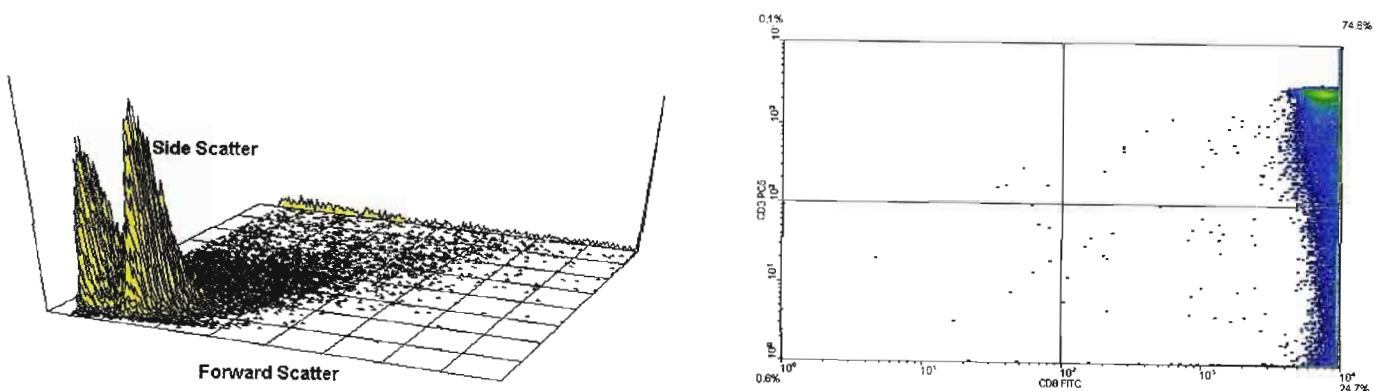


Figure 44i 200µM FA 3D contour and density plots at 24 hour incubation.

The actual mechanism by which FA causes apoptosis is not known although mechanisms have been proposed. Evidence indicates that apoptosis is modulated by intracellular excess or deficiency of Zn^{2+} . Zinc deficiency resulting from dietary deprivation or exposure of cultured cells to membrane permeable Zn^{2+} plays a critical role in apoptosis, possibly by modulating the activity of endonucleases (Fernandez-Pol *et al.*, 2001).

This activity is consistent with the hypothesis that Zn^{2+} prevents apoptosis by blocking the activation or inhibiting the activity of Ca^{2+}/Mg^{2+} dependant endonuclease. Chelation of intracellular Zn^{2+} can trigger apoptosis in cells. Similarly PA a Zn^{2+}/Fe^{2+} chelator induces apoptosis in many cells by chelating pools of intracellular Zn^{2+}/Fe^{2+} , since influx of Zn^{2+}/Fe^{2+} prevented apoptosis in the presence of PA, while chelation of Zn^{2+}/Fe^{2+} induced apoptosis. It is possible that FA acts in a similar way to induce apoptosis in cells (Fernandez-Pol *et al.*, 2001).

In support of the contention delineated above are the studies which found that PA, dipicolinic acid, and isonicotinamide strongly induce apoptosis in human acute myelomonocytic leukemia cells. After treatments with PA dipicolinic acid, and isonicotinamide, apoptosis started within 4 hours and it was induced in about 50% of cells in 8 hours (Fernandez-Pol *et al.*, 2001). Similar results were obtained in the current study in which FA was used to induce apoptosis in healthy human lymphocytes.

Numerous assays are currently used to measure apoptosis including morphological changes by light microscopy, electron microscopy SCGE or flow cytometry using fluorescent dyes. Quantification of apoptosis by microscopy is cumbersome, whereas most of the fluorescent dyes used in flow cytometry are non vital dyes, ie, they stain apoptotic cells only after membrane damage. DNA cleavage by endonucleases discussed

in previous chapters (SCGE and fragmentation analysis) is also used to detect apoptosis. Although flow cytometry is also employed in the detection of apoptosis on a per cell basis it is substantially more rapid than other techniques and allows the analysis of a significantly larger sample number.

Annexin V was used for detection of apoptosis in FA treated lymphocytes. Placing these lymphocytes under these apoptotic inducing conditions resulted in the staining of annexin V in a population of cells. Any procedure that affects the integrity of the plasma membrane of what would otherwise be intact cells will allow access of annexin V to the inner plasma membrane, resulting in cells that will be scored as positive for apoptosis. One hour incubations with various concentrations of FA yielded a substantial increase in annexin V positive lymphocytes. Double positive annexin V and PI lymphocytes also significantly increased. This indicates that lymphocytes rapidly lose their membrane phospholipid asymmetry and expose phosphatidylserine on their surfaces. After 24 hours of incubation a prominent subpopulation of lymphocytes was found which was virtually absent in the 1 and 4 hour incubated lymphocytes. Further examination of these lymphocytes indicated that they were both annexin V positive and annexin V/ PI positive. Double stained lymphocytes were more apparent at higher FA concentrations. This population of double stained lymphocytes was also significantly higher when compared with that of the 1 and 4 hour incubations.

This large increase in necrotic cells could be explained by the fact that the current model is an *in vitro* apoptosis assay. Although the characteristic features of apoptosis strongly contrast that of necrosis, the features of necrosis can become superimposed on those of apoptosis if the dead cell for some reason fails to be recognized and engulfed by a

phagocyte. Thus apoptotic cells *in vitro*, after a rapid rise in buoyant density, exhibit a progressive fall in density to subnormal levels over the ensuing few hours. The membranes of these cells become permeable to dyes that had previously been excluded, such as trypan blue and PI. A similar scenario is seen *in vivo* in apoptotic cells that have, for example been shed from an epithelium into a duct lumen. This process has been termed secondary necrosis (Wyllie, 1997). This could account for the extensive necrosis after the initial rise in apoptosis at higher concentrations of FA after 24 hours of incubation.

Chapter 7

7. Cell cycle analysis

The continuous growth and division of cells is called the cell cycle. It is characterized by five phases: The G₁ ("gap 1") phase which is a period of growth before DNA replication; S ("synapsis") phase which is characterized by DNA replication; G₂ ("gap2") a period of growth that follows DNA replication; M ("mitosis") a period of cell division.

After mitosis cells may proceed to the G₁ phase or may enter the fifth or G₀ phase in which they are said to be "quiescent". During this phase growth and replication stops. These cells may either re-enter the G₁ phase or perhaps die after their lifespan expires.

7.1 Cell cycle and flow cytometry

The versatility of flow cytometry (FC) in a number of methodologies applicable to individual cells or cell organelles has more recently led to its widespread use in studies of cell proliferation (cell cycle).

The use of FC in proliferation assays serve two main purposes : 1) the revelation of distribution of cells in particular phases of the cycle or the determination of the kinetics of progression through these phases; 2) the elucidation of molecular and functional mechanisms associated with the cell cycle. These may be immunohistochemical detection of components such as, cyclins, inhibitors of cyclin-dependant kinases (cdk's), proto-oncogenes that are associated with the cell cycle such as c-myc and ras, and tumour suppressor genes such as p53 and prb (Darzynkiewicz *et al.*, 2001). This kind of assay is widely used in the study of cancer cells. In Medicine, these assays are used to classify some cancers with respect to prognosis, which may impact upon the treatment or therapy

selected by the physician. In research, it is often used to evaluate the effects of drugs on the growth and division of cells.

DNA (cell cycle position or DNA ploidy) is a marker of cellular maturity in the cell cycle. The DNA content contained by a cell corresponds to the specific phase that the cell is in. Cells in $G_{0/1}$ (quiescent cells) have DNA content set equal to 1 unit of DNA; cells in the S phase undergo DNA duplication increasing its content in proportion to progression through S; and upon entering G_2 and afterwards M have twice the amount of DNA as the $G_{0/1}$ phase (2 units). Univariate analysis of cellular DNA content effectively allows discrimination among the phases and is the most frequently employed method of revealing cells in these cell cycle phases (Darzynkiewicz *et al.*, 2001).

In the most common protocols, cells are stimulated with a mitogen such as phytohaemagglutinin (PHA), fixed or permeabilized with a detergent and then stained with a nucleic acid-specific fluorochrome, PI. Once PI intercalates into the double stranded DNA complex it emits red fluorescence when excited with blue light (488nm). A minor setback of the procedure occurs when PI stains double stranded RNA. It is therefore necessary to incubate samples with Rnase (Darzynkiewicz *et al.*, 2001).

The results of fluorescence measurements of proliferating cells are displayed as cellular DNA content frequency histograms (Fig 45) or three dimensional contour plots (Fig 46). The different phases of the cell cycle are represented by different fluorescence intensities. Cells in G_1 are characterized by the initial high peak at low fluorescence intensity. Cells in G_2 and M usually combine to form a peak at twice that fluorescence intensity, since the DNA has been replicated. Between these two peaks, there is a flat "plateau" which includes cells that contain various amounts of DNA between G_1 and G_2 , typical of the S

phase. The flow cytometer's computer can *integrate* the graph in these three regions to determine the relative amount, or fraction, of the cell population in each phase. Typically, most of the cells are in the G₁ phase. By measuring the fractions in S and G₂/M, one can obtain information on how rapidly cells are proliferating.

Apoptosis of cells may lead to a loss of DNA in shedding apoptotic bodies, and DNA that has undergone internucleosomal cleavage may be extracted during fixation and staining. As a result apoptotic cells in frequency histograms are distinguished by their fractional DNA content ("sub-G₁" cells) (Fig 45) (Darzynkiewicz *et al.*, 2001).

The simplicity of univariate analysis of DNA content makes it ideal for its use in clinical studies to obtain the cell cycle distributions in tumours or other proliferative disorders. Cells found in the S and G₂/M phases are considered to indicate increased proliferative potential. If asynchronously growing cells are treated *in vitro* or *in vivo* with an agent that interferes with progression through the cell cycle, cells tend to accumulate in the phase where their progression was affected maximally, showing up as an increase in relative proportion of cells in that phase of the cycle on the DNA content frequency histograms (Darzynkiewicz *et al.*, 2001).

A drawback with frequency histograms is that they don't yield information about the rate of the cell cycle progression or kinetics. For these purposes duration of the cell cycle is required, or the doubling time of cells in culture (Darzynkiewicz *et al.*, 2001).

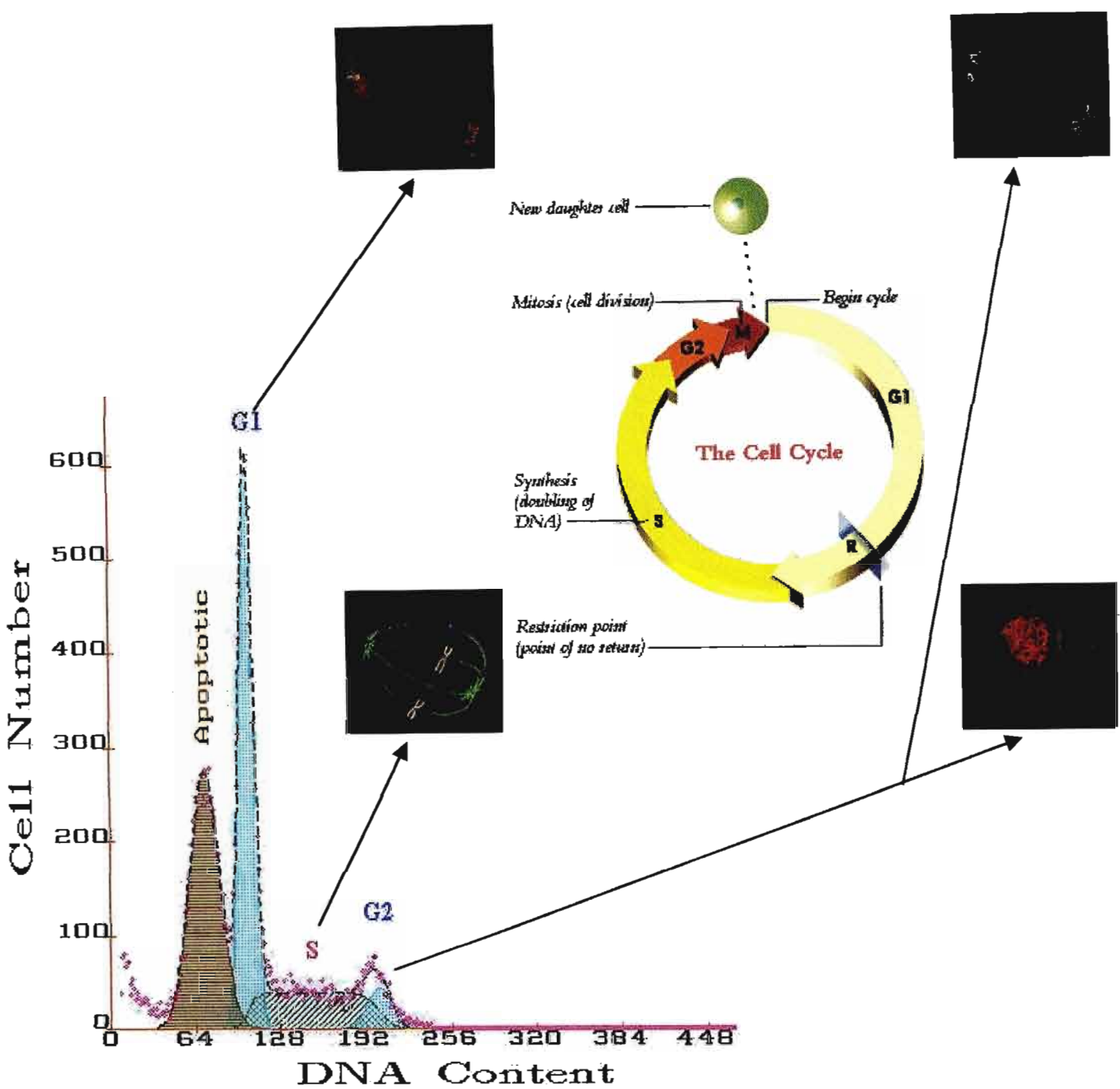


Figure 45 Typical flow cytometric histogram representing various phases of the cell cycle. The inset depicts cartoons of cells in the various phases of the cell cycle (www.geocities.com/CollegePark/Lab/1580/cycle.html).

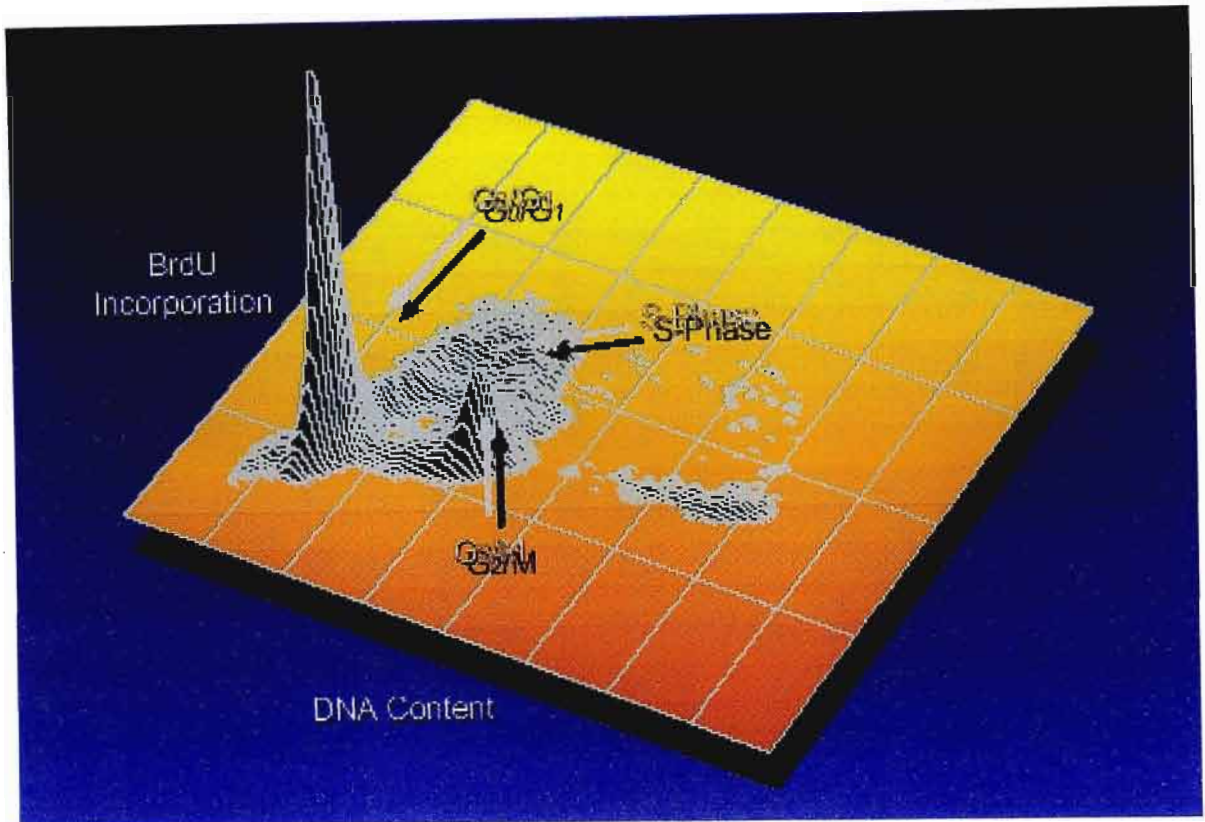


Figure 46 Three dimensional contour plot of cells in various phases of the cell cycle (www.fcm-ntsrvr01.utmb.edu/apo.pdf).

7.2 Detection of cyclins in individual cells using flow cytometry

The progression of cells through successive phases and checkpoints of the cell cycle is possible through sequential phosphorylation of different sets of nuclear and cytoplasmic proteins by cyclin-dependant kinases (CDKs).

The activation of partner CDKs and targeting them to the respective protein substrates allows cyclins to play a key regulatory role in the cell cycle process. The cyclins B1, A, E and D are expressed discontinuously during the cell cycle. The synthesis and degradation of these cyclins occurs at specific time points in the cell cycle (Table 5) (Fig 47). Cyclin

B2 is responsible for the activation of CDC2 whose kinase activity is essential for cell transition from G₂ to M phase (Morgan, 1995).

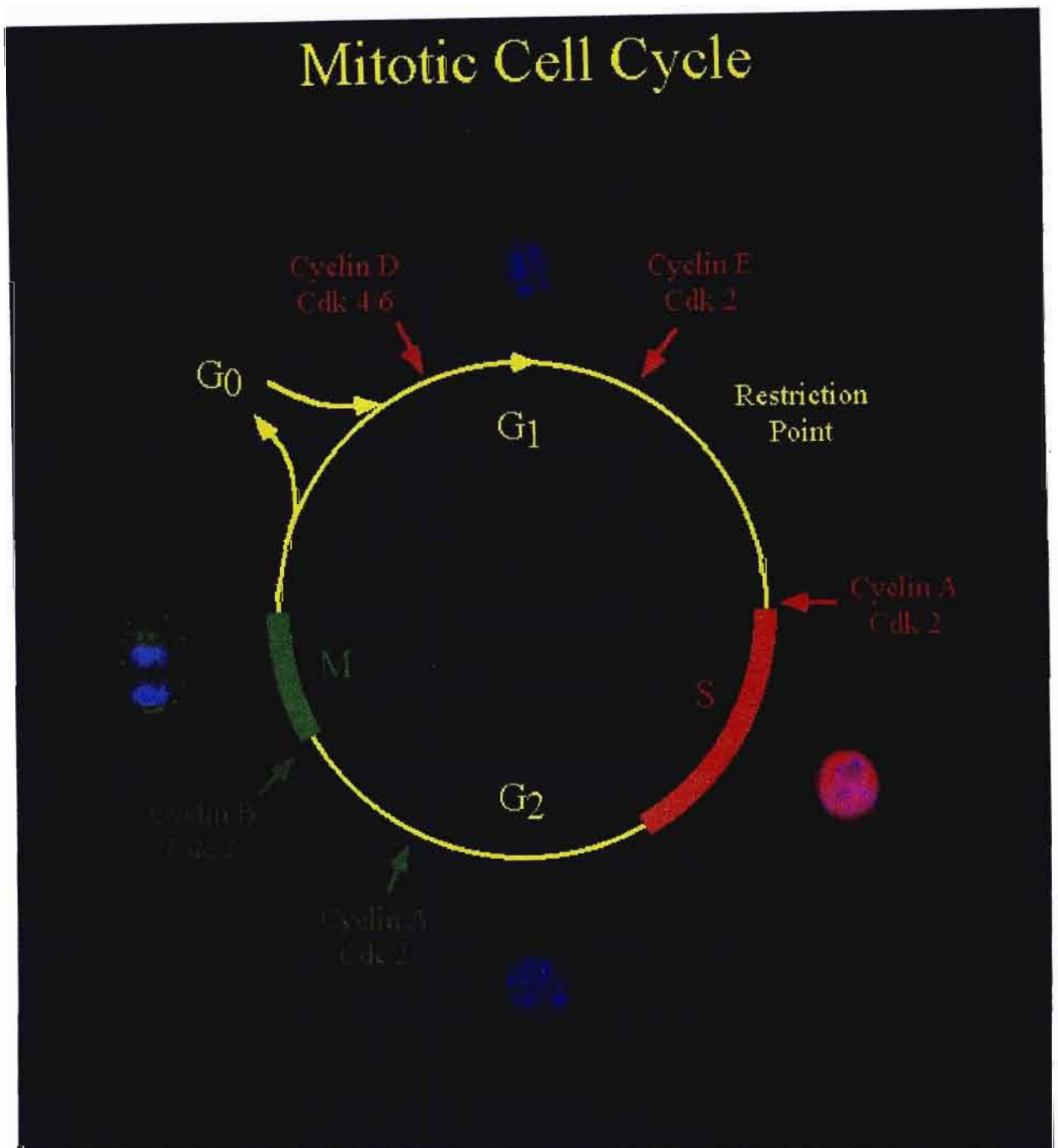


Figure 47 Schematic diagram of the occurrence of various cyclins at different time points in the cell cycle (www.chemcases.com/cisplat/cisplat19.htm).

TABLE 5 CYCLINS AND THEIR PARTNER CDKS DURING THE CELL CYCLE

Cyclin	Primary CDK partner	Presumed role in cell cycle	Peak of expression	Localization
D	CDK4 and CDK6	pRB phosphorylation, commitment to S phase	Early in G ₁	Nucleus
E	CDK2	Initiation of S	G ₁ /S transition	Nucleus
A	CDK2 and CDC2	S and G ₂ traverse	During G ₂ M	Nucleus
B1	CDC2	G ₂ traverse entrance to M	Late G ₂ /M	Cytoplasm/ Nucleus ^a

Cyclin B1 is localized in the cytoplasm during G₂ and undergoes translocation to nucleus during prophase (Juan and Darzynkiewicz, 1998).

Cyclin B2 usually accumulates at the time of cell exit from S. Maximal levels of cyclin B1 indicate cells entering mitosis. Cyclin B1 is degraded rapidly during the transition to anaphase (Juan and Darzynkiewicz, 1998). Once cyclin A complexes with either CDC 2 or CDK2 the kinase activity of the complex drives the cell through S and G₂ phases of the cell cycle. Cyclin A is found abundantly in the cell early in S and its maximal expression is seen at the end of G₂. It is rapidly degraded in prometaphase and the metaphase cells are essentially cyclin A negative. Cyclin E complexes with CDK2 and this holoenzyme is essential for the cell transition from G₁ to S phase. Cyclin E expression increases in

mid-G₁ and is maximally expressed at the time of the cell entrance to S. It is continuously broken down as the cell progresses through S (Dulic *et al.*, 1992).

The D family of cyclins (D1, D2 and D3) are maximally expressed in response to mitogenic stimulation of G₀ cells or by mitogen and growth factors. The levels of these cyclins seems to decrease during the exponential phase of growth (Ohtsubo *et al.*, 1993). Cyclins D activate CDK4/CDK6 and the complex phosphorylates the retinoblastoma tumour suppressor gene RB (pRB) (Weinberg, 1995). Phosphorylation of pRB leads to the release of E2F factor that initiates transcription of the components of the DNA replication machinery, and in this way the cell is committed to the S phase (Shirodkar *et al.*, 1992). This event is the most important regulatory point during G₁ which appears to be defective in most tumours. Cyclins exhibit cell cycle phase specificity. Due to this specificity, analysis of the expression of cyclin proteins can be used in addition to DNA content, as yet another marker of a cells position in the cell cycle.

The aim of this study was determine the effect of FA on the cell cycle of the lymphocyte.

7.3 Materials and method

7.3.1 Materials

The chemicals used in the experiments were purchased from the following suppliers :
Rnase from Roche Biochemicals; Ethanol from Merck; sodium citrate from Saarchem.

7.3.2 Methods

7.3.2.1 Chemicals required

- a) DNA stain: 5 milligrams of PI in 100 milliliters of 1.12% (w/v) of sodium citrate.
- b) Rnase solution : 500 units per ml. In 1.12% (w/v) of sodium citrate. A highly purified Rnase is required to avoid destruction of the cells by contaminating proteases and /or Dnases. The Rnase solution can be purified by heating to 75 degrees celsius for 30 minutes. It should then be cooled to room temperature before treating cells.
- c) 100% ethanol.
- d) Foetal or newborn bovine serum, (optional) for removal of debris.
- e) Cells in suspension, counted and viability checked with exclusion dye such as Trypan Blue. The procedure is for 10^6 cells but can be scaled up if required. The cells should preferably be suspended in culture media or phosphate buffered saline (PBS) without serum, as the ethanol fixation step will precipitate the proteins in the serum.

The procedure does not necessarily require 100% viable cells, but generally the more dead cells, the more debris and multi-cell aggregates can be expected.

7.3.2.2 Preparation of lymphocyte samples

Whole blood 4ml (6 tubes of 4ml each) was collected in lithium heparin Vacutainer tubes by venopuncture from a healthy donor. Lymphocyte isolations were carried out as described in chapter 2. The lymphocyte suspensions (10^6 cells/ml) were prepared and

treated in a sterile environment as in chapter 2 and incubated for 24, 48 and 72 hours. Lymphocyte suspensions were treated with a range of serial dilutions and made up to final concentrations of 10 μ M, 50 μ M, 100 μ M and 200 μ M FA. Positive control cells were not treated with FA. Positive control cells and all FA treated lymphocytes were treated with 10 μ g/ml PHA. Negative control lymphocytes were not treated with PHA or FA. After each respective time interval the lymphocytes (10⁶ cells/ml) were collected by centrifugation at 300 \times g for 5 minutes.

7.3.2.2.1 Fixation

Lymphocytes (10⁶) were resuspended in 500 μ l volume of PBS and chilled well on ice. A 12 \times 75 mm tube containing 500 μ l of ice-cold 100% ethanol was prepared. The lymphocyte suspension was rapidly pipetted into the cold ethanol and mixed by forcing bubbles through the suspension. Pasteur type pipettes worked best for this purpose. The suspension was then allowed to stand on ice for 15 minutes.

7.3.2.2.2 Debris removal

The lymphocyte suspension was carefully under layered with 1ml ice-cold foetal calf serum and centrifuged at room temperature for 3 minutes at 300 \times g. After centrifugation care was taken not to disturb the pellet as the liquid was aspirated. 2ml of PBS was then added to the pellet and then vortexed.

7.3.2.2.3 DNA Staining

The lymphocyte suspension from the debris removal step was then centrifuged at room temperature for 3 minutes at 300 \times g and as much liquid as possible was removed without disturbing the pellet which was easily dislodged at this stage. Rnase solution (125 μ l) was then added to the pellet and then vortexed. The suspension was then incubated at 37 $^{\circ}$ C in

a water bath for 15 minutes. The suspension was then removed from the water bath and 125 μ l of PI stain was added and then vortexed. The suspension was allowed to stand at room temperature for at least 30 minutes before analysing on a flow cytometer.

7.3.2.2.4 Statistical analysis

All experiments were performed in duplicate on at least two separate occasions. Differences between the groups were tested for statistical significance by using Chi-squared test. P-values of < 0.0001 were considered statistically significant. Values are quoted as the mean of both experiments conducted.

7.4 Results and Discussion

Phytohaemagglutinin stimulated lymphocytes led to a significant average increase in DNA synthesis and thus lymphocyte proliferation at 48 and 72 hours (Table 6). Co-incubation of PHA stimulation of lymphocytes led to a significant decrease of G₀/G₁ phase and an increase in S and G₂/M phase at 48 and 72 hours of incubation.

Significant changes in the various phases due to co-incubation with FA occurred predominantly after 48 and 72 hours. The percentages of cells found treated with the various concentrations of FA in all the phases was comparable with that of the control percentages at 24 hours. FA substantially inhibited cells 48 and 72 hours after incubation in the S and G₂/M phases at 100 μ M and 200 μ M concentrations. Frequency histograms (Fig 48 a-c, 49a-c and 50 a-c) illustrate changes in the various phases at different time intervals and concentrations.

TABLE 6 PERCENTAGES OF CELLS IN DIFFERENT PHASES OF THE CELL CYCLE AFTER TREATMENT WITH FUSARIC ACID AT VARIOUS TIME INTERVALS

	24 HOURS			48 HOUR			72 HOUR		
	G ₁	S	G ₂ M	G ₁	S	G ₂ M	G ₁	S	G ₂ M
-VE C *	65.77	0.44	9.20	98.15	0.37	8.16	81.66	1.37	5.44
+VE C	59.48	0.95	9.44 ⊗	40.41	13.51	15.07	45.50	15.17	15.18
10μM FA	56.35	0.78	9.20 ⊗	46.12	14.93	14.21	42.40	14.97	17.55
50μM FA	57.86	0.80	7.53	43.47	7.11	8.20	47.90	13.68	12.29
100μM FA	49.86	0.62	8.83	58.29	1.31	9.04	67.74	2.1	5.14
200μM FA	49.26	0.86	9.29	34.57	1.28	5.47	56.34	0.74	6.10 ⊗

- NO PHA INCLUDED IN NEGATIVE CONTROL (-ve C).
- ALL OTHER CONCENTRATIONS TREATED WITH 10μg/ml PHA

Significance of all values (percentages of cells in the respective phases of the cell cycle) in comparison to the controls ($P < 0.0001$) and to PHA ($P < 0.0001$). All values except those marked ⊗ were found to be extremely significant when compared to the control values.

Twenty four hour cell cycle histograms

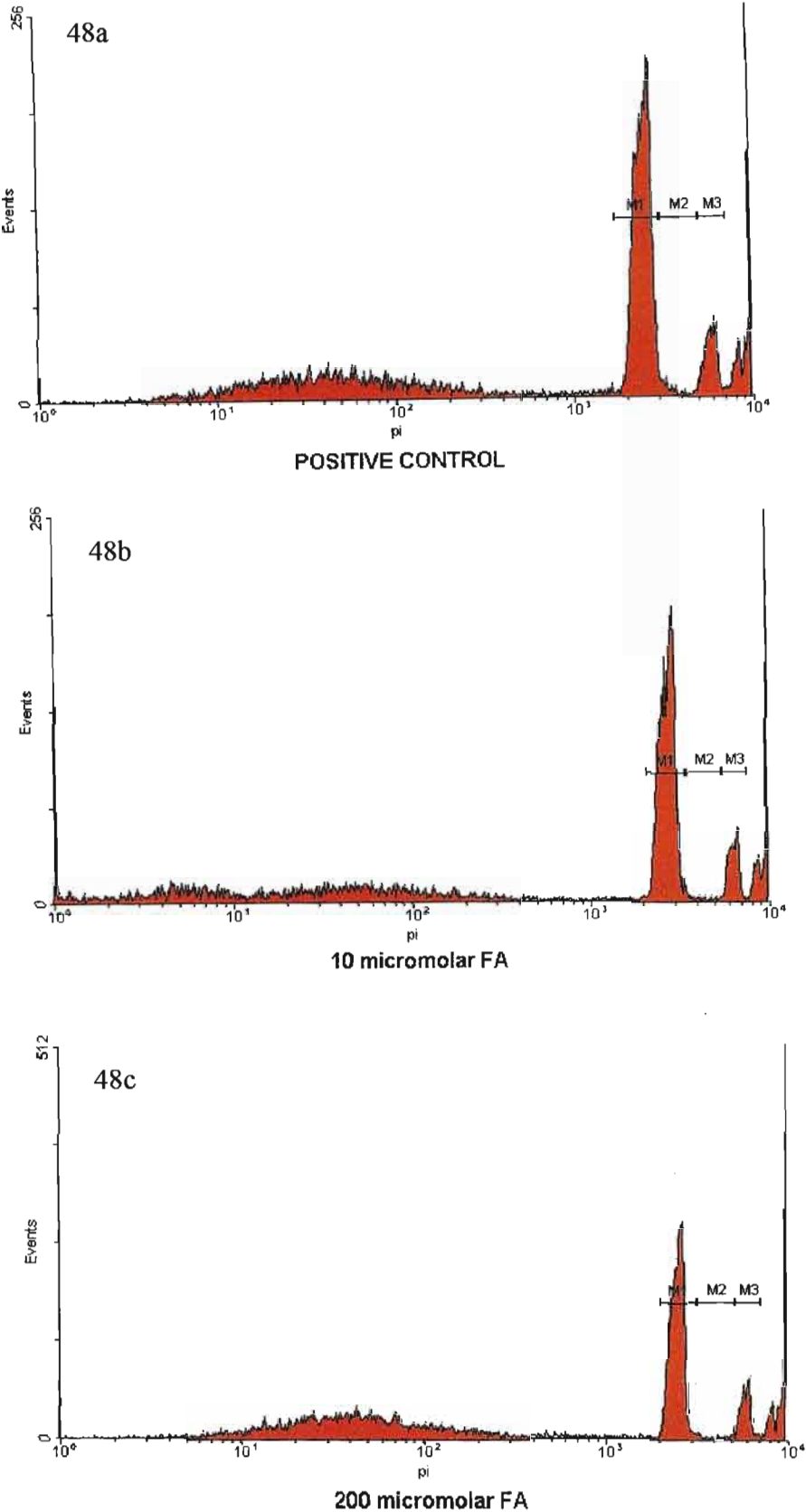


Figure 48a Positive control exhibiting normal distribution of phases after 24 hours. 48b Slight decrease in G_0/G_1 and G_2/M peaks after $10\mu\text{M}$ FA treatments. 48c more pronounced decrease in G_0/G_1 and G_2/M peaks after $200\mu\text{M}$ FA treatments.

Forty eight hour cell cycle histograms

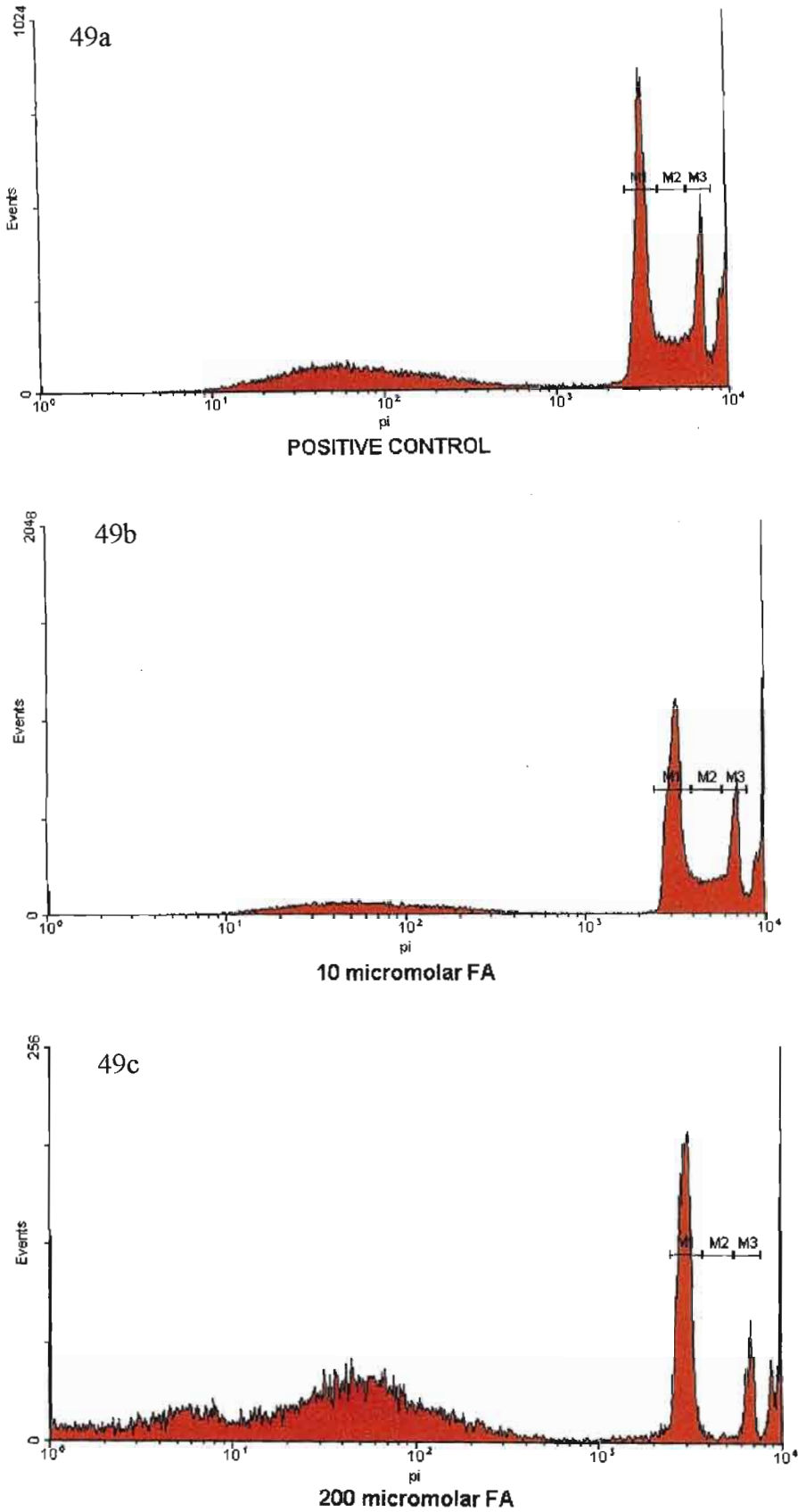


Figure 49a Positive control exhibiting pronounced S phase. 49b All phase peaks smaller than positive control due to 10 μ M FA treatment although S phase still prominent. 49c All phase peaks smaller than positive control due to 200 μ M FA treatment. S phase still present.

Seventy two hour cell cycle histograms

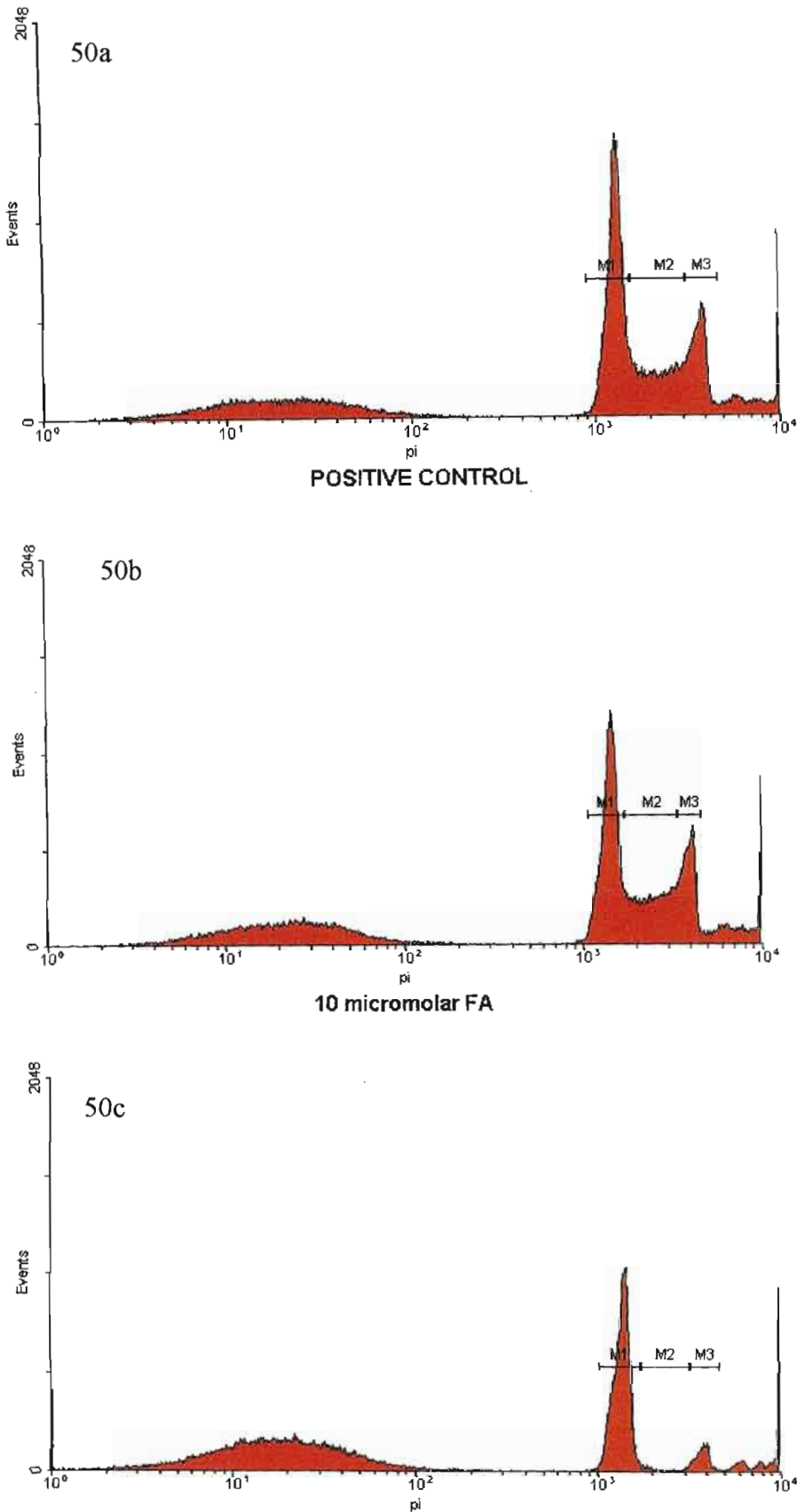


Figure 50a Full expression of PHA indicated in all phase peaks after 72 hours. 50b Significant decrease in all phase peaks due to 10 μ M FA treatment after 72 hours. 50c Fusaric acid has almost totally stopped replication of cells as exhibited by an absence of an S phase and a very small G₂/M phase.

Previous studies demonstrated that addition of the pyridine derivative, α PA, to the culture medium reversibly arrests normal rat kidney (NRK) cell growth in the G_1 phase of the cell cycle (Johnson and Fernandez-Pol, 1977). Research has led to the belief that α PA could act through alterations in cyclic adenosine mono phosphate (cAMP) levels. Cyclic AMP plays an instrumental role in growth control (Pastan *et al.*, 1975). In this regard certain pyridine derivatives influence cAMP metabolism in some cells. Nicotinic acid has been shown to prevent the ACTH-glucagon- or epinephrine-induced elevation of cAMP levels in fat cells and NAD^+ is required for the activation of adenylate cyclase by cholera toxin in erythrocytes and certain tumour cells (Gill, 1975; Bitensky *et al.*, 1975). Cultures of peripheral blood lymphocytes are predominantly found in the resting state exhibiting low degrees of [3H] thymidine incorporation into DNA. The addition of a mitogen such as PHA to these resting cells transforms them into proliferative active blast cells. Cyclic AMP has been implicated in the regulation of this process.

Cyclic AMP plays an important role in mitogen activated lymphocytes. Peripheral nucleotides which are treated with high concentrations of PHA initiates a slight increase in intracellular cyclic AMP. This is observed with the first few minutes of treatment. Studies have also found that cAMP levels in PHA- activated lymphocytes fall within 6 hours to below the levels found in control cultures (Smith *et al.*, 1971). Purity of the PHA preparations have also been found to influence cAMP levels. The more pure the PHA the less the expression of cAMP. Cyclic AMP has been demonstrated to inhibit DNA synthesis in PHA stimulated lymphocytes from patients with chronic lymphocytic leukemia (Johnson and Abel, 1970). Bt_2cAMP produced maximal inhibition of PHA induced DNA synthesis if present during the first hour after initial exposure to PHA.

Moreover, numerous agents that elevate intracellular cAMP levels (aminophylline, isoproterenol, and prostaglandins) also inhibited [³H]- thymidine incorporation (Smith *et al.*, 1971).

It has been postulated that the effect of PA on NRK cell growth inhibition is not a direct one, and it is possible that it may be converted into another molecule. (Johnson and Fernandez-Pol, 1977).

FA could act by metal ion chelation or by interference with NAD⁺ metabolism or NAD⁺ functions. FA could possibly bind to and activate a specific protein-metal iron complex in a manner similar to the binding of nicotinic acid to leghaemoglobin. Numerous pyridine derivatives undergo an exchange reaction with the nicotinamide moiety of NAD⁺ to form NAD⁺ analogues. It is possible that FA could be incorporated into a similar molecule that is an active species (Fernandez-Pol *et al.*, 1977).

Kinetic and radioisotopic studies have shown that PA both inhibits incorporation of iron into the cells and effectively removes radio iron from the cells. It is conceivable that the inhibition of cell proliferation *in vitro* by FA results at least in part from selective depletion of iron in the cells. The chelation of FA is however is not limited to iron and thus, it may act simultaneously on various transition metal ion requiring systems. FA can chelate Zn²⁺, Cu²⁺ and Mn²⁺ ions which are important structural and functional components in numerous proteins associated with cell proliferation, differentiation, and protection against free radicals such as the transcriptionally active zinc finger proteins and the Cu²⁺ and Mn²⁺ containing superoxide dismutases (Fernandez-Pol *et al.*, 1993).

The inhibition of growth by FA may be primarily due to inhibition of the activity of the iron-requiring enzyme ribonucleotide reductase. Ribonucleotide reductase is a rate

controlling enzyme in the DNA synthetic pathway and is thus a possible target for the action of FA (Fernandez-Pol *et al.*, 1993).

The only difference in cytotoxicity between PA and FA is due to the 5-butyl side chain of FA which because of its lipid solubility may presumably allow better cellular penetrability of this agent. Of course other mechanisms of action are possible (Fernandez-Pol *et al.*, 1993).

8 Conclusion

Apoptosis is a co-ordinated process characterised by changes occurring at the cell surface as well as in the nucleus and cytoplasm. After a lethal stimulus is delivered the time to onset of apoptosis is variable, but once initiated the changes are rapid. To date much has been elucidated regarding the molecular basis of apoptosis. Numerous genes are known that are involved and are mainly concerned with triggering events, a common effector pathway and modulation of susceptibility to apoptosis.

Fusaric acid is a small molecule (MW 179); and is water soluble. Chemically, FA molecules are little differentiated, and they can therefore manifest themselves into the most varied functions and sub structures of the host cells. Apart from the molecule as a whole, some of its chemical groups also interfere independently in vital cellular processes of the host. The pyridine ring (of FA) at low concentrations may impair oxidative phosphorylation whereas the aliphatic side chain in the β position may block the cytochrome oxidase at higher concentrations.

It is possible that FA undergoes different changes within the host. The two main changes that may occur are decarboxylation and methylation. Provided that FA undergoes only decarboxylation, the first cleavage product will be 3-n-butylpyridine. This structure is believed to be 100 times more toxic than the parent FA. The 3-n-butylpyridine thus acts as a protoxin which increases its lethal toxicity inside the host cell.

In addition to its chelating ability FA impairs the semi-permeability of the plasma membranes. The site of action of FA within the host cells are probably as numerous as the objectives; thus, the receptor for impairment of semi-permeability are chiefly in the

boundary layers of the plasma, whereas those for the impairment of respiration are in the mitochondria.

In this study FA showed acute toxicity on lymphocytes at high concentrations (24 hours incubation). The MTT assay was effective and sensitive in determining the cytotoxicity of FA. The results of the MTT assay were used to select the relevant concentrations to investigate the induction of apoptosis and cell growth inhibition in healthy lymphocytes. The SCGE assay detected DNA strand breakages in lymphocytes treated with low concentrations of FA. Results obtained for the SCGE assay correlate with those obtained for the DNA fragmentation assays. Ultrastructural studies (TEM) revealed that FA induced apoptosis, which was evidenced at the nuclear level. This was predominantly displayed by nuclear material migrating to the periphery of the nucleus, mitochondrial damage and budding of membrane bound vesicles from the parent lymphocyte. Flow cytometry was effectively employed in this study and was useful in detecting the early morphological changes in lymphocytes undergoing apoptosis.

Fusaric acid was also found to be a potent inhibitor of lymphocyte proliferation *in vitro*. Inhibition of proliferating lymphocytes occurred at high concentrations of FA and later time intervals. It seemed to once again impose its mode of action by chelating ions that are instrumental in the growth of normal and cancerous cells. The results obtained in this study correlated with those obtained for cell growth inhibition studies on various cell lines *in vitro*.

The current study proved that FA induced apoptosis in human lymphocytes and is a potent inhibitor of lymphocyte proliferation *in vitro*. An interesting prospect for future

studies will be to raise an antibody against FA to trace its mode of pathogenicity in the cell.

9 References

1. Abd-Allah G. A., R. I. El-Fayoumi, M. J. Smith, R. A. Heckmann and K. L. O'Neil. 1999. A comparative evaluation of aflatoxin B₁ genotootoxicity in fish models using the comet assay, *Mutation Research*, 446: 181-188.
2. Allbritton N., C. R. Verret, R. C. Wolley and H. N. Eisen. 1988. Calcium ion concentrations and DNA fragmentation in target cell destruction by murine cloned cytotoxic T lymphocytes, *Journal of Experimental Medicine*, 167: 514-527.
3. Anderson D. T., W. Yu, R. J. Hambly, M. Mendy and C. P. Wild. 1999. Aflatoxin exposure and DNA damage in the comet assay in Individuals from The Gambia, West Africa, *Teratogenesis, Carcinogenesis, and Mutagenesis*, 19: 147-155.
4. Arends M. J., R. G. Morris and A. H. Wyllie. 1990. Apoptosis: The Role of the Endonuclease, *American Journal of Pathology*, 136: 593-608.
5. Arias J. A., 1985. Secretory organelle and mitochondrial alterations induced by fusaric acid in root cells of *Zea mays*, *Physiological Plant Pathology*, 27: 149-158.
6. Bacon C.W., J. K. Porter, and W. P. Norred. 1995. Toxic interactions of fumonisin B1 and fusaric acid measured by injection into fertile chicken egg, *Mycopathologia*, 129: 29-35.
7. Bacon C.W., J. K. Porter, W. P. Norred and J. F. Leslie. 1996. Production of Fusaric Acid by *Fusarium* Species, *Applied and Environmental Microbiology*, 62: 4039-4043.
8. Bassé F., J. G. Stout, P. J. Sims and T. Wiedmer. 1996. Isolation of an erythrocyte membrane protein that mediates Ca²⁺-dependent transbilayer movement of phospholipids, *Journal of Biological Chemistry*, 271: 17205-17210.

9. Beleznay Z., A. Zachowski, P. F. Devaux, M. P. Navazo and P. Ott. 1993. ATP-dependent aminophospholipid translocation in erythrocyte vesicles: Stoichiometry of transport, *Biochemistry*, 32: 3146-3152.
10. Bitensky M. W., M. A. Wheeler, H. Mehta and N. Miki. 1975. Cholera toxin activation of adenylate cyclase in cancer cell membrane fragments, *Proceedings of the National Academy of Sciences USA*, 72: 2572-2576.
11. Brown R. 1997. The bcl-2 family of proteins, *British Medical Bulletin*, 53: 466-477.
12. Buendia B., A. Santa-Maria and J. C. Courvalin. 1999. Caspase-dependant proteolysis of integral and peripheral proteins of nuclear membranes and nuclear pore complex proteins during apoptosis, *Journal of Cell Science*, 112: 1743-1753.
13. Canman C. E. and M. B. Kastan. 1996. Three paths to stress relief, *Nature*, 384: 213-214.
14. Chaouloff F., D. Laude, D. Merino, B. Serrurier and J. L. Elghozi. 1986. Peripheral and short-term effects of fusaric acid, a DBH inhibitor, on tryptophan and serotonin metabolism in the rat, *Journal of Neural Transmission*, 65: 219-232.
15. Cohen J. J. and R. C. Duke. 1984. Glucocorticoid activation of a calcium-dependant endonuclease in thymocyte nuclei leads to cell death, *The Journal of Immunology*, 132: 38-42.
16. Connor J., C. H. Pak, R. F. A. Zwaal and A. J. Schroit. 1992. Bidirectional transbilayer movement of phospholipid analogues in human red blood cells, *Journal of Biological Chemistry*, 267: 19412-19417.

17. Connor J. and A. J. Schroit. 1988. Transbilayer movement of phosphatidylserine in erythrocytes. Inhibition of transport and preferential labelling of a 31,000 Dalton protein by sulfhydryl reactive reagents, *Biochemistry*, 27: 848-851.
18. Coulombe R. A. 1993. Symposium: the biological action of mycotoxins. *Journal of Dairy Science*, 76: 880-891.
19. Creutz C. E. 1992. The annexins and exocytosis, *Science*, 258: 924-931.
20. Darzynkiewicz Z., E. Bedner and P. Smolewski. 2001. Flow cytometry in analysis of cell cycle and apoptosis, *Seminars in Hematology*, 38: 179-193.
21. Distelhorst C. W. 1988. Glucocorticosteroids induce DNA fragmentation in human lymphoid leukaemia cells, *Blood*, 72: 1305-1309.
22. Duke R. C., J. J. Cohen and R. Chervenak. 1986. Differences in target cell DNA fragmentation induced by mouse cytotoxic T lymphocytes and natural killer cells, *Journal of Immunology*, 137: 1442-1447.
23. Dulic V., E. Lees and S. I. Reed. 1992. Association of human cyclin E with a periodic G1-S phase protein kinase, *Science*, 257: 1958-1961.
24. Elghozi J. L., D. Laude and F. Chaouloff. 1985. Fusaric acid-induced elevation of homovanilic acid in the CSF as an index of brain noradrenaline synthesis, *European Journal of Pharmacology*, 117: 363-367.
25. Erenpreisa J., T. Freivaids, H. Roach and R. Alston. 1997. Apoptotic cell nuclei favour aggregation and fluorescence quenching of DNA dyes, *Histochemical Cell Biology*, 108: 67-75.

26. Fernandez-Pol J. A., V. H. Jr. Bono and G. S. Johnson. 1977. Control of growth by picolinic acid: Differential response of normal and transformed cells, *Proceedings of the National Academy of Sciences USA*, 74: 2889-2893.
27. Fernandez-Pol J. A., P. D. Hamilton and D. J. Klos. 2001. Essential viral and cellular zinc and iron containing metalloproteins as targets for novel antiviral and anticancer agents : implications for prevention and therapy of viral diseases and cancer, *Anticancer Research*, 21: 931-958.
28. Fernandez-Pol J. A and G. S. Johnson. 1977. Selective toxicity induced by picolinic acid in simian virus 40 transformed cells in tissue culture, *Cancer Research*, 37: 4276-4279.
29. Fernandez-Pol J. A., D. J. Klos and P. D. Hamilton. 1993. Cytotoxic activity of fusaric acid on human adenocarcinoma cells in tissue culture, *Anticancer Research*, 13: 57-64.
30. Finch J. T. and A. Klug. 1976. Solenoidal model for superstructure in chromatin, *Proceedings of the National Academy of Sciences USA*, 73: 1897-1901.
31. Fisher T. C., A. E. Milner and C. D. Gregory. 1993. Bcl-2 modulation of apoptosis induced by anticancer drugs: resistance to thymidylate stress is independent of classical resistance pathways, *Cancer Research*, 53: 3321-3326.
32. Friedberg E. C. 1996. Relationships between DNA repair and transcription, *Annual Reviews of Biochemistry*, 65: 15-42.
33. Gedik C.M., S.W.B. Ewen and A.R. Collins. 1992. Single-cell gel electrophoresis applied to the analysis of UV-C damage and its repair in human cells, *International Journal of Radiation Biology*, 62: 315-320.

34. Ghadially F. N. 1982. *Ultrastructural Pathology of the Cell and Matrix*, 2, 1-122 and 149-250.
35. Gill D. M. 1975. Involvement of nicotinamide adenine dinucleotide in the action of cholera toxin *in vitro*, *Proceedings of the National Academy of Sciences USA*, 72: 2064-2068.
36. Glenney J. R., M. Boudreau, R. Galyean, T. Hunter, B. Tack. 1986. Association of the S-100- related calpactin I light chain with the NH₂- terminal tail of the 36-kDa heavy chain, *Journal of Biological Chemistry*, 261: 10485-10488.
37. Gorczyca W., R. Myron and Z. Darzynkiewicz. 1997. Analysis of apoptosis by flow cytometry. *Flow cytometry protocols*, 91: 217-238.
38. Green M. H. L., J. E. Lowe, S. A. Harcourt, P. Akinluyi, T. Rowe, A. V. Anstey and C. F. Arlett. 1992. UV-C sensitivity of stimulated and unstimulated human lymphocytes from normal and xeroderma pigmentosum donors in the comet assay: A potential diagnostic technique, *Mutation Research*, 273: 137-144.
39. Hengartner M. O. 2000. The Biochemistry of Apoptosis, *Nature*, 407: 770-776.
40. Hermann A., A. Zachowski and P. F. Devaux. 1990. Protein-mediated phospholipid translocation in the endoplasmic reticulum with a low lipid specificity, *Biochemistry*, 29: 2023-2027.
41. Hickman J. A. and C. C. Boyle. 1996. Apoptosis and Cytotoxins, *British Medical Bulletin*, 52: 632- 643.
42. Hsieh D. P. H. 1987. *Mycotoxins in food* (Mode of action of mycotoxins), 149-176.

43. Ishida R., H. Akiyoshi and T. Takahoshi. 1974. Isolation and purification of calcium and magnesium dependant endonuclease from rat liver nuclei, *Biochemical Biophysical Research Communications*, 56: 703-710.
44. Johnson L. D. and C. W. Abell. 1970. The Effects of Isoproterenol and Cyclic Adenosine 3', 5'-Phosphate on Phytohemagglutinin-stimulated DNA Synthesis in Lymphocytes Obtained from Patients with Chronic Lymphocytic Leukemia, *Cancer Research*, 30: 2718-2723.
45. Johnson G. S. and J. A. Fernandez-Pol. 1977. NRK Cells Synchronized in G1 by picolinic acid are super-sensitive to prostaglandin E1 stimulation, *FEBS LETTERS*, 74: 201-204.
46. Juan G. and Z. Darzynkiewicz. 1998. Detection of cyclins in individual cells by flow and laser scanning cytometry, *Methods in Molecular Biology: Flow Cytometry Protocols*, 91: 67-75.
47. Knudson C. M., K. S. K. Tung and W. G. Tourtellotte. 1995. BAX-deficient mice with lymphoid hyperplasia and male germ cell death, *Science*, 270: 96-99.
48. Koopman G., C. Reutelingsperger, G. A. M. Kuijten, R. M. J. Keehnen, S. T. Pals, and M. H. J. van Oers. 1994. Annexin V for flow cytometric detection of phosphatidylserine expression of B cells undergoing apoptosis, *Blood*, 84: 1415-1420.
49. Kothakota S. 1997. Caspase-3-generated fragment of gelsolin: effector of morphological change in apoptosis, *Science*, 278: 294-298.

50. Koury M. J. and M. C. Bondurant. 1990. Erythropoietin retards DNA breakdown and prevents programmed death in erythroid progenitor cells, *Science*, 248: 378-381.
51. Krammer P. H. 2000. CD 95's deadly mission in the immune system, *Nature*, 407: 789-795.
52. Kyprianou N. and J. T. Isaacs. 1988. Activation of programmed cell death in the rat ventral prostate after castration, *Endocrinology*, 122: 552-562.
53. Lah B., T. Cepeljnik, F. V. Nekrep and R. Marin_ek Logar. 2001. Development of a new pollution biotest using comet assay on *Tetrahymena thermophila*.
<http://www.bfro.uni-lj.si/zoo/org/microtech/Comet2001.pdf>.
54. Lam M., G. Dudyak and L. Chen. 1994. Evidence that Bcl-2 represses apoptosis by regulating endoplasmic reticulum-associated Ca⁺ fluxes, *Proceedings of the National Academy of Sciences USA*, 91: 6569-6573.
55. Leuthauser S. W. C., L. W. Oberley and T. D. Oberley. 1982. Antitumor Activity of Picolinic Acid in CBA/J Mice, *JNCI*, 68: 123-126.
56. Levin B.C., J. Chen and D.J. Reeder. 1998. Single-strand DNA Breaks from Combined Therapeutic AIDS Agents, <http://www.cstl.nist.gov/biotech/techact98.html>
57. Loeffler M. and G. Kroemer. 2000. The mitochondrion in cell death control: certainties and incognita, *Experimental Cell Research*, 256: 19-26.
58. Loffler H. J. M. and J. R. Mouris. 1992. Fusaric acid: phytotoxicity and in vitro production by *Fusarium oxysporum* f.sp. *lilii*, the causal agent of basal rot in lillies, *Netherlands Journal of Plant Pathology*, 98: 107-115.
59. Malini S. 1966. Heavy Metal Chelates of Fusaric Acid: in vitro spectrophotometry, *Phytopathology*, 57: 221-231.

60. Marasas W. F. O. 1993. Occurrence of *Fusarium moniliforme* and fumonisins in maize in relation to human health, *South African Medical Journal*, 83: 383-384.
61. Matta R. J. and G. F. Wooten. 1973. Pharmacology of fusaric acid in man, *Clinical Pharmacology and Therapeutics*, 14: 541-546.
62. Mckelvey-Martin V. J., M. H. L. Green, P. Schmezer, B.L. Pool-Zobel, M. P. Demeo and A. Collins. 1993. The single cell gel electrophoresis assay (comet assay): A European review, *Mutation Research*, 288: 47-63.
63. Medema J. P. 1997. Cleavage of FLICE (caspase-8) by granzyme B during cytotoxic T lymphocyte induced apoptosis, *European Journal of Immunology*, 407: 789-795.
64. Mehler A. H. and E. L. May. 1956. Studies with carboxyl-labelled 3-hydroxy-anthranilic and picolinic acids *in vivo* and *in vitro*, *Journal of Biological Chemistry*, 23: 449-455.
65. Miyashita T. and J. C. Reed. 1995. Tumour suppressor p53 is a direct transcriptional activator of the human BAX gene, *Cell*, 80: 293-299.
66. Morgan D. O. 1995. Principles of CDK regulation, *Nature*, 374: 131-134.
67. Morrot G., P. Herve, A. Zachowski, P. Fellmann and P. F. Devaux. 1989. Aminophospholipid translocase of human erythrocytes: Phospholipid substrate specificity and effect of cholesterol, *Biochemistry*, 28: 3456-3462.
68. Mosmann T. 1983. Rapid colorimetric assay for cellular growth and survival: Application to proliferation and cytotoxicity assays, *Journal of Immunological Methods*, 65: 55-63.

- 69) Nagatsu T., H. Hidaka, H. Kuzuya and K. Takeya. 1970. Inhibition of dopamine β -hydroxylase by fusaric acid (5-butylpicolinic acid) *in vitro* and *in vivo*, *Biochemical Pharmacology*, 19: 35-44.
- 70) Nakamura M., Y. Sakaki, N. Watanabe and Y. Takagi. 1981. Purification and characterization of the Ca^{2+} plus Mg^{2+} dependent endodeoxyribonuclease from calf thymus chromatin, *Journal of Biochemistry*, 89: 143-152.
71. Ogata S., M. Takeuchi, H. Fujita, K. Shibata, K. Okumura and H. Taguchi. 2000. Apoptosis induced by Niacin-related compounds in K562 cells but not in normal lymphocytes, *Bioscience, Biotechnology, Biochemistry*, 64 (6): 1142-1146.
72. Ohtsubo M. and J. M. Roberts. 1993. Cyclin dependent regulation of G1 in mammalian fibroblasts, *Science*, 259: 1908-1912.
73. Olive P. L., D. Wlodek, R. E. Durand and J. P. Banath. 1992. Factors influencing DNA migration from individual cells subjected to gel electrophoresis, *Experimental Cell Research*, 198: 259-267.
74. Omerod M. G., F. P. M. Cheetham and X. M. Sun. 1995. Discrimination of apoptotic thymocytes by forward light scatter, *Cytometry*, 21: 300-304.
75. Pastan I., G. S. Johnson and W. B. Anderson. 1975. Role of cyclic nucleotides in growth control, *Annual Reviews in Biochemistry*, 44: 491-552.
76. Pollard H. B. and E. Rojas. 1988. Ca^{2+} activated synexin forms highly selective, voltage-gated Ca^{2+} channels in phosphatidylserine bilayer membranes. *Proceedings of the National Academy of Sciences USA*, 85: 2974-2978.
77. Reed J. C. 1997. Double identity of the proteins of the Bcl-2 family, *Nature*, 387: 773-776.

78. Richmond T. J., J. T. Finch, B. Rushton, D. Rhodes and A. Klug. 1984. Structure of the nucleosome core particle at 7A resolution, *Nature*, 311: 532-537.
79. Rudel T. and G. M. Bokoch. 1997. Membrane and morphological changes in apoptotic cells regulated by caspase-mediated activation of PAK-2, *Science*, 276: 1571-1574.
80. Schlaepfer D. D. and H. T. Haigler. 1988. *In vitro* protein kinase C phosphorylation sites of placental lipocortin, *Biochemistry*, 27: 4253-4258.
81. Schwartzman R. A. and J. A. Cidlowski. 1993. Apoptosis: The biochemistry and molecular biology of programmed cell death, *Endocrine Reviews*, 14: 133-151.
82. Seigneuret M. and P. F. Devaux. 1984. Asymmetric distribution of spin-labelled phospholipids in the erythrocyte membrane: Relation to shape changes, *Proceedings of the National Academy of Sciences USA*, 81: 3751-3755.
83. Shirodkar S., M. Ewen, J. A. DiCaprio, J. Morgan, D. M. Livingston and T. Chitenden. 1992. The transcription factor E2F interacts with the retinoblastoma gene product and a p107-cyclin A complex in a cell cycle-regulated manner, *Cell*, 68: 157-166.
84. Singh N. P., M. T. Macoy, R. R. Tice and E. L. Schneider. 1988. A simple technique for the quantification of low levels of DNA damage in individual cells, *Experimental Cell Research*, 175: 184-191.
85. Singh N. P., R. R. Tice, R. E. Stephens and E. L. Schneider. 1991. A microgel electrophoresis technique for the direct quantitation of DNA damage and repair in individual fibroblasts cultured on microscope slides, *Mutation Research*, 252: 289-296.

86. Slater T. F., B. Sawyer and U. D. Strauli. 1963. Studies on Succinate-Tetrazolium Reductase Systems 8. Points of coupling of Four Different Tetrazolium Salts, *Biochimica Biophysica Acta*, 77: 383-393.
87. Smith T. K. and E. J. MacDonald. 1991. Effect of fusaric acid on brain regional neurochemistry and vomiting behaviour in swine, *Journal of Animal Science*, 69: 2044-2049.
88. Smith T. K. and M. G. Sousadias. 1993. Fusaric acid content of swine feedstuffs, *Journal of Agriculture and Food Chemistry*, 41: 2296-2298.
89. Smith J. W., A. L. Steiner, W. M. Jr. Newberry and C. W. Parker. 1971. Cyclic Adenosine 3', 5'-Monophosphate in Human Lymphocytes. Alterations after Phytohemagglutinin Stimulation, *Journal of Clinical Investigation*, 50: 432-441.
90. Strasser A., A. H. Harris, T. Jacks and S. Cory. 1993. DNA damage can induce apoptosis in proliferating lymphoid cells via p53-independent mechanisms inhibitable by Bcl-2, *Cell*, 79: 329-339.
91. Strasser A., L. O' Connor and V. M. Dixit. 2000. Apoptosis signalling, *Annual Reviews in Biochemistry*, 69: 217-245.
92. Sulpice J. C., A. Zachowski, P. F. Devaux and F. Giraud. 1994. Requirement for phosphatidylinositol 4,5-bisphosphate in the Ca²⁺-induced phospholipid redistribution in the human erythrocyte membrane, *Journal of Biological Chemistry*, 269: 6347-6354.
93. Thompson C. B. 1995. Apoptosis in the pathogenesis and treatment of disease, *Science*, 267: 1456-1462.

94. Thress K., S. Kornbluth and J. J. Smith. 1999. Mitochondria at the crossroad of apoptotic cell death, *Journal of Bioenergetics and Biomembranes*, 31: 321-326.
95. Tilly R. H. J., J. M. G. Senden, P. Comfurius, E. M. Bevers and R. F. A. Zwaal. 1990. Increased aminophospholipid translocase activity in human platelets during secretion, *Biochimica Biophysica Acta*, 1029: 188-190.
96. Towle C. A. and Treadwell, B. V. 1992. Identification of a novel mammalian annexin, *Journal of Biological Chemistry*, 267: 5416-5423.
97. Troncone L. R. P. and S. Tufik. 1991. Effects of selective adrenoceptor agonists and antagonists on aggressive behaviour elicited by apomorphine, DL-DOPA and fusaric acid in REM-sleep-deprived rats, *Physiology and Behavior*, 50: 173-178.
98. Valverde M., P. Ostrosky-Wegman, Emilio Rojas, M. Teresa Fortoul, M.C. Fernando Meneses, M.C. Matiana Ramírez, F. Díaz-Barriga and C. Mariano. 1999. The application of single cell gel electrophoresis or comet assay to human monitoring studies, *S113 salud pública de méxico*, 41, suplemento 2: S109-S113.
99. Varesio L., M. Clayton, E. Blasi, R. Ruffman and D. Radzioch. 1990. Picolinic acid, a catabolite of tryptophan, as the second signal in the activation of IFN- γ -primed macrophages, *The Journal of Immunology*, 145: 4265-4271.
100. Veis D. J., C. M. Sorenson, J. R. Shutter and S. J. Korsmeyer. 1993. Bcl-2 deficient mice demonstrate fulminant lymphoid apoptosis, polycystic kidneys, and hypopigmented hair, *Cell*, 75: 229-240.
101. Verheij M., R. Bose and X. H. Lin. 1996. Requirement of ceramide-initiated SAPK/JNK signalling in stress-induced apoptosis, *Nature*, 380: 75-79.

102. Verheij H. M., J. J. Volwerk, E. H. J. M. Jansen, W. C. Puyk, B. W. Dijkstra, J. Drenth. and G. H. de Haas. 1980. Methylation of histidine-48 in pancreatic phospholipase A2. Role of histidine and calcium ion in the catalytic mechanism, *Biochemistry*, 19: 743-750.
103. Verhoeven B., R. A. Schlegel and P. Williamson. 1995. Mechanisms of phosphatidylserine exposure, a phagocyte recognition signal, on apoptotic T lymphocytes, *Journal of Experimental Medicine*, 182: 1597-1601.
104. Vermes I., C. Haanen, H. Steffens Nakken and C. Reutelingsperger. 1995. A novel assay for apoptosis. Flow cytometric determination of phosphatidylserine expression on early apoptotic cells using fluorescein labelled Annexin V. *Journal of Immunological Methods*, 184: 39-51.
105. Vijayalaxmi R., R. Tice and G. H. S. Strauss. 1992. Assessment of radiation-induced DNA damage in human blood lymphocytes using the single-cell gel electrophoresis technique, *Mutation Research*, 271: 243-252.
106. Wang H. and T. B. Ng. 1999. Pharmacological activities of fusaric acid (5-Butylpicolinic acid), *Life Sciences*, 65: 849-856.
107. Waring P. 1990. DNA fragmentation induced in macrophages by gliotoxin does not require protein synthesis and is preceded by raised inositol triphosphate levels, *Journal of Biological Chemistry*, 265: 14476-14480.
108. Warrant R. W. and S. H. Kim. 1978. Alpha-helix double helix shown in the structure of a protamine-transfer RNA complex and a nucleoprotamine model, *Nature*, 271: 130-135.

109. Weinberg R. A. 1995. The retinoblastoma protein and the cell cycle control, *Cell*, 81: 323-330.
110. Wheater P. R., H. G. Burkitt and V. G. Daniels. 1987. *Functional Histology: A text and colour atlas*, 2: 36-51.
111. www.bssv01.lancs.ac.uk/StuWork/BIOS316/Bios31697/annexinv.htm
112. www.chemcases.com/cisplat/cisplat19.htm
113. www.fcm-ntsrvr01.utmb.edu/apo.pdf
114. www.geocities.com/CollegePark/Lab/1580/cycle.html
115. www.hsc.virginia.edu/./pathology/educ/innes/text/nh/wcb.html
116. www.idexx.com/.../InClinic/Catalog/lasergraphics.cfm
117. www.learninglab.co.uk/headstart/cycle3.htm
118. www.southernbiotech.com/techbul/10010.pdf
119. Wyllie A. H. 1980. Glucocorticoid-induced thymocyte apoptosis is associated with endogenous nuclease activation, *Nature*, 284: 555-556.
120. Wyllie A. H. 1997. Apoptosis: an overview, *British Medical Bulletin*, 53: 451-465.
121. Yang E. and S. J. Korsmeyer. 1996. Molecular apoptosis: a discourse on the Bcl-2 family and cell death, *Blood*, 88: 386-401.
122. Yin D. X. and R.T. Schimke. 1995. Bcl-2 expression delays drug-induced apoptosis but does not increase clonogenic survival after drug treatment in HeLa cells, *Cancer Research*, 55: 4922-4928.
123. Zachowski A., J. P. Henry and P. F. Devaux. 1989. Control of transmembrane lipid asymmetry in chromaffin granules by an ATP-dependent protein, *Nature*, 340: 75-76.

124. Zwaal R. F. A and Alan J. Schroit. 1997. Pathophysiologic implications of membrane phospholipid asymmetry in blood cells, *Blood*, 89 (4): 1121-1132.

10 APPENDICES

Appendix 1

Buffer A	(50 ml)
Tris	60.57mg
MgCl ₂	30.50mg
Phenylmethane sulphonyl fluoride	2.61mg
Mercaptoethanol	6.99μl

Appendix 2

Lysis buffer	(50ml)
Tris	300mg
EDTA	186mg
Sodium N lauryl sarcosinate	250mg

Appendix 3

TBE Buffer (10× stock)

(1 Litre)

Tris

108g

Boric acid

55g

EDTA

4ml (0.5M stock, pH 8)

Appendix 4

Lysing solution	(250ml)
NaCl	36.52mg
EDTA	50ml (0.5M stock, pH 8)
Triton X	2.5ml
Tris	0.3g
DMSO	25ml

Appendix 5

Electrophoresis buffer	(pH 13)	(500ml)
EDTA		1ml (0.5M stock, pH 8)
NaOH		6g

Appendix 6

Electronic compensation

1. While viewing a FSC vs SSC dot plot, run the control tube of unstained cells and set the acquisition gate on the population of interest. *Because apoptotic cells may undergo changes in light scattering properties, the gate used to identify the cells of interest should accommodate these changes.*
2. Generate a log FL1 vs log FL2 (or FL3) dot plot of the gated cells. Adjust emission PMTs so that >98% of the total events are located within the lower left quadrant and are within the first log decade on both the X and Y axis of the FL1 vs FL2 (or FL3) dot plot.
3. While viewing the FL1 vs FL2 (or FL3) dot plot of the gated cells, run tube #2 (annexin V-FITC only) to ensure that no events are recorded in the upper left and upper right quadrants of the display. If necessary, correct the compensation by increasing FL2 (or FL3) - %FL1 compensation (this may range from 15-25%).
4. While viewing the FL1 vs FL2 (or FL3) dot plot of the gated cells, run tube #3 (PI only) to ensure that no events are recorded in the upper and lower right quadrants of the display. If PI stained cells are visible in any other than the upper left quadrant, decrease the FL1 - %FL2 (or FL3) compensation (this may range from 0-1%).
5. If the flow cytometer has been properly compensated, singly stained cells should be centrally located within the upper left (FL2 or FL3/PI) or lower right (FL1/annexin V-FITC) quadrants.
6. Run samples and collect a minimum of 10,000 cells in list mode.
7. To properly set the quadrant markers for determining the frequency of cells undergoing apoptosis, FL1 vs FL2 (or FL3)

analysis should first be performed on the untreated/uninduced cell samples as follows :

a) the largest cluster of events located in the lower left region of the FL1 vs FL2 (or FL3) dot plot is the annexin V-negative population (normally this population will reside within the first two log decades of the FL1 axis). Set the vertical cursor 0.1 to 0.2 log units beyond the right edge of this annexin V-negative population.

b) discrimination of PI + and PI - subpopulations is aided if necrotic cells are present in the sample; if so it may be possible to identify an additional cluster of events in the upper right area of the dot plot (annexin V + PI +); if no PI + cells are present in the sample, distinguishing PI + cells is best estimated by placing the horizontal cursor 0.1 to 0.3 log units above the edge of the double-negative cluster of events (annexin V - PI -).

8. Cells that have been experimentally treated or are suspected of undergoing apoptosis can now be analyzed. Those events falling outside the negative staining region are considered positive staining events for either annexin V only. The subpopulation of cells staining with annexin V-FITC only are those cells in the apoptotic pathway, while those that stain with both annexin V-FITC and PI are either necrotic or are in transition from the apoptotic to the necrotic state.